Summer 2019

Evaluating Volumetric Strain as a Predictor of Yield and Peak Strength for the Multistage Triaxial Test: A Case Study with Utah Coal Specimens

Emmanuel Orilogi

Evaluating Volumetric Strain as a Predictor of Yield and Peak Strength for the Multistage Triaxial Test: A Case Study with Utah Coal Specimens

by

Emmanuel Orilogi, Mary MacLaughlin, and Steve Berry

A project submitted in partial fulfillment of the requirements for the degree of

Master of Science in Geoscience

Geological Engineering Option

Montana Technological University

2019

Abstract

Failure envelopes used to characterize the shear strength of geological materials are generally obtained through conventional triaxial testing of multiple specimens and most of the specimens are heterogonous and expensive to obtain. Therefore, the multistage triaxial test was introduced to make use of a single specimen for material strength characterization, compared to the conventional triaxial test that requires at least three specimens. In the multistage triaxial test, the challenge to obtaining meaningful data is identifying when to terminate each loading stage. The goal is to be as close to the peak strength of the material but below the stress threshold that causes damage (referred to as the yield point), and consequently underestimation of the strength during the subsequent stages. In brittle rock, failure can occur suddenly, making it difficult to terminate each stage before yield and failure. In a document adopted by the the International Society of Rock Mechanics (ISRM), Kovari et al. (1983) suggest that axial load should be increased until the axial stress-strain curve shows a horizontal tangent, accepting that some damage will be done. More recently, alternatives have been suggested that terminate each stage of the multistage test based on volumetric strain measurements: the point of dilation (where the specimen volume has become larger than its original volume, due to the formation of microcracks) or the point of inflection (where the specimen stops contracting and starts expanding (due to the initiation of microcracks).

In this study, stress-strain curves available from 72 conventional triaxial tests on Utah coal from a previous study sponsored by the NIOSH Spokane Mining Research Division were used to identify the stresses associated with the volumetric dilation and inflection points, to investigate whether either of these would provide an adequate failure termination point for multistage tests performed on this material. In many of the tests, the volumetric dilation stress was higher than the yield stress, so the inflection point was identified as a better choice for the failure termination point. Three successful multistage tests were performed on specimens of the Utah coal using volumetric inflection as the termination point. The shear strength parameters obtained from these multistage triaxial tests are in very good agreement with those obtained from the conventional triaxial tests (average friction angle within 1°, average cohesion within 6%).

Keywords: Coal, multistage triaxial, volumetric strain, failure envelope.

Acknowledgements

This study made use of data from conventional triaxial tests performed by SB to fulfil research contract 214-2017-M-93216 funded by the NIOSH Spokane Mining Research Division under the direction of Dr. Bo Kim.

EO created the data plots and performed the interpretation and analysis, under the guidance of SB and MM. EO also wrote the draft report and participated in the multistage tests, supervised by SB. SB and MM contributed content to the report and MM had the lead role in the final editing.

Financial support was provided by the Department of Geological Engineering at Montana Technological University.

Table of Contents

1. Introduction

Characterization of the shear strength of materials is important for engineering design purposes. Shear strength data are often obtained in the laboratory using the triaxial test. In a typical conventional triaxial test, a cylindrical specimen is subjected to confining pressure to simulate confinement at depth and is subsequently loaded axially to failure. The primary drawback of the conventional test is that data from multiple specimens must be combined to establish a model for shear strength, and due to the inherent heterogeneity of geological materials, these specimens are not identical and could have different shear strength. Also, obtaining, preparing, and testing multiple specimens is expensive. For these reasons, the multistage triaxial test procedure for rock was introduced that uses a single specimen instead of three or more (Kim & Ko, 1979).

The goal of the multistage triaxial test is to identify the peak stresses at failure associated with at least three different confining pressures (applied in different stages) using a single specimen. The primary issue is that loading a specimen to the point of failure causes damage, which can result in underestimation of the intact strength for subsequent stages, particularly with brittle specimens. Ideally, each stage of the test would be terminated close to but just before failure in order to identify peak strength, but avoid damage. Identifying this termination point just prior to failure is challenging (Crawford & Wylie, 1987; Pagoulatos, 2004)

The termination point for each loading stage of the multistage triaxial test is generally identified using the graph of the stress vs. strain data being collected during the test. Alternatives used by previous researchers are a) when the stress vs. axial strain graph becomes horizontal (Kovari & Tisa, 1975; Kim & Ko, 1979) which is the generally accepted point at which peak stress is reached and it is understood that some damage will have occurred, b) when the volumetric strain reaches zero (Crawford & Wylie, 1987), and c) when the volumetric strain reaches its minimum at the inflection point (Pagoulatos, 2004). Alternative “c” was developed because many specimens, particularly those composed of brittle rock, reach failure or are significantly damaged before “a” or “b” are reached.

In this study, stress-strain curves from 72 conventional triaxial tests that had previously been performed on specimens of Utah coal were used to identify the stress values associated with alternatives “b” and “c,” in order to evaluate how well these stresses agree with the peak stress and whether they are below or above the stress level that causes damage to the specimen. Three multistage triaxial tests were then performed to allow the shear strength models formulated using the multistage and conventional triaxial test data to be compared.

2. Conventional Triaxial Test and Shear Strength Models

The triaxial test method was developed to evaluate the shear strength of materials subjected to confinement, simulating in situ stress conditions experienced by materials at depth. The test provides the peak stress and confining pressure data needed to establish a model for shear strength. As shown in Figure 2-1, a typical conventional triaxial test involves applying constant confining pressure around a cylindrical test specimen while the axial load applied through a hydraulic piston is gradually increased until the specimen fails. Failure of the specimen occurs at peak stress, the maximum stress the specimen can hold under a specific confining pressure.

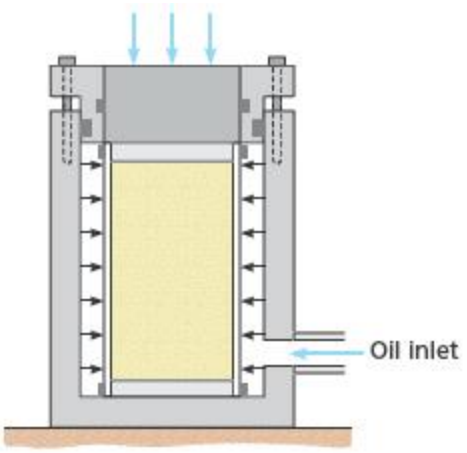

Figure 2-1: Diagram of a triaxial test apparatus showing (vertical) axial stress and (horizontal) confining stress (Gonzalez de Vallejo & Ferrer, 2011, p. 155).

2.1. Specimen Preparation

Specifications for the dimensions, shape, and surface tolerances of rock core specimens have been established to allow consistent interpretation of laboratory test data. Based on ASTM D4543-08 (2008), the length to diameter ratio of a rock specimen should be 2.0 to 2.5 with a diameter of not less than 47 mm. Also, the ends of the specimens should be parallel with a tolerance not to exceed 0.001 in (0.025 mm). The International Society for Rock Mechanics (Fairhurst & Hudson, 1999) suggests a length to diameter ratio of 2.0 to 3.0, a diameter not less than 50 mm, and specimen ends flattened to within 0.01 mm.

2.2. Test Procedures

Although the details of the triaxial test can vary, the ISRM (Kovari, et al., 1983) and ASTM (D7012-14, 2014) agree on the following basic concepts:

- A specific value of confining pressure (often referred to as p_c or σ_3) is achieved by introducing a fluid (oil, water, or compressed air) into the testing chamber to surround the specimen, and subsequently pressurizing the fluid. (The specimen is wrapped in membrane to prevent it from being saturated by the confining fluid.)
- The axial stress (σ_{axial} = applied force / specimen cross-sectional area, often referred to as σ_1) is applied by compressing the specimen with the loading ram, and steadily increased until the specimen fails.

It is generally recommended that deformation of the specimen be measured as a function of axial stress until peak stress and failure are observed. Although specifying a constant rate of axial stress increase is allowable, stress-controlled tests almost always result in uncontrolled failure at peak stress because the specimens can't carry the next specified stress increments and often fail violently. Strain-rate-controlled loading is preferable, with computer feedback to allow the testing machine to *decrease* the applied stress after the peak has been reached, facilitating continuation of the test into the post-peak region. To accomplish post-peak data collection, the test apparatus must also have a system stiffness that is higher than the specimen stiffness; the stiffer the testing system, the more likely that it will be able to capture post-peak behavior. Specimen stiffness is a function of its dimensions (wider, shorter specimens have lower stiffness) and the elastic modulus of the material. Rock specimens can display brittle or non-brittle behavior based on both the nature of the material (weaker, more deformable rock types tend to have less brittle behavior) and the confinement (specimens under higher confining pressure tend to be less brittle).

In terms of specimen deformation, axial loading alters both the axial and lateral dimensions. Axial compressive stress causes shortening of the specimen, expressed as axial strain. Axial strain (ε_{axial}) is defined as the change in length divided by the original length of the specimen ($\Delta L/L_0$). Axial compressive stress also causes lateral expansion, expressed as lateral strain. Lateral strain ($\varepsilon_{lateral}$) is defined as the change in the specimen diameter by its original diameter ($\Delta D/D_0$). During the triaxial test, axial and lateral strain or displacement measurements can be made using strain gages, linear variable differential transformers (LVDTs), or other suitable instrumentation (ASTM D7012-14, 2014).

2.3. Stress-Strain Curves

Use of instrumentation for measuring strain or displacement during the triaxial test allows strain-rate control (as described in section 2.2) and observation of the specimen behavior in real-time during the test or after the test is completed. The most common data plot is axial stress vs. axial strain, as shown in Figure 2-2. Initially, when the axial stress is increased, microcracks and voids in the sample are closed, causing non-linear response as depicted as region 1 in Figure 2-2; this nonlinearity may also be attributed to closure of the gaps between the ends of the specimen and the endcaps, even if the specimen is prepared to appropriate flatness tolerances. The linear portion of the curve, identified as region 2, is known as the elastic region where the increases in axial stress and axial strain are proportional. The point at which the curve deviates from linear,

presumably due to microcrack formation associated with high stress values, is referred to as the yield point and it is generally accepted that damage has initiated at this point. Beyond the yield point (region 3), new cracks grow and coalesce, resulting in "failure" at the peak stress. Post-peak behavior (region 4) may be obtained with a stiff testing machine.

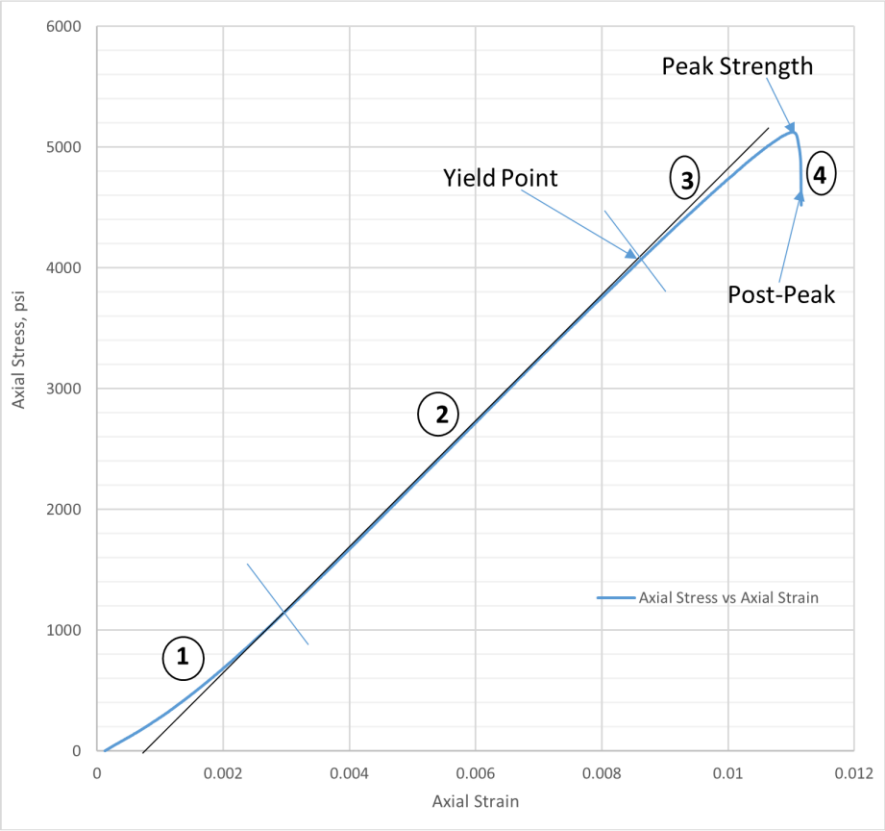

Figure 2-2: Axial stress –axial strain curve showing yield point and peak strength; (1) nonlinear region due to closure of void spaces and gaps, (2) elastic region, (3) nonlinear behavior approaching failure due to microcrack formation, (4) post-peak region. (Compressive stress and strain positive.)

In order to more fully evaluate the behavior of the specimen during the triaxial test, plots of lateral and volumetric strain can be added to the axial stress vs. axial strain graph. Volumetric strain is the change in volume over initial volume ($\Delta V/V_0$) and is often calculated as (Goodman, 1989):

$$\frac{\Delta V}{V} = \boldsymbol{\varepsilon_{axial}} + \boldsymbol{2\varepsilon_{lateral}} \qquad \text{(Equation 1)}$$

Changes in volumetric strain provide insight into the specimen's condition. During the initial stages of loading, the axial compression is dominant and the specimen's volume decreases. At some point, the axial stress becomes high enough to cause the initiation of microcracks, which in turn cause volume increase. This volume change is illustrated in Figure 2-3, which shows a plot of axial stress vs. axial, lateral, and volumetric strain. The point at which the specimen ceases to

compress and starts to expand due to the initiation of microcracks is called the volumetric strain inflection point. Also shown in Figure 2-3 is the volumetric dilation point, the point at which the specimen's overall volume has become larger than its original value, due to crack growth. Note that the volumetric dilation point may not perfectly coincide with the y-axis due to the strain accumulated during application of the confining pressure.

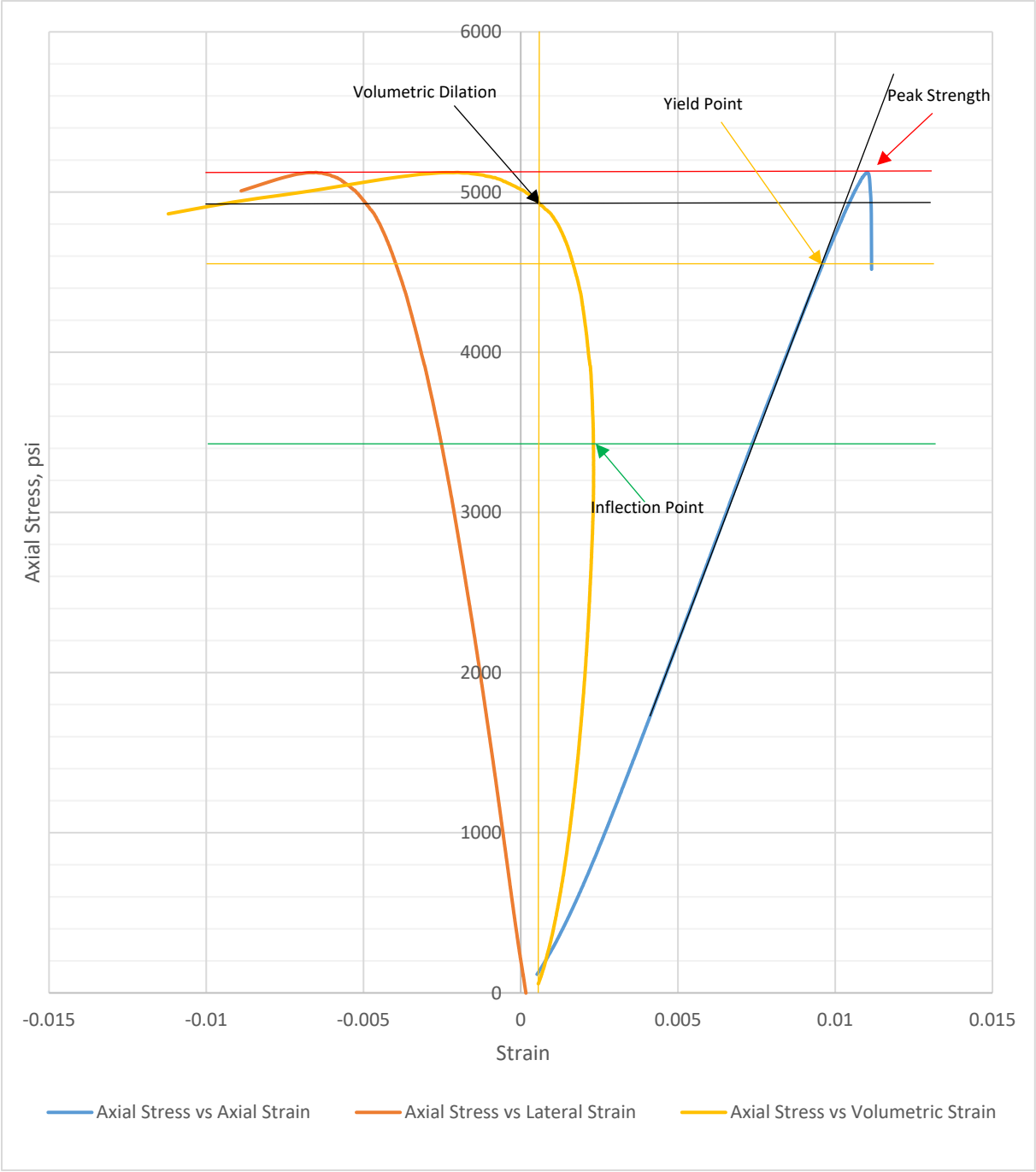

Figure 2-3: Plot of axial stress vs volumetric, lateral and axial strain. (Compressive stress and strain positive.)

2.4. Shear Strength Interpretation

Triaxial test data are commonly used to construct models of the shear strength of geological materials, including intact rock. One of the simplest and most common shear strength models is the Mohr-Coulomb (MC) failure envelope. It describes a linear relationship between normal stress and shear strength, and consequently has two parameters: the inclination of the line is known as the friction angle and the y-intercept is referred to as the shear strength intercept or cohesion (Goodman, 1989; Gonzales de Vallejo & Ferrer, 2011).

To develop the MC failure envelope, Mohr's circles of stress are plotted on a graph of shear stress (τ) vs. normal stress (σ_n) using data from the triaxial test. The confining pressure (σ_3) and corresponding peak stress (σ_1) are plotted on the normal stress (x) axis, and a circle is drawn through the two points, depicting the state of stress in the specimen at failure, including the shear stress values on all possible planes within the specimen. (In some instances, the yield point is substituted for the peak stress.) The MC failure envelope is drawn tangent to at least two Mohr's circles corresponding to failure at two different confining pressures. In practice, three circles are generally used to provide confidence in the results. Figure 2-4 displays the MC failure envelope constructed using triaxial test data.

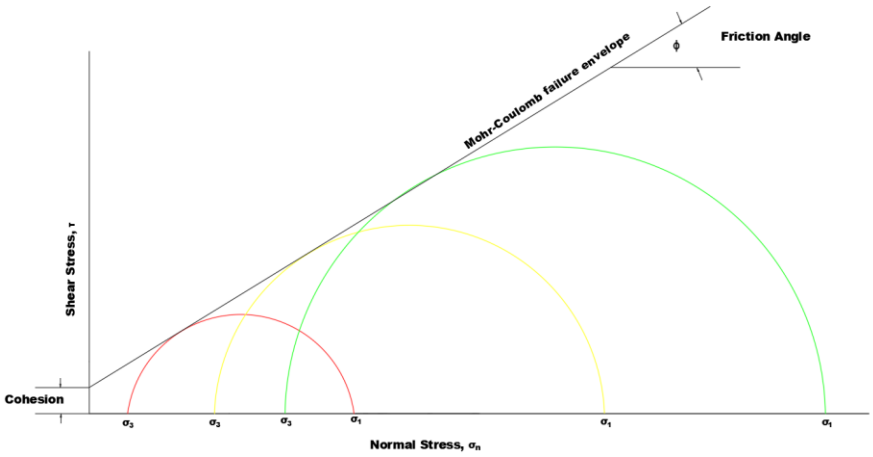

Figure 2-4: Construction of the Mohr-Coulomb failure envelope from three Mohr's circles of stress.

One significant problem with this approach is that the MC failure envelope is constructed using data from tests on multiple specimens that are not identical. Inherent heterogeneity in the specimens due to variability of the rock material as well as the presence of discontinuities causes variability in their strength. Because of this, along with the fact that obtaining and testing multiple specimens is expensive, an alternative approach referred to as the multistage triaxial test was introduced. This approach makes use of a single specimen instead of multiple specimens.

3. Multistage Triaxial Test

While development of a shear strength model is generally done using a minimum of three conventional triaxial tests, requiring at least three specimens, the multistage triaxial test can provide the required data with one specimen. A multistage triaxial test consists of different stages as shown in Figure 3-1, with each stage terminated at the peak stress, or ideally, a point just prior to failure to avoid specimen damage. Subsequent stages are achieved by applying higher levels of confining pressure on the single test specimen, which is brought to failure in the last stage of the test. It should be noted that if the specimen being tested reaches failure during one of the initial stages, the test will not provide adequate data to form a meaningful shear strength envelope and consequently will not yield an accurate estimate of the material's intact strength, so using a conservative indicator of imminent failure is recommended.

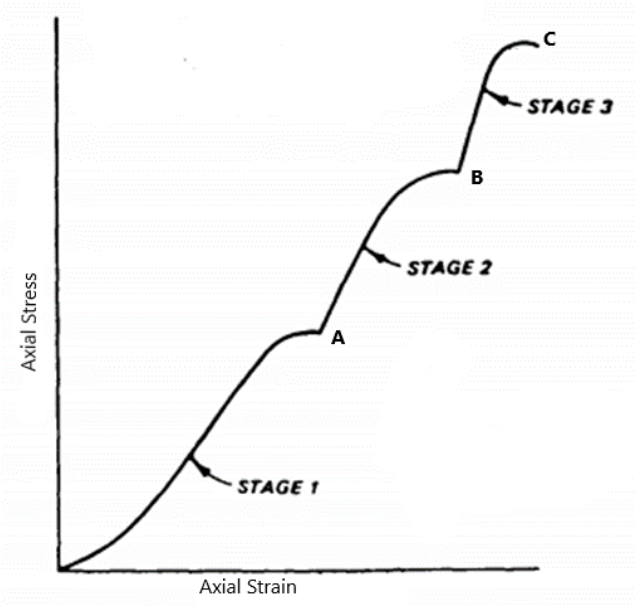

Figure 3-1: Multistage triaxial test stress-strain curve (modified from US Army Corps of Engineers, 1993, RTH 204-80).

3.1. Multistage Triaxial Test Procedures

ISRM (Kovari et al., 1983) recommends a multistage triaxial test procedure in which the first step involves increasing the axial load and the confining pressure until both reach the value of the confining pressure of the first stage, establishing a hydrostatic (equal stress in all directions) condition. Then, Stage 1 is conducted by increasing the axial stress while keeping confining pressure constant, until the peak stress is observed on the axial stress vs. axial strain curve at Point A of Figure 3-1. In Stage 2 of the test, the confining pressure is first increased to the next level while keeping the axial stress constant, then the axial stress is increased until peak stress is observed at Point B. The final stage of the test (Stage 3) is achieved by another sequential increase in the confining pressure and then the axial stress, continued until failure of the specimen is observed (Point C).

The modified multistage triaxial testing method (Crawford & Wylie, 1987) includes slight adjustments to the testing method suggested by ISRM. In this method, after reaching the first failure point, the axial stress is reduced to the level of the confining pressure, re-establishing a hydrostatic state. To start the next stage, the next desired confining pressure is attained while maintaining a hydrostatic state (keeping the axial stress equal to the confining pressure while the confining pressure is being increased), and then the axial stress is increased until the next peak stress is reached; this is repeated as many times as desired. Returning to the hydrostatic state between stages has several benefits, notably that the test procedure more closely resembles the stress path applied during conventional triaxial tests.

Although a great deal of success has been achieved using these multistage triaxial test methods, most published studies have involved testing of specimens that display primarily ductile behavior; the test is much more difficult to perform on brittle specimens because of the tendency for sudden failure as experienced when tests were performed on specimens of Lyons Sandstone (Kim & Ko, 1979) and Lac du Bonnet Granite (Crawford & Wylie, 1987). To overcome this challenge, Youn & Tonon (2010) proposed the use of radial strain control rather than axial strain control when loading brittle rock specimens. In their study, specimens of Edwards Limestone were tested and imminent failure (termination point) is defined as the point when the axial stress vs. radial strain curve becomes flat. Figure 3-2 shows differences in volumetric and axial stress-strain curves obtained using axial (left) and radial (right) strain rate control, in tests on specimens subjected to the same confining stress (1 MPa). The use of radial strain rate control provides denser data near the failure point, which allows the specimen to approach failure more slowly. The drastic strength difference observed was explained as local material variation (verified using other index tests).

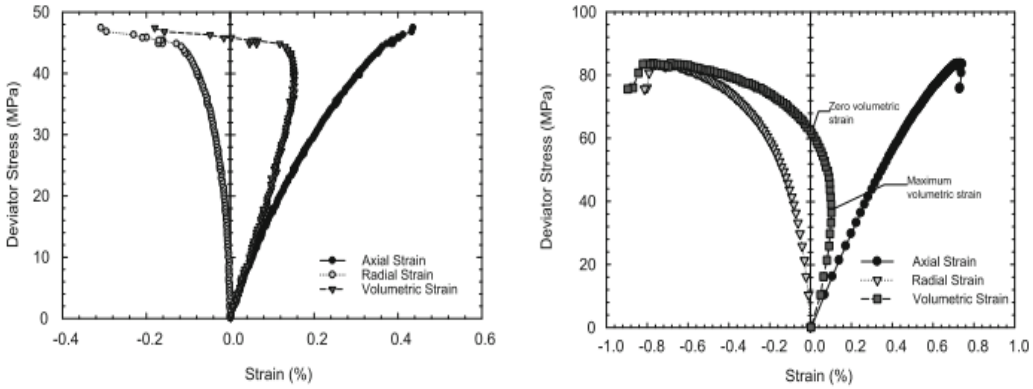

Figure 3-2: Triaxial test stress-strain plots for specimens of Edwards Limestone subjected to confining stress values of 1 MPa: a) axial strain control, b) radial strain control (Youn & Tonon, 2010).

Youn and Tonon (2010) also suggest a slight modification of the multistage procedure: after a stage is terminated, both confining stress and axial stress are increased, maintaining a constant stress difference. In additional tests performed on Edwards Limestone with radial strain control, excellent agreement was observed between the results of the conventional and modified multistage triaxial tests.

3.2. Identification of the Termination Point for Each Loading Stage

The primary issue with multistage triaxial test is knowing exactly when to terminate each stage, getting as close to peak stress as possible without causing damage to the specimen (Crawford & Wylie, 1987). Researchers have suggested several different approaches for performing multistage triaxial test and identifying the termination point for each loading stage of the test.

Kovari & Tisa (1975) summarize the results of "multiple failure state" (MFS) tests (an early version of the multistage test) and "continuous failure state" tests conducted on Buchberg Sandstone and Carrara Marble to allow determination of the failure envelope from a single specimen. The point of termination of each stage loading was when flattening of the stress-strain curve was detected. The test was then stopped and the confining pressure was increased to the next level without removing the axial load. The authors state that "a rigid testing machine and sensitive axial load measurement are required" to get good results with brittle rock specimens.

Kim and Ko (1979) carried out an investigation comparing the results of conventional and multistage triaxial tests on specimens of Pierre Shale, Raton Shale and Lyons Sandstone. During the multistage tests, each loading stage of the test was stopped when the stress-strain plot became horizontal. The results of the tests on Pierre Shale and Raton Shale showed good agreement between the conventional and multistage procedures. The strength values identified via the multistage test were within 6% of those yielded by the conventional tests, with the multistage test results slightly lower than conventional for the Pierre Shale and slightly higher than conventional for the Raton Shale. The results from the multistage tests performed on the Lyons Sandstone were not in good agreement with the conventional test results; the authors concluded that to achieve meaningful results with brittle materials like Lyons Sandstone, the tests need to be carried out under very high confining pressures using a high capacity, stiff testing machine.

Crawford and Wylie (1987) were among the first to make use of volumetric strain to determine the termination point of MFS (multistage) triaxial tests performed on specimens of Berea Sandstone and Lac du Bonnet Granite. The imminent failure termination point was defined

as the point at which volumetric strain (ΔV/V), initially negative, reaches zero on a volumetric strain versus axial strain plot; this is commonly referred to as the volumetric dilation point. The strength envelope for the Berea Sandstone obtained using the modified MFS method was slightly lower than that developed using conventional triaxial test data, as shown in Figure 3-4. During tests performed on Lac du bonnet Granite, a brittle material, it was observed that the point of zero volumetric strain could not be attained before failure of the specimens and the tests could not be performed successfully using volumetric dilation to terminate the loading stages. Additional tests were performed using maximum volumetric strain (also referred to as volumetric inflection) as the loading stage termination point, but the strength envelopes did not agree with those established via conventional triaxial tests. The authors indicate that the best results were achieved by terminating the tests below but near the volumetric dilation point and extrapolating the stress-strain curves.

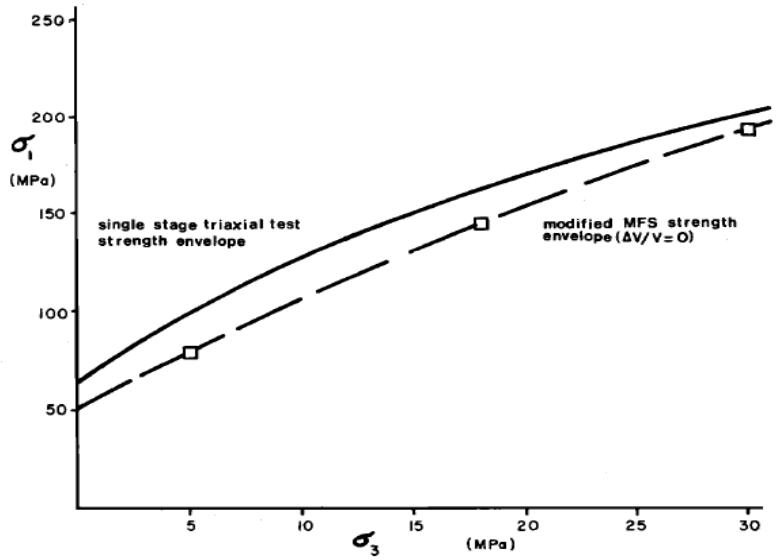

Figure 3-3: Berea sample strength envelopes for conventional triaxial and modified multiple failure state (multistage) triaxial methods.

Pagoulatos (2004) proposed the use of inflection point of the volumetric strain curve for termination of the multistage test initial loading stages. The volumetric inflection point can be readily and objectively determined, and it has been observed that the corresponding stress is always less than peak stress and almost always below yield stress. Multistage triaxial tests performed on Berea Sandstone showed good agreement with conventional triaxial tests when volumetric inflection was used as the loading stage termination point, and the results were adjusted to compensate for the difference between inflection point stress and peak stress.

4. Evaluation of Alternatives for the Termination Point

The alternatives that have been proposed for identifying the termination point for each loading stage of the multistage triaxial test are described in Section 3.2. They may be summarized as:

a) when the stress vs. axial strain graph becomes horizontal (Kovari & Tisa, 1975; Kim & Ko, 1979). This is generally accepted as the point of failure, when peak stress has been reached. There has clearly been some damage done to the specimen at this point. For non-brittle materials that do not lose strength after failure, the strength identified in subsequent stages could be a good representation of the material strength, but for brittle materials that lose strength upon failure, subsequent tests will likely underestimate the undamaged strength.

b) when the volumetric strain reaches zero (Crawford & Wylie, 1987). This is known as the volumetric dilation point, at which the specimen volume becomes larger than the original volume, presumably due to the formation of microcracks as the specimen starts to fail. This point should be close to, but below, the peak stress. In practice, however, it has been observed that many specimens fail before reaching the volumetric dilation point.

c) when the volumetric strain reaches its minimum (Pagoulatos, 2004). This is referred to as the volumetric strain inflection point, at which the specimen stops compressing under the applied stress and starts expanding as microcracks begin to form. This should be a more conservative estimate of the onset of failure than alternatives “a” or “b.” This alternative was developed because many specimens, particularly those composed of brittle rock, reach failure or are significantly damaged before “a” or “b” are reached.

In this project, alternatives “b” and “c” (based on volumetric strain) for identifying the multistage triaxial test loading stage termination point were evaluated using data available for 72 conventional triaxial tests that had previously been conducted on specimens of coal. Ideally, the stress values would be close to the peak stress but below the “damage level” stress, suggesting that the alternative is a good choice for the termination point in multistage triaxial tests performed on this material.

The fact that the tests were performed on specimens of coal under low confining pressures is significant in that brittle behavior is expected, and was observed. Achieving success with the multistage triaxial test is difficult with truly brittle materials because of the tendency for sudden, violent failure and because significant damage has usually occurred before signs of failure are perceptible. This is further exacerbated by the fact that coal contains multiple planes of weakness.

4.1. Specimens, Test Data, and Interpretation

The tests that provided data for this study were conducted for a research project to investigate the behavior of coal under very low confining stresses, sponsored by NIOSH Spokane Mining Research Division under the direction of Dr. Bo Kim (Kim et al., 2018). The 72 conventional triaxial tests were performed on specimens of Utah coal cored to an approximate diameter of 44 mm and with a length to diameter ratio of 2 to 2.5 according to ASTM D 4542-01, and with a flatness tolerance of 0.025 mm.

Coal contains multiple closely-spaced planes of weakness referred to as “cleats.” In order to investigate the influence of the cleat orientations on the coal’s shear strength, four groups of specimens were created, each with a specific angle between the coal cleats and the long axis of the core: 0°, 15°, 30°, and 45°. The specimens were subjected to confining pressure values ranging from 10 psi to 1628 psi; because the focus of the study was on behavior at low confinement, the majority (nearly 80%) of the confining stresses were 211 psi or lower. Three different specimens were tested at each confining pressure to allow evaluation of the consistency of the data. Appendix A contains a table listing the 72 specimens and their respective confining pressure values.

The test results from the previous study were imported into Microsoft Excel for analysis. Figure 4-1 shows a portion of one of the test datafiles. Each datafile contains the measurements of axial stress, axial strain, lateral strain, and confining pressure applied during the test. Volumetric strain is a derived value calculated by the testing software (using equation 1).

In the Microsoft Excel spreadsheet, stress-strain curves for the 72 tests were created by plotting axial stress vs. axial strain along with volumetric and lateral strain. Figure 4-2 shows the axial stress vs. axial, lateral, and volumetric strain graph for one of the 72 datafiles (Tri_0_1a_32psi). The stress-strain plots can be found in Appendix B and entire set of 72 datafiles is available online at https://digitalcommons.mtech.edu/geol_engr/.

The axial stress vs. axial strain plot is used to identify the peak stress as well as the yield stress at which the specimen deviates from linear elastic behavior, presumably due to new formation of new microcracks as failure initiates (assumed to be the onset of significant damage). The axial stress vs. volumetric strain curve is used to identify the volumetric dilation and inflection points, which are the alternatives for identifying the onset of damage. The lateral strain curve was not explicitly used for this study, but is plotted for completeness and as a check on data consistency. The peak stress, yield stress, dilation point, and inflection point are referred to in this study as “crucial” points.

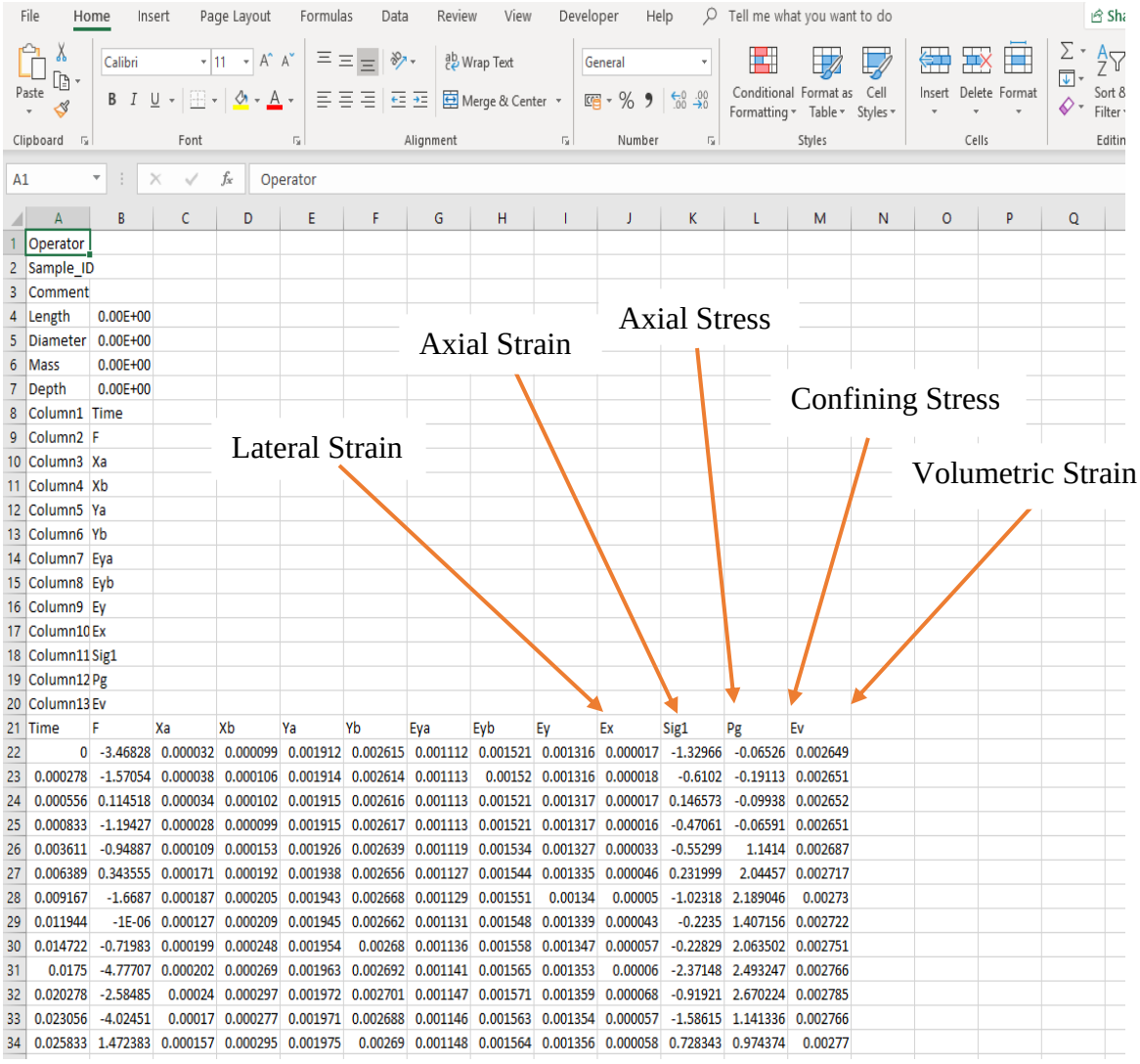

	A	B	C	D	E	F	G	H	I	J	K	L	M	N	O	P	Q
1	Operator																
2	Sample_ID																
3	Comment																
4	Length	0.00E+00															
5	Diameter	0.00E+00															
6	Mass	0.00E+00															
7	Depth	0.00E+00															
8	Column1	Time															
9	Column2	F															
10	Column3	Xa															
11	Column4	Xb															
12	Column5	Ya															
13	Column6	Yb															
14	Column7	Eya															
15	Column8	Eyb															
16	Column9	Ey															
17	Column10	Ex															
18	Column11	Sig1															
19	Column12	Pg															
20	Column13	Ev															
21	Time	F	Xa	Xb	Ya	Yb	Eya	Eyb	Ey	Ex	Sig1	Pg	Ev				
22	0	-3.46828	0.000032	0.000099	0.001912	0.002615	0.001112	0.001521	0.001316	0.000017	-1.32966	-0.06526	0.002649				
23	0.000278	-1.57054	0.000038	0.000106	0.001914	0.002614	0.001113	0.00152	0.001316	0.000018	-0.6102	-0.19113	0.002651				
24	0.000556	0.114518	0.000034	0.000102	0.001915	0.002616	0.001113	0.001521	0.001317	0.000017	0.146573	-0.09938	0.002652				
25	0.000833	-1.19427	0.000028	0.000099	0.001915	0.002617	0.001113	0.001521	0.001317	0.000016	-0.47061	-0.06591	0.002651				
26	0.003611	-0.94887	0.000109	0.000153	0.001926	0.002639	0.001119	0.001534	0.001327	0.000033	-0.55299	1.1414	0.002687				
27	0.006389	0.343555	0.000171	0.000192	0.001938	0.002656	0.001127	0.001544	0.001335	0.000046	0.231999	2.04457	0.002717				
28	0.009167	-1.6687	0.000187	0.000205	0.001943	0.002668	0.001129	0.001551	0.00134	0.00005	-1.02318	2.189046	0.00273				
29	0.011944	-1E-06	0.000127	0.000209	0.001945	0.002662	0.001131	0.001548	0.001339	0.000043	-0.2235	1.407156	0.002722				
30	0.014722	-0.71983	0.000199	0.000248	0.001954	0.00268	0.001136	0.001558	0.001347	0.000057	-0.22829	2.063502	0.002751				
31	0.0175	-4.77707	0.000202	0.000269	0.001963	0.002692	0.001141	0.001565	0.001353	0.00006	-2.37148	2.493247	0.002766				
32	0.020278	-2.58485	0.00024	0.000297	0.001972	0.002701	0.001147	0.001571	0.001359	0.000068	-0.91921	2.670224	0.002785				
33	0.023056	-4.02451	0.00017	0.000277	0.001971	0.002688	0.001146	0.001563	0.001354	0.000057	-1.58615	1.141336	0.002766				
34	0.025833	1.472383	0.000157	0.000295	0.001975	0.00269	0.001148	0.001564	0.001356	0.000058	0.728343	0.974374	0.00277				

Figure 4-1: Visual view of a portion of one of the datafiles from conventional triaxial tests in Microsoft Excel, with important data columns labelled.

The peak stress and yield point for each of the 72 conventional triaxial tests were identified using the axial stress vs. axial strain curve. The peak stress is readily determined as the maximum axial stress. To select the point of yield from each plot, the curve was expanded and a straight line was manually superimposed over the data to distinguish where the curve begins to deviate, as shown in Figure 4-3. It is noted that the yield point defined as the initial deviation from linear may occur significantly earlier in the test (at a lower axial stress value) than the yield point defined as deviation from linear as readily apparent in the full scale stress-strain curve (and in the testing software during the test). It is also noted that while the other three crucial points are well-defined, the determination of the yield point is much more subjective.

The volumetric dilation and inflection points were determined from the axial stress vs. volumetric strain plots. The initial portion of the curves were inspected to adjust the "zero" point if necessary due to initial offsets in the strain data. To precisely pick the point of inflection, the axial stress vs. volumetric strain curve was expanded to be able to pick the inflection point, as shown in Figure 4-4. This point was also verified by finding the maximum value of the volumetric strain data defined as compression positive (which correspond to the minimum specimen volume). The axial stress values at the yield point, peak point, inflection point, and volumetric dilation point for the 72 tests are tabulated in Appendix C.

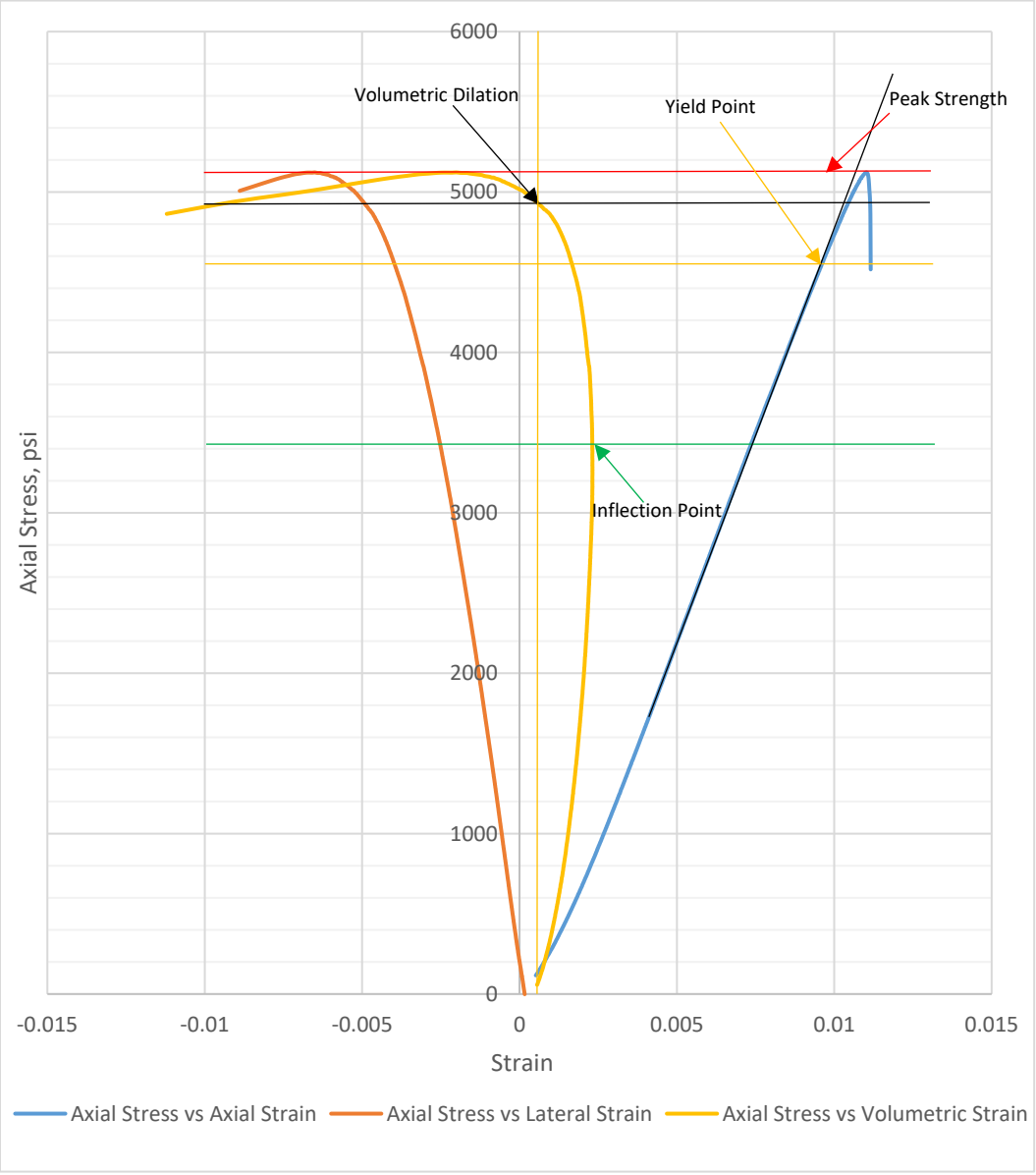

Figure 4-2: Axial stress vs. axial, lateral, and volumetric strain for conventional triaxial test Tri_0_32psi.

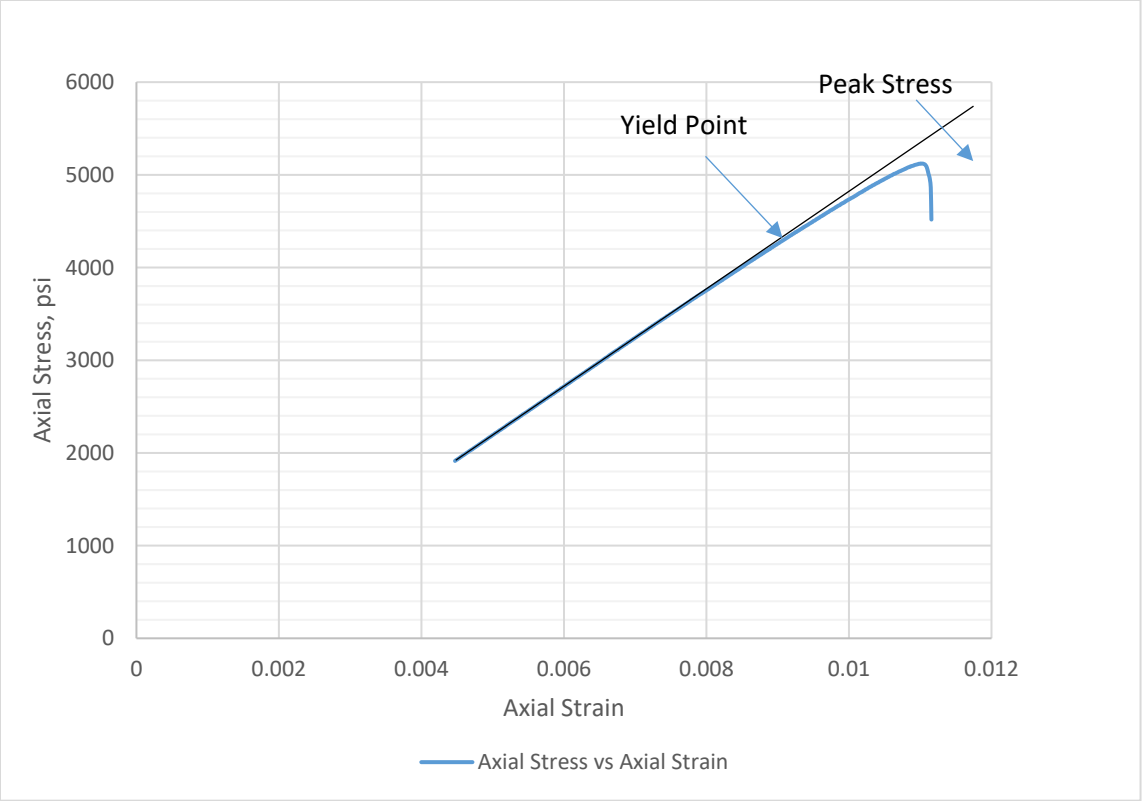

Figure 4-3: Axial stress vs. axial strain curve expanded to identify the yield point.

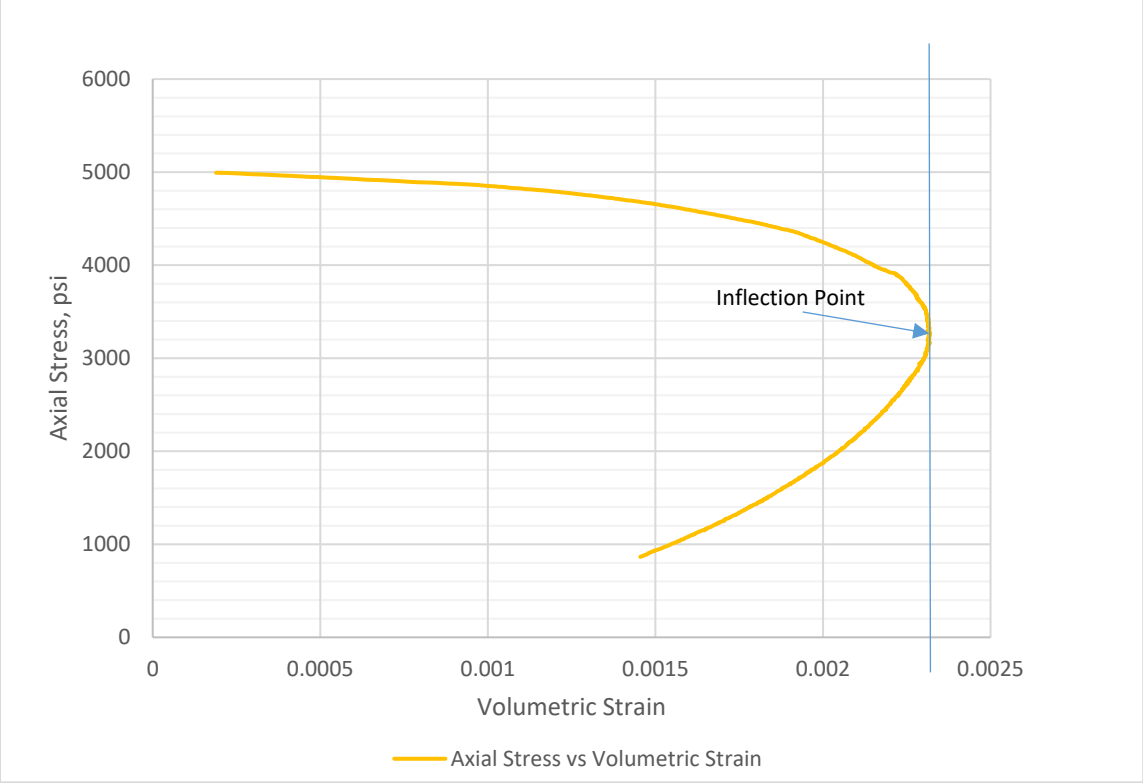

Figure 4-4: Axial stress vs. volumetric strain curve expanded to select the inflection point.

4.2. Conventional Triaxial Test Data Analysis

The primary goal of this project is to investigate the effectiveness of using the volumetric dilation point and/or volumetric inflection point as the multistage triaxial test loading stage termination point when conducting tests on this material. The stress values associated with an ideal termination point would be close to the peak stress but below the "damage level" (yield) stress. In the first stage of the analysis, the relationship between all of the crucial points identified on the stress-strain and volumetric strain curves (peak stress, yield stress, volumetric dilation point stress, and volumetric inflection point stress) for the 72 tests are shown graphically in Figure 4-5 to allow for identification of whether or not the data for each individual specimen followed the anticipated pattern: in an ideal situation, the inflection point stress (green) and the dilation point stress (yellow) would be near but slightly lower than the yield stress (orange), and all three would be near but below the peak stress (red). Volumetric inflection or dilation point stress above the yield stress would indicate that damage has occurred. After inspecting the data and graphs, the following conclusions can be drawn:

- In many cases (65/72), the volumetric dilation point stress values are higher than the yield stress values (45/72) and close to the peak stress values of the samples, or dilation was not reached prior to failure (20/72). This suggests that if the volumetric dilation point is used for the multistage triaxial test loading stage termination point, there is a significant chance that the specimen may fail before it begins to dilate, resulting in an unsuccessful multistage test. At best, even if dilation is reached prior to failure, the specimen is likely to be damaged, resulting in underestimation of the strength measured in subsequent stages.
- In contrast, the volumetric inflection point stress is below the yield point stress for 58 of the 72 specimens (80%). This suggests that the volumetric inflection point is a good choice to use for the multistage triaxial test loading stage termination because significant damage is not likely to be inflicted on the specimen during the initial loading stages.

To further investigate these relationships, the dilation point and inflection point stresses as a percentage of the yield point and peak stresses (dilation or inflection point stress equal to yield or peak stress would be "100%") were calculated for each of the 72 specimens and are tabulated in Appendix D. With the inflection point being identified as a better candidate than the dilation point for terminating the stages of a multistage triaxial test, the range and average of inflection point stress as a percentage of yield and peak stress are displayed in Table 4-1, organized by the four groups corresponding to different cleat orientations.

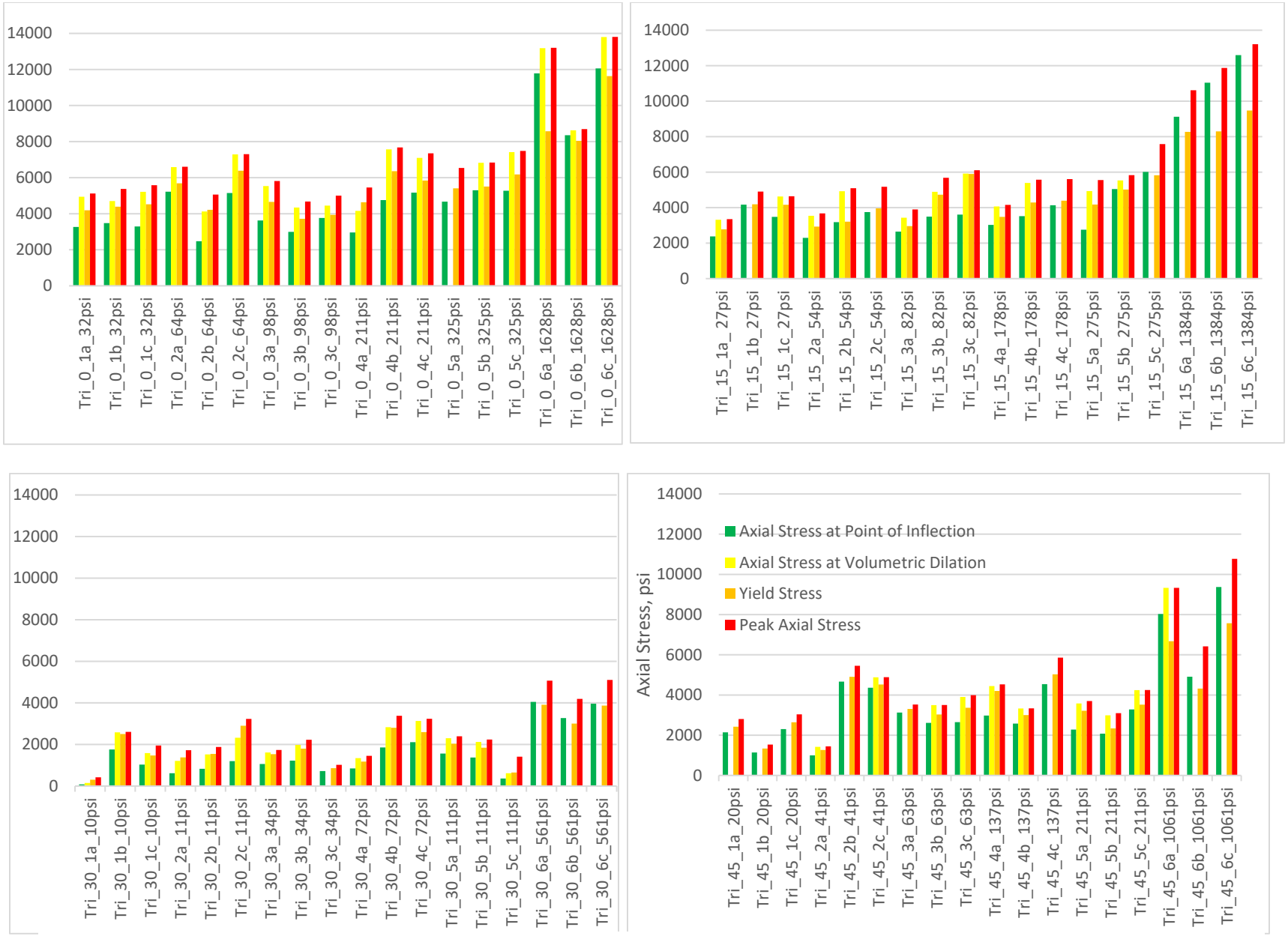

Figure 4-5: Peak stress, yield stress, volumetric dilation point stress, and inflection point stress for 72 specimens of Utah coal. Top left: Group 1 with cleats oriented parallel (0°) to the long axis of the core. Top right: Group 2 with cleats oriented 15° from the long axis. Bottom left: Group 3 with cleats oriented at 30°. Bottom right: Group 4 with cleats oriented at 45°. The data for dilation point stress are absent for tests in which dilation was not observed prior to peak stress.

Table 4-1: Inflection point stress as a percentage of yield and peak stress

Group	Cleat angle	Range of confining pressure [psi]	Inflection point as a % of yield stress: average [range]	Inflection point as a % of peak stress: average [range]
1	0°	32 to 1628	86% [59% to 137%]	70% [49% to 96%]
2	15°	32 to 275	93% [61% to 133%]	73% [50% to 95%]
3	30°	10 to 561	70% [26% to 109%]	56% [19% to 80%]
4	45°	20 to 1062	92% [71% to 124%]	76% [62% to 89%]

One aspect of performing multistage tests on brittle materials that is particularly critical is establishing three values of undamaged shear strength. If the specimen is loaded past yield in any stage, significant damage may occur and there is a potential for violent failure. Consequently, it is critical to select a loading stage termination point that is near yield and ideally below it. A methodology to account for the fact that the peak stresses are underestimated in the initial stages of the multistage triaxial test has been developed (Pagoulatos, 2004) and is discussed further in Section 6.2. The data summarized in Table 4-1 indicate that the inflection point stress as a percentage of the yield stress was on average less than 100% for each of the four groups of coal specimens. Furthermore, it is generally expected that closer and more consistent agreement between the termination point and the peak stress will provide more accurate shear strength parameters. As shown in Table 4-1, for specimens in groups 1, 2, and 4, the inflection point stresses are on average 70-76% of the peak stress, and within the range of 49-95%. In contrast, the inflection point stresses for the specimens in group 3 range from 19-80% of the peak stress and are on average 56% of the peak stress. The difference between the data from group 3 and the other groups is also evident in Figure 4-6, which displays plots of peak stress and inflection point stress as a percentage of peak stress vs. confining pressure. The generally lower peak strength values, higher variability, and larger average difference between inflection point stresses and peak stresses associated with the data from group 3 are explained by the fact that the cleats have the most unfavorable orientation, aligned with the plane that has the most adverse combination of normal and shear stresses. This suggests that the shear strength parameters identified for specimens with adversely oriented discontinuities may be less accurate, but more conservative, than those identified for specimens with less adversely oriented discontinuities.

One final analysis was performed to further inspect the influence of confining pressure. Figure 4-7 shows plots of the inflection point stress as a percentage of the yield stress for each of the 72 individual specimens, with white fill highlighting values above 100%. From this plot it

can be seen that for the 14 cases in which the inflection point was above yield, twelve were at the highest confining stress values applied to each group and the other two were at the second highest confining stress. This suggests that for higher confining stresses, there is a higher likelihood that some damage will have occurred at the inflection point.

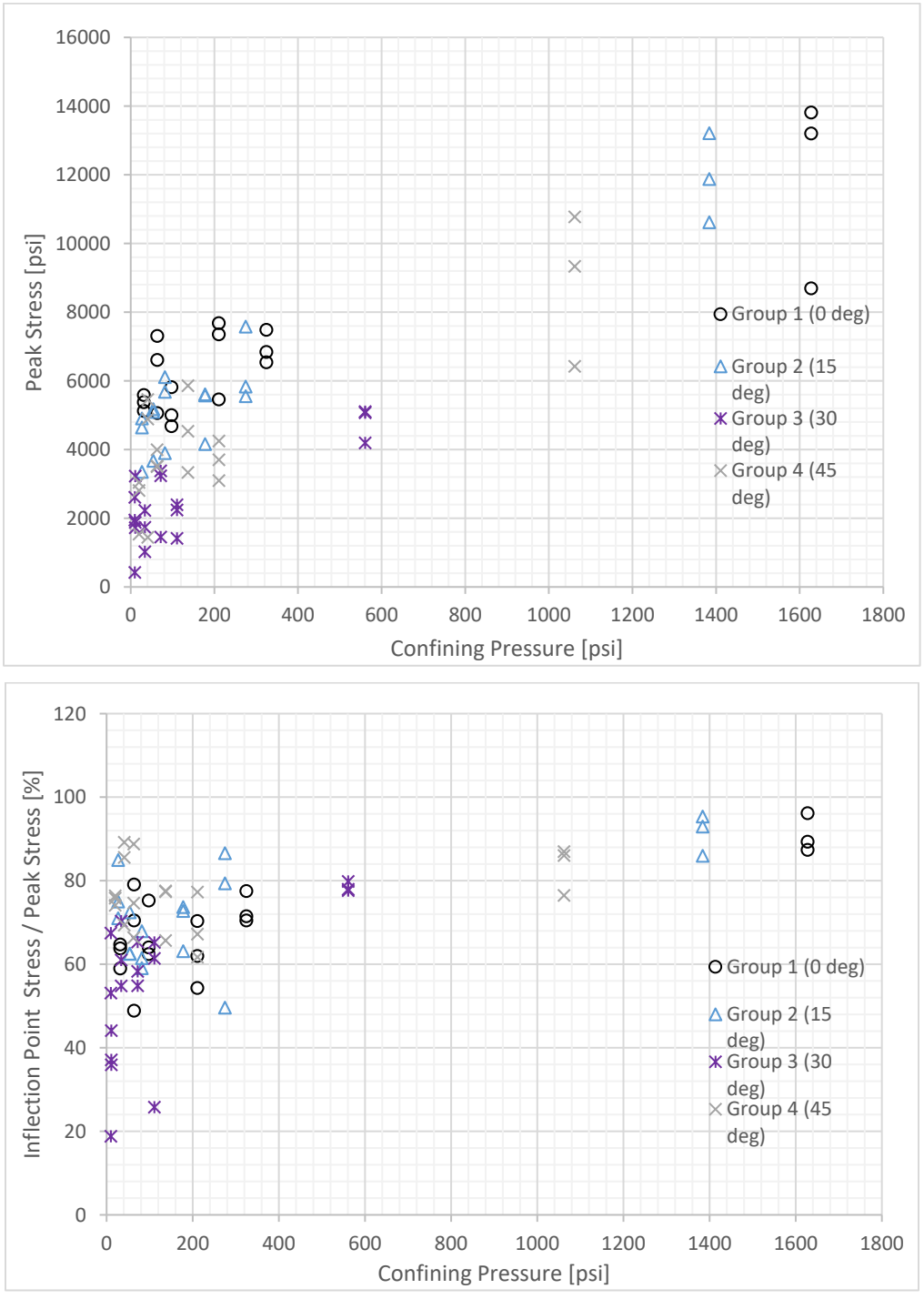

Figure 4-6: Graphs showing peak stress vs. confining pressure (top), and inflection point stress as a percentage of yield stress vs. confining pressure (bottom).

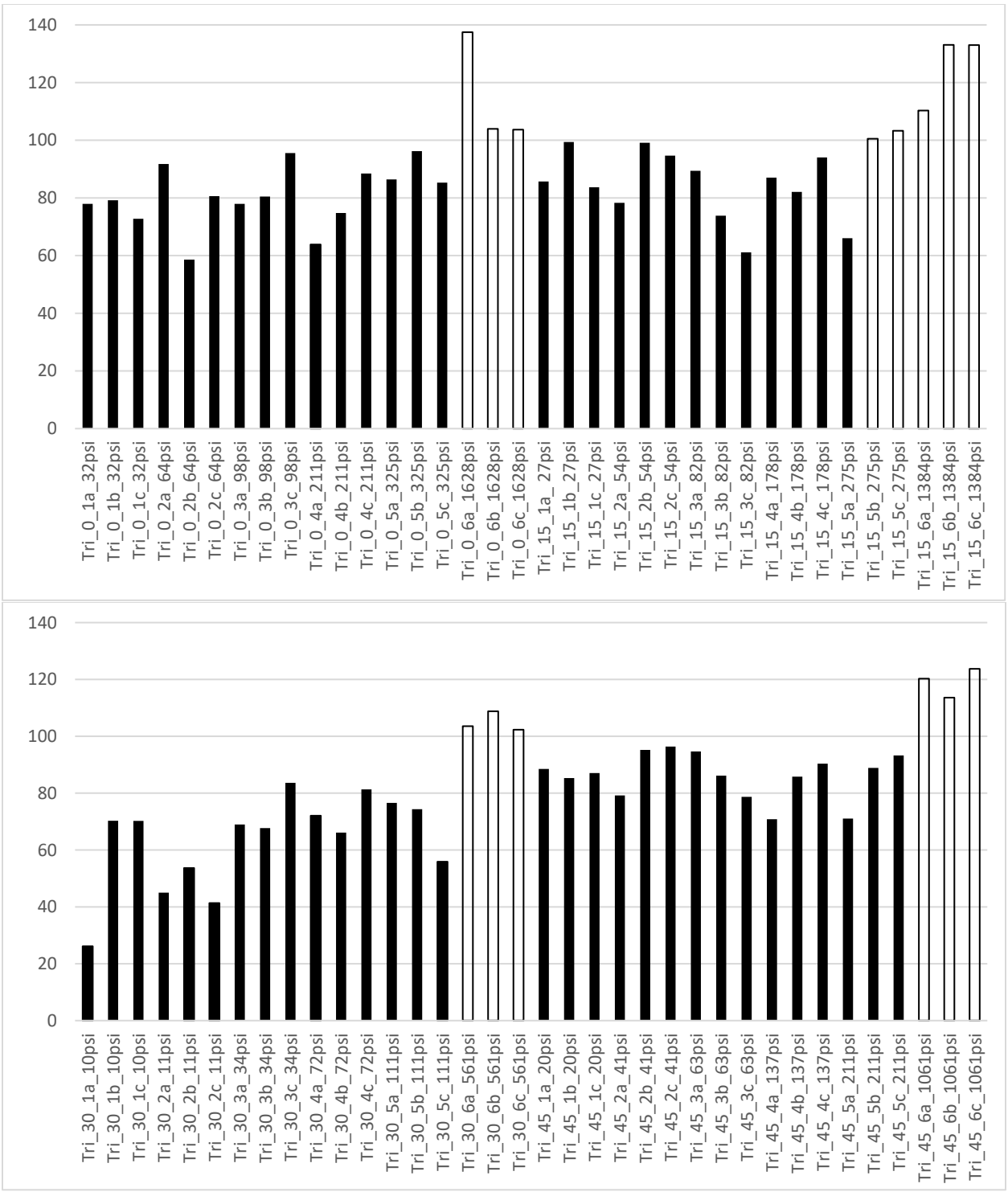

Figure 4-7: Graphs showing inflection point stress as a percentage of yield stress for the 72 specimens.

5. Multistage Triaxial Tests using the Volumetric Inflection Point

Analysis of the data from the 72 conventional triaxial tests indicated that the volumetric strain inflection point corresponds to a stress that is usually below the yield point, suggesting that the inflection point is a good choice for terminating each stage of multistage triaxial test. To verify this, three multistage triaxial tests were performed on the specimens shown in Figure 5-1. The specimens were prepared for the previous study (group 1, cleats at 0°, oriented parallel to the long axis of the core) but not tested. The confining pressures selected for use in the multistage triaxial test were 212, 326, and 1628 psi; these values are quite low for rock but near the high end of the range of confining pressures used in the previous study.

Figure 5-1: Three specimens prepared for the multistage triaxial test.

The multistage triaxial tests were carried out using a TerraTek servo-controlled hydraulic load frame, shown in Figure 5-2. The maximum force that the hydraulic piston can apply is 330,000 lb and the maximum confining pressure that can be applied is 20,000 psi.

Figure 5-2: Montana Technological University's TerraTek servo-controlled triaxial testing machine used for this project.

Samples were jacketed with a membrane to prevent penetration of confining pressure fluid. Figure 5-3 shows one specimen and its strain monitoring devices (axial LVDTs attached to the specimen endcaps, and the strain-gage-based radial strain device mounted on the specimen) before (left) and after (right) placement in the load frame.

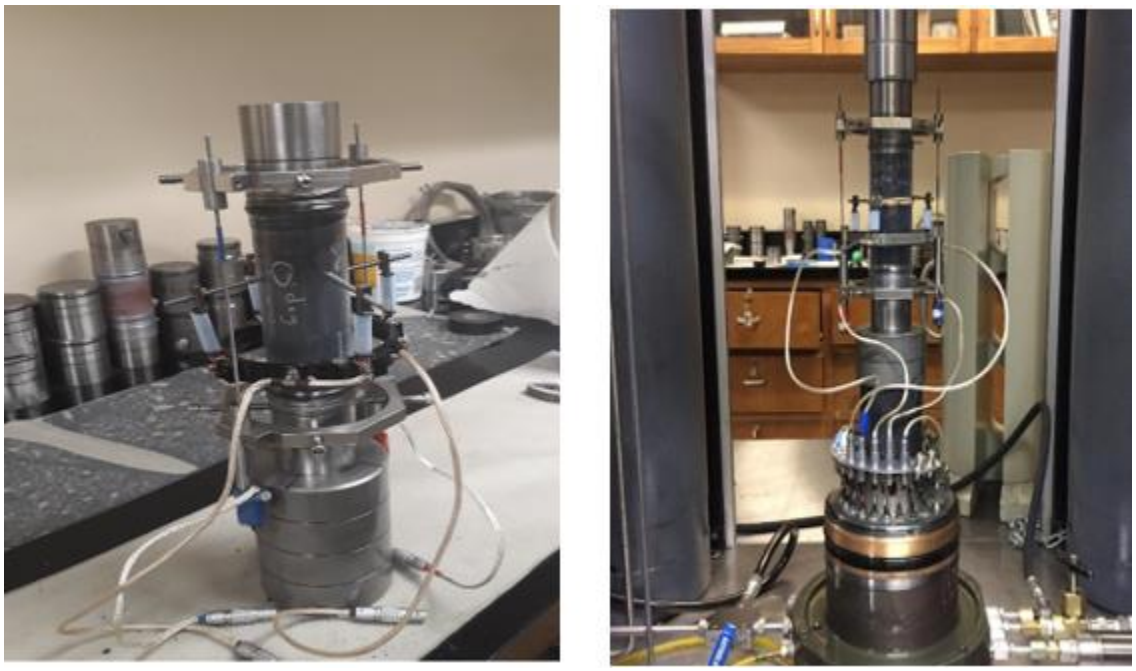

Figure 5-3: Specimen wrapped in a membrane with axial and lateral strain monitoring devices mounted, before (left) and after (right) placement into the load frame.

The procedure used for the multistage triaxial tests included the following steps:

1. The specimen, wrapped in a membrane with axial LVDTs and radial strain assembly attached, was placed into the load frame
2. Specimen dimensions and mass were entered into the test software
3. The LVDTs and radial strain device were adjusted to allow the displacement measurement channels to capture all of the deformation of the specimen
4. The specimen was raised into the testing chamber, the loading ram was positioned 0.1" above the specimen, and the initial confining pressure (212 psi) was applied
5. The axial loading ram was brought down into contact with the specimen
6. Axial stress was applied to the specimen to achieve an axial strain rate of $1x10^{-5}$ in/in/sec
7. Real time plots of axial stress and volumetric strain vs. axial strain were monitored (Figure 5-4)
8. Each stage of the test was terminated when point of volumetric inflection was reached
9. The axial stress was reduced to half of its value at the termination point
10. The confining pressure was increased to 325 psi and steps 6 to 9 were repeated
11. The final confining pressure of 1628 was applied and the specimen was loaded to failure (using the same axial strain rate) to obtain actual peak stress

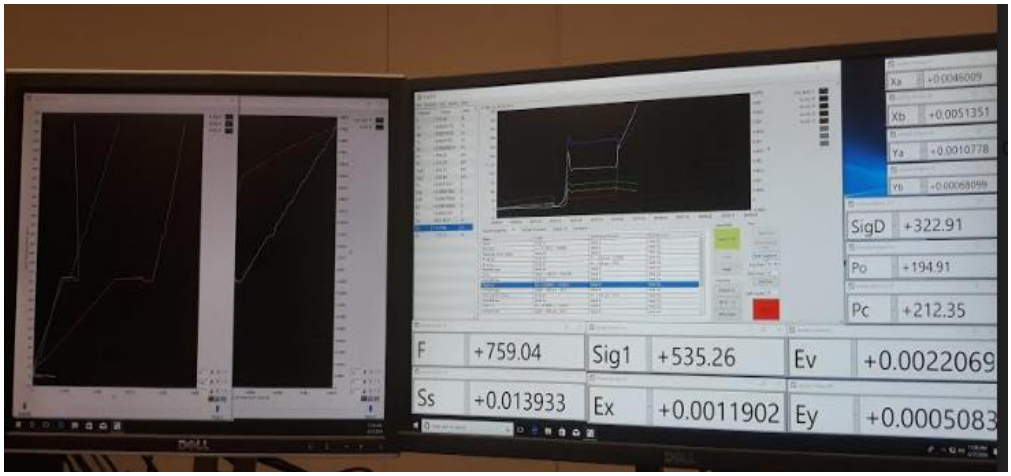

Figure 5-5: Testing software displaying real time plot of volumetric stain, stress-strain curve, confining pressure, and applied axial force.

Figure 5-5 contains photos of the specimens that were subjected to the multistage triaxial test. Shear failure is evident in all specimens as diagonal cracks. Despite the brittle nature of the coal and the low confining pressures, all three multistage tests were successful in that sudden, brittle failure and associated damage were not observed in the initial loading stages. Files containing the test data are available online at https://digitalcommons.mtech.edu/geol_engr/. Figure 5-6 shows plots of the axial stress vs. axial and volumetric strain data, similar to those that were observed during the tests; at the volumetric strain inflection point, the axial stress vs. volumetric strain curve reaches vertical, which is difficult to determine. The other real time plot that is monitored to allow identification that the inflection point has been reached is a plot of volumetric strain vs. axial strain. This curve becomes horizontal at the inflection point and is much easier to distinguish. When the inflection point has been achieved, indicating that the specimen has ceased to contract and is about to start expanding, the stage is terminated and the next stage is initiated. Test results are quantitatively summarized and discussed in Section 6.2.

Figure 5-5: Specimens after being subjected to the multistage triaxial test, displaying shear failure evident as diagonal cracks.

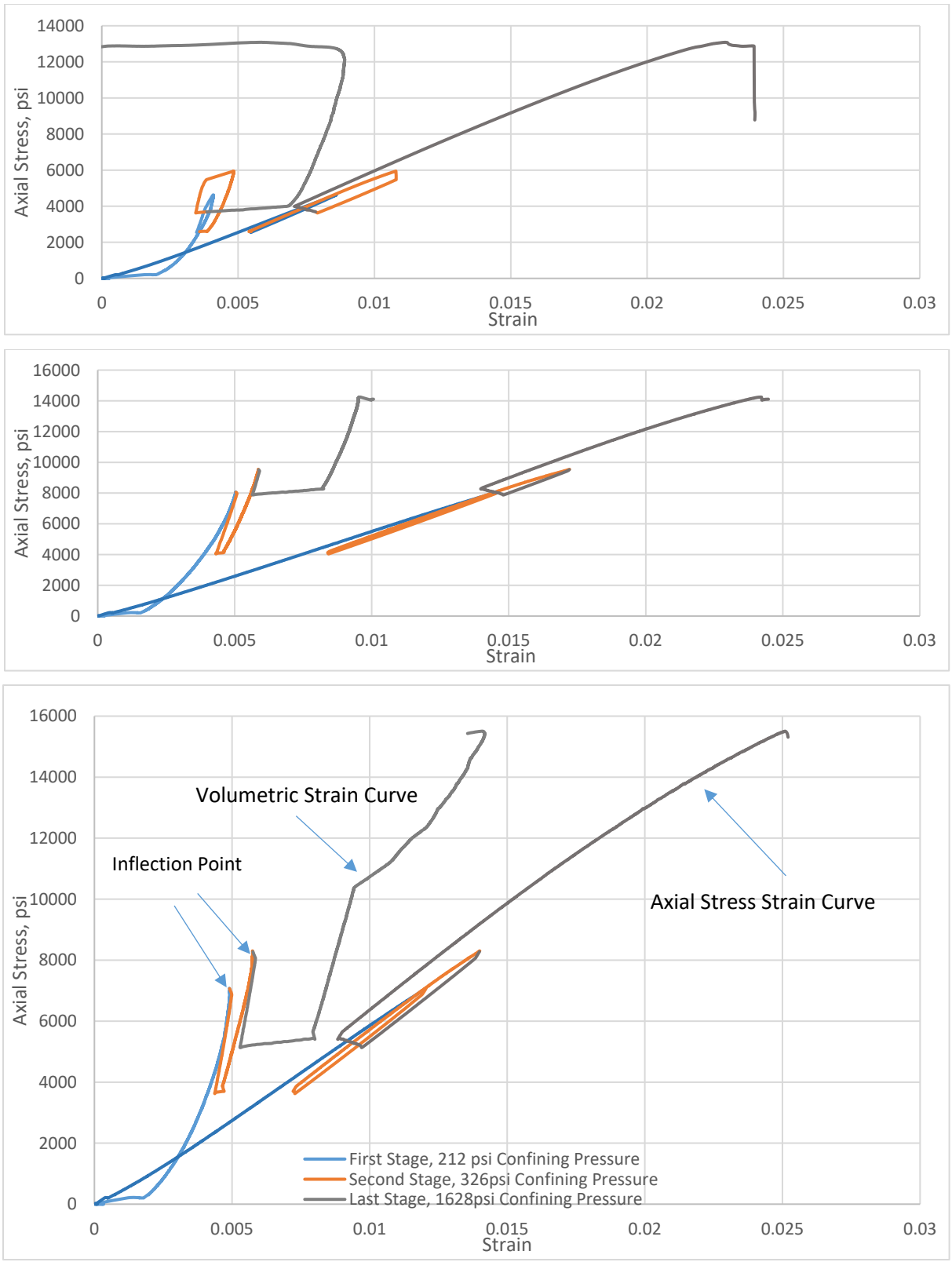

Figure 5-6: Plots of axial stress vs. axial and volumetric strain from the three multistage triaxial tests performed for this study. (Compressive stress and strain positive.)

6. Comparison of Conventional and Multistage Shear Strength Models

The final component of this project was to perform a comparison of the Mohr-Coulomb shear strength models obtained from the conventional and multistage triaxial test results. The shear strength parameters (friction angle and cohesion) were obtained by constructing a Mohr Coulomb (MC) failure envelope. The MC envelope was plotted using the peak strength and corresponding confining pressure data with the aid of Rocscience RocData software to graph the Mohr's circles and calculate best-fit tangent lines.

6.1. Mohr Coulomb Failure Envelopes from Conventional Triaxial Tests

The three specimens subjected to the multistage triaxial tests were members of "group 1" of the previous study (corresponding to cleats oriented at 0° from the long axis of the core). The results of these multistage tests were consequently compared to the conventional triaxial test results for the specimens in group 1 (0°) subjected to approximately the same confining pressures (217, 332, and 1625 psi) used in the multistage triaxial tests. Table 6-1 lists the conventional triaxial test data for the three sets of three specimens (9 out of the 18 total specimens in group 1) used for the comparison. Figure 6-1 shows the Mohr's circles associated with each of the 9 tests, and the Mohr Coulomb failure envelope best fit to all 9 circles. One outlier (peak stress 8689 psi for confining stress 1628 psi) is evident.

Table 6-1: Conventional triaxial test data for 9 specimens in Group 1 with confining pressures similar to those used in the multistage triaxial tests.

Confining Pressure (psi)	Peak Strength Values (psi)	Average Peak Strength (psi)
211 psi	5456, 7675, 7348	6826
325 psi	6536, 6839, 7481	6952
1628 psi	13197, 8689*, 13807	11898 (13502**)
	*outlier	**without outlier

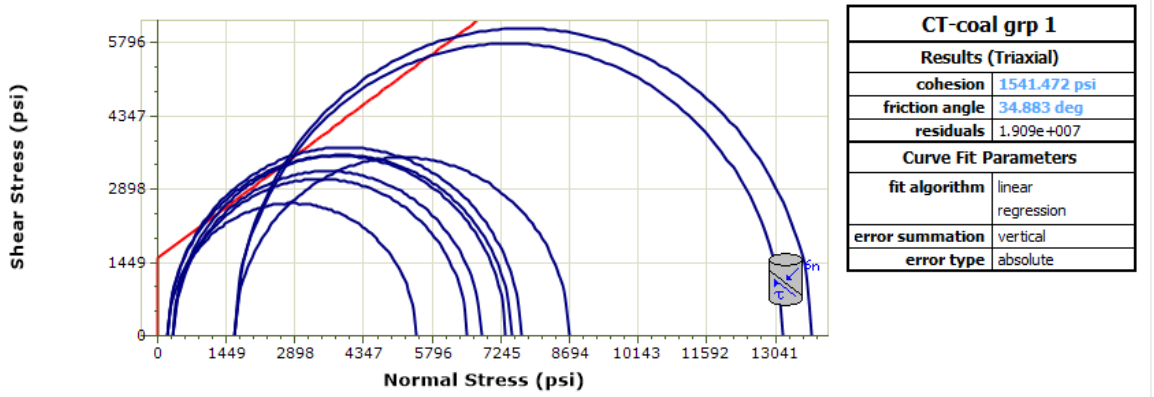

Figure 6-1: Mohr's circles of stress associated with 9 conventional triaxial tests, with Mohr-Coulomb failure envelope best fit to all 9 circles.

Figure 6-2 shows plots of Mohr's circles constructed using the average peak stress and corresponding confining stress values, with the outlier datapoint included (top) and removed (bottom). When the average peak stresses are used, the conventional triaxial tests yield friction angle and cohesion values of 35° and 1541 psi with the outlier included; note that these parameters match the friction angle and cohesion best fit to the entire 9-specimen dataset (Figure 6-1). Eliminating the outlier changes the friction angle to 41° and the cohesion to 1271 psi.

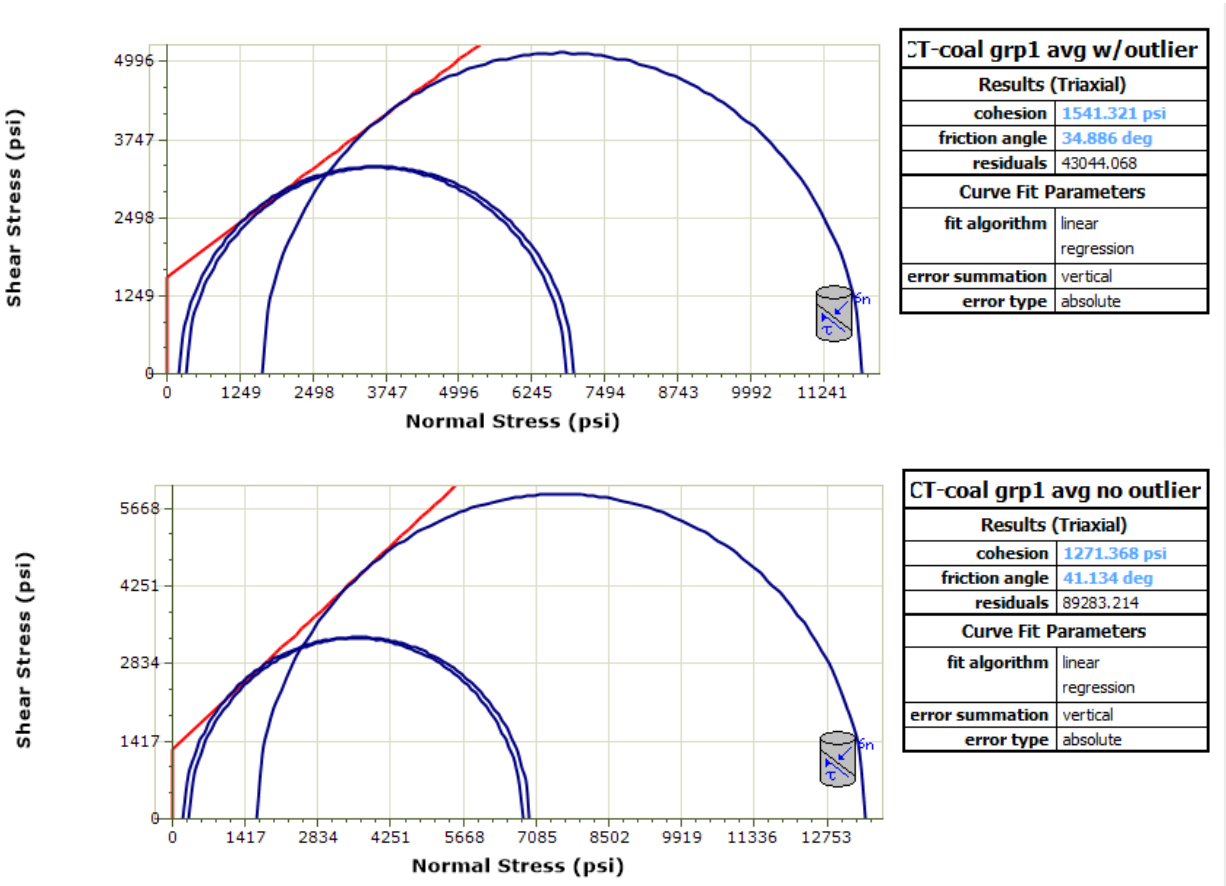

Figure 6-2: Conventional triaxial test Mohr Coulomb envelopes constructed using the average shear strength values associated with each of the three confining pressures. The top diagram corresponds to the data with the outlier included, and the bottom diagram corresponds to the data with the outlier removed.

To investigate the variability in the shear strength parameters resulting from the conventional triaxial tests, the 27 different combinations of peak stress data (formed by selecting one peak stress from the 3 members of the lowest confining pressure set, one peak stress from the middle confining pressure set, and one peak stress from the highest confining pressure set) were used to determine 27 different strength envelopes. Appendix E shows the shear strength parameters from all 27 possible peak stress combinations, with the 9 sets associated with the outlier data point highlighted in yellow. With the values associated with the outlier eliminated, friction angle values ranged from 37° to 44° and cohesion values ranged from 924 to 1601 psi.

6.2. Mohr Coulomb Failure Envelopes from Multistage Triaxial Tests

To complete this study, three multistage triaxial tests were performed using confining pressure values of 217, 332, and 1625 psi. The first two stages (with confining pressures of 212 and 326 psi) were terminated at the volumetric strain inflection point. In the third stage, the specimen was loaded past the inflection point to failure, to determine its peak strength. Figure 6-3 shows the MC plots for the three specimens constructed using the inflection point stresses.

It is understood, however, that the inflection point stress is a conservative estimate of the peak strength of the specimen. In previous studies, the inflection point failure envelope has been adjusted by shifting it upward to a position tangent to the peak stress Mohr circle (e.g. Pagoulatos, 2004). For this study, the inflection point stress values were "adjusted" using the ratio of the peak stress to inflection point stress observed in the third stage. For the three multistage tests performed for this study, the calculated ratios of peak stress to inflection point stress are 13,085/12,150=1.0769, 14,107/14,050=1.0041, and 15,506/15,400=1.0069. Figure 6-4 shows the MC plots for the three specimens constructed using the peak stress measured in the third stage combined with the "adjusted" stresses from the first and second stages.

Table 6-2 contains a summary of the results of all three multistage triaxial tests, interpreted with inflection point and peak stress values, and their corresponding shear strength parameters. These results suggest that for these specimens, adjusting from inflection point to peak stress makes a very minimal difference of 0° to 2° in the friction angle and up to 32 psi (3.7%) in the cohesion. The friction angle and cohesion values associated with the average inflection point and peak stress values are also tabulated, and shown in Figure 6-5. For comparison, the bottom line of the table displays the average values for the conventional triaxial tests (with outlier removed). The results of the multistage and conventional triaxial tests are in very good agreement.

Table 6-2: Shear strength data and Mohr-Coulomb parameters from multistage and conventional triaxial tests

		Confining Pressure Values			MC Parameters	
Test Type		**217 psi**	**332 psi**	**1625 psi**	**Cohesion [psi]**	**Friction Angle**
		Inflection Point Stress Values				
Multistage Triaxial Test	1	4628	5946	12150	866	42°
	2	8070	9544	14050	1956	36°
	3	7077	8303	15400	1287	44°
	Average	6592	7931	13867	1339	41°
		Peak Stress Values (*adjusted)				
Multistage Triaxial Test (adjustment ratio)	1 (1.0769)	4984*	6403*	13085	898	44°
	2 (1.0041)	8103*	9583*	14107	1961	36°
	3 (1.0069)	7126*	8361*	15506	1291	45°
	Average	6738	8116	14233	1347	42°
Average of 3 Conventional Triaxial Tests (** Average of 2 Tests with Outlier Removed)		6826	6952	13502**	1271	41°

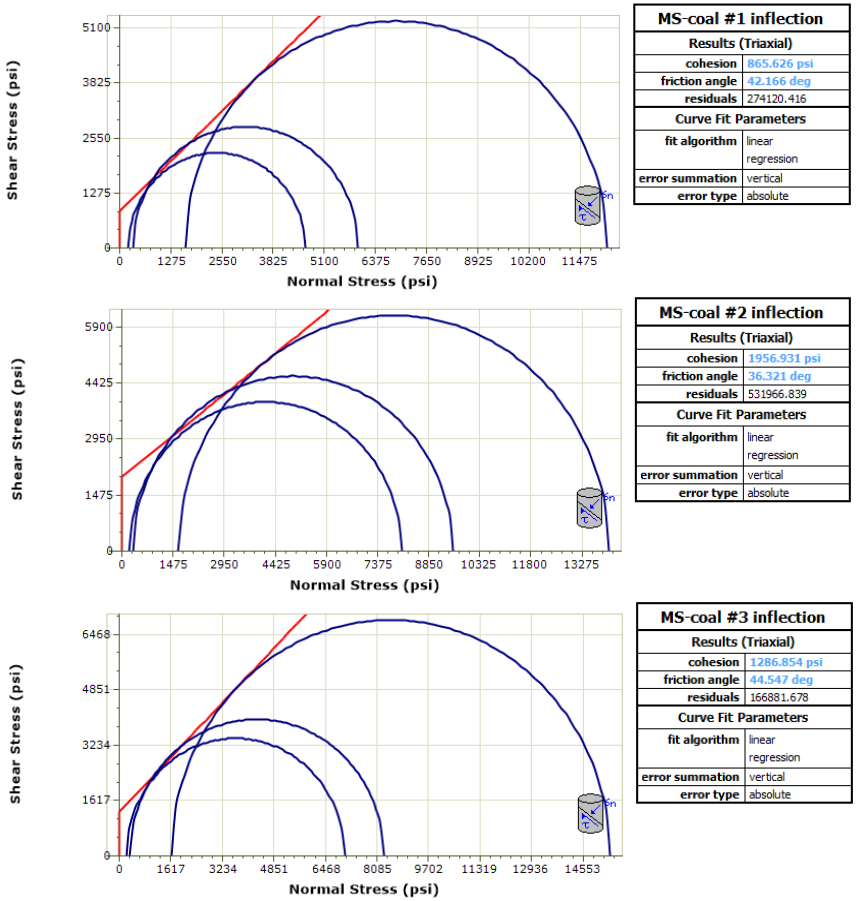

Figure 6-3: Mohr's circles of stress plotted using inflection point stress values, and corresponding MC failure envelopes, for the three multistage triaxial tests.

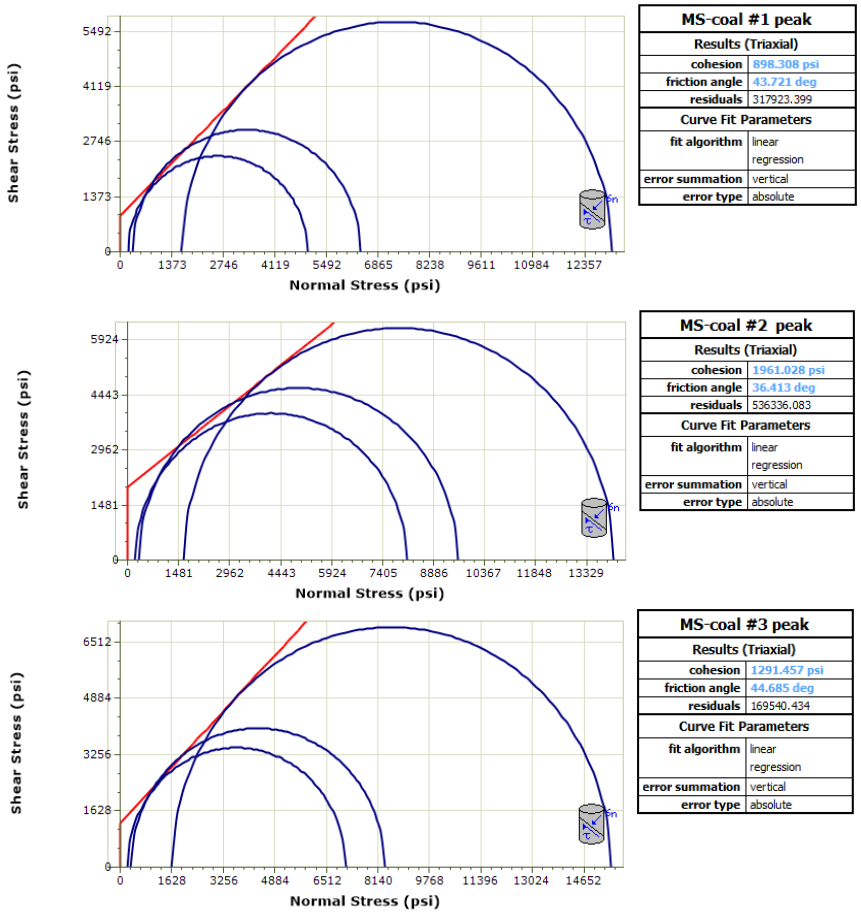

Figure 6-4: Mohr's circles of stress plotted using peak stress values, and corresponding MC failure envelopes, for the three multistage triaxial tests. Note that the peak stress values for the two lower confining pressure tests have been calculated by applying an adjustment factor to the inflection point stress values.

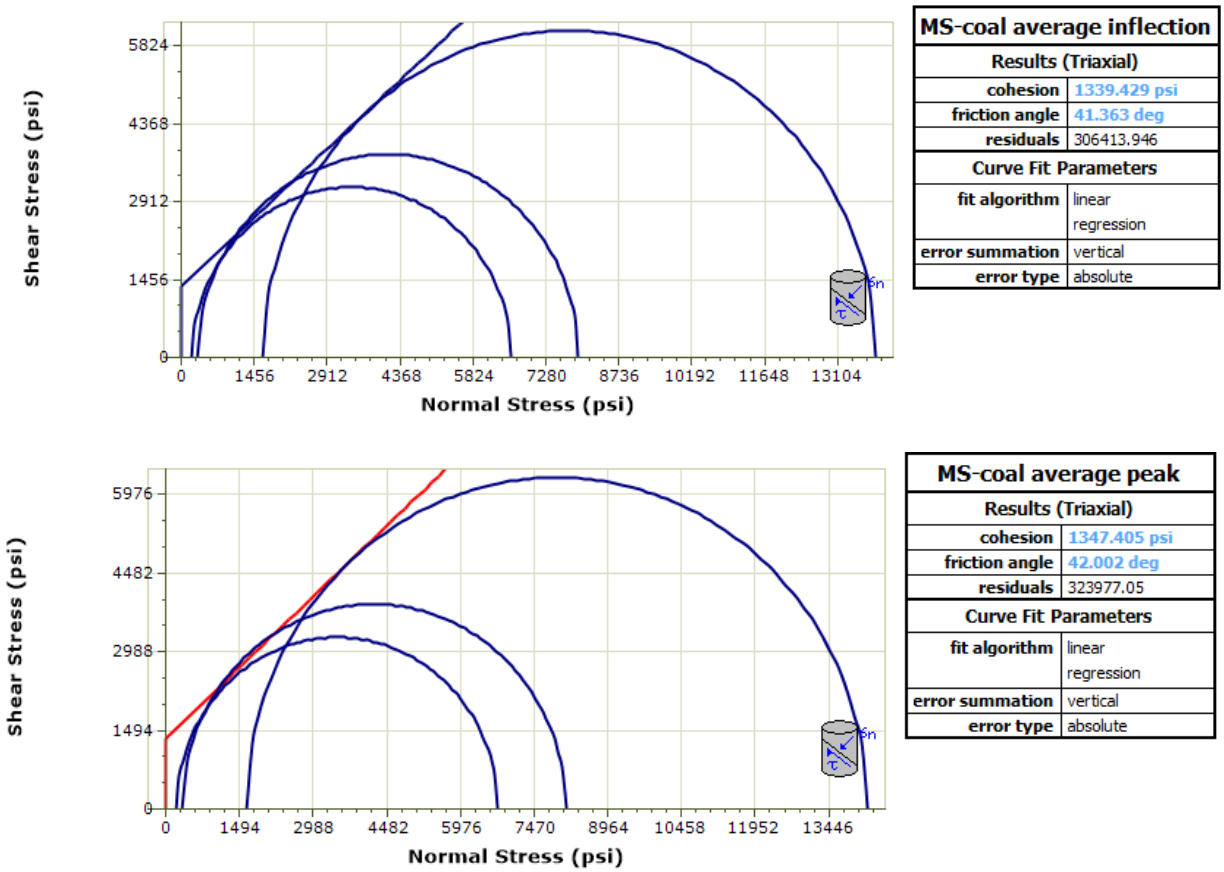

Figure 6-5: Mohr's circles of stress plotted using average inflection point (top) and average peak (bottom) stress values, and corresponding MC failure envelopes, for the three multistage triaxial tests. Note that in the bottom graph, the peak stress values for the two lower confining pressure tests have been calculated by applying an adjustment factor to the inflection point stress values.

7. Conclusions and Recommendations

The multistage triaxial test has been established as a viable alternative to the conventional triaxial test for establishing the shear strength parameters of rock specimens, but identifying when to terminate each stage of the test remains a challenge. It is generally accepted that using the most easily recognizable termination point (peak stress) induces damage in the specimen and leads to underestimation of the strength parameters. Two observable points in the volumetric strain data have been proposed as alternatives: volumetric dilation (the point at which the specimen volume becomes larger than its original volume) and volumetric inflection (the point at which the specimen stops compressing and starts expanding due to formation of microcracks). Data from 72 conventional triaxial tests performed on specimens of Utah coal for a previous study indicate that in the vast majority of cases (65/72), volumetric dilation is either not achieved prior to failure, or occurs after yield. In contrast, the volumetric inflection point is reached at least 5% below peak stress in all tests and below yield stress in 80% of the tests. This suggests that inflection point is the better choice for the loading stage termination point for this material.

The results of three multistage triaxial tests performed on specimens of the Utah coal using the volumetric inflection point as the loading stage termination yielded shear strength parameters that are in very good agreement with those obtained from the conventional triaxial tests. The friction angles determined from the average shear strength at each loading stage were within 1°, and cohesion values were within 6%.

References

ASTM D4543-08. (2008.) *Standard Practices for Preparing Rock Core as Cylindrical Test Specimens and Verifying Conformance to Dimensional and Shape Tolerances*, ASTM International, West Conshohocken, PA.

ASTM D7012-14. (2014). *Standard Test Method for Compressive Strength and Elastic Moduli of intact Rock Core Specimens under Varying Stress of Stress and Temperatures.* ASTM International, West Conshohocken, PA.

Crawford, A., & Wylie, D. (1987). A modified multiple failure state triaxial testing method. *28th US Symposium on Rock Mechanics*, (pp. 133-140). Tuscon.

Fairhurst, C.E., & Hudson, J.A. (1999). Draft ISRM Suggested Method for the Complete Stress-Strain Curve for Intact Rock in Uniaxial Compression, ISRM Suggested Methods, Second Series. International Journal of Rock Mechanics and Mining Sciences 36 (1999):279-289.

Gonzalez de Vallejo, L. I., & Ferrer. M. (2011). *Geological Engineering.* CRC Press/Balkema, Boca Raton, FL.

Goodman, E. R. (1989). *Introduction to Rock Mechanics Second Edition.* John Wiley & Son, New York, NY.

Kim, B.-H., Larson, M., & Berry, S. (2018). Laboratory Investigation of Confinement-Dependent mechanical Behaviour of a Utah Coal. *37th International Conference on Ground Control in Mining* (pp. 248-254). Society for Mining, Metallurgy & Exploration, Morgantown, WV.

Kim, M. M., & Ko, H.-Y. (1979). Multistage Triaxial Testing of Rocks. *Geotechnical Testing Journal*, 2:98-105.

Kovari, K., & Tisa, A. (1975). Multiple Failure State and Strain Controlled Triaxial Tests. *Rock Mechanics*, 7:17-33.

Kovari, K., Tisa, A., Einstein, H., & Franklin, J. (1983). Suggested Methods for Determining the Strength of Rock Materials in Triaxial Compression. *International Journal of Rock Mechanics and Mining Sciences*, 20(6):285-290.

Pagoulatos, A. (2004). *Evaluation of multistage triaxial testing on berea sandstone,* Master of Science Thesis. The University of Oklahoma, Norman, OK.

US Army Corps of Engineers. (1993). *Rock Testing Handbook (Test Standards 1993),* US Army Engineer Waterways Experiment Station, Vicksburg, MS.

Youn, H., & Tonon, F. (2010). Multi-stage triaxial test on brittle rock. *International Journal of Rock Mechanics & Mining Sciences*, 4(47):678-684.

Appendix A: 72 Specimens and their Confining Pressure Values

Table A-1: Confining pressures applied during the 72 conventional triaxial tests, showing three samples subjected to the same confining pressure

Group	Samples	Confining Pressures (psi)	Group	Samples	Confining Pressures (psi)
1 (0°)	Tri_0_1a_32psi	32	2 (15°)	Tri_15_1a_27psi	27
	Tri_0_1b_32psi	32		Tri_15_1b_27psi	27
	Tri_0_1c_32psi	32		Tri_15_1c_27psi	27
	Tri_0_2a_64psi	64		Tri_15_2a_54psi	54
	Tri_0_2b_64psi	64		Tri_15_2b_54psi	54
	Tri_0_2c_64psi	64		Tri_15_2c_54psi	54
	Tri_0_3a_98psi	98		Tri_15_3a_82psi	82
	Tri_0_3b_98psi	98		Tri_15_3b_82psi	82
	Tri_0_3c_98psi	98		Tri_15_3c_82psi	82
	Tri_0_4a_211psi	211		Tri_15_4a_178psi	178
	Tri_0_4b_211psi	211		Tri_15_4b_178psi	178
	Tri_0_4c_211psi	211		Tri_15_4c_178psi	178
	Tri_0_5a_325psi	325		Tri_15_5a_275psi	275
	Tri_0_5b_325psi	325		Tri_15_5b_275psi	275
	Tri_0_5_325psi	325		Tri_15_5c_275psi	275
	Tri_0_6a_1628psi	1628		Tri_15_6a_275psi	1384
	Tri_0_6b_1628psi	1628		Tri_15_6b_275psi	1384
	Tri_0_6c_1628psi	1628		Tri_15_6c_275psi	1384
3 (30°)	Tri_30_1a_10psi	10	4 (45°)	Tri_45_1a_20psi	20
	Tri_30_1b_10psi	10		Tri_45_1b_20psi	20
	Tri_30_1c_10psi	10		Tri_45_1c_20psi	20
	Tri_30_2a_11psi	11		Tri_45_2a_41psi	41
	Tri_30_2b_11psi	11		Tri_45_2b_41psi	41
	Tri_30_3a_11psi	11		Tri_45_2c_41psi	41
	Tri_30_3a_34psi	34		Tri_45_3a_63psi	63
	Tri_30_3b_34psi	34		Tri_45_3b_63psi	63
	Tri_30_3c_34psi	34		Tri_45c_63psi	63
	Tri_30_4a_72psi	72		Tri_45_4a_137psi	137
	Tri_30_4b_72psi	72		Tri_45_4b_137psi	137
	Tri_30_4c_72psi	72		Tri_45_4c_137psi	137
	Tri_30_5a_111psi	111		Tri_45_5a_211psi	211
	Tri_30_5b_111psi	111		Tri_45_5b_211psi	211
	Tri_30_5c_111psi	111		Tri_45_5c_211psi	211
	Tri_30_6a_561psi	561		Tri_45_6a_1psi	1062
	Tri_30_6b_561psi	561		Tri_45_6b_1psi	1062
	Tri_30_6c_561psi	561		Tri_45_6c_1psi	1062

Appendix B: Stress-Strain Plots for All 72 Conventional TriaxialTests


SPECIMEN TRI_0_1A_32PSI
Volumetric Dilation
Axial Stress = 4908 psi
Yield Point Axial Stress =
4506 psi
Peak Axial Stress = 5122 psi
Inflection Point Stress = 3265 psi
AXIAL STRESS, PSI
AXIAL STRAIN
Axial Stress vs Axial Strain
Axial Stress vs Lateral Strain
Axial Stress vs Volumetric Strain

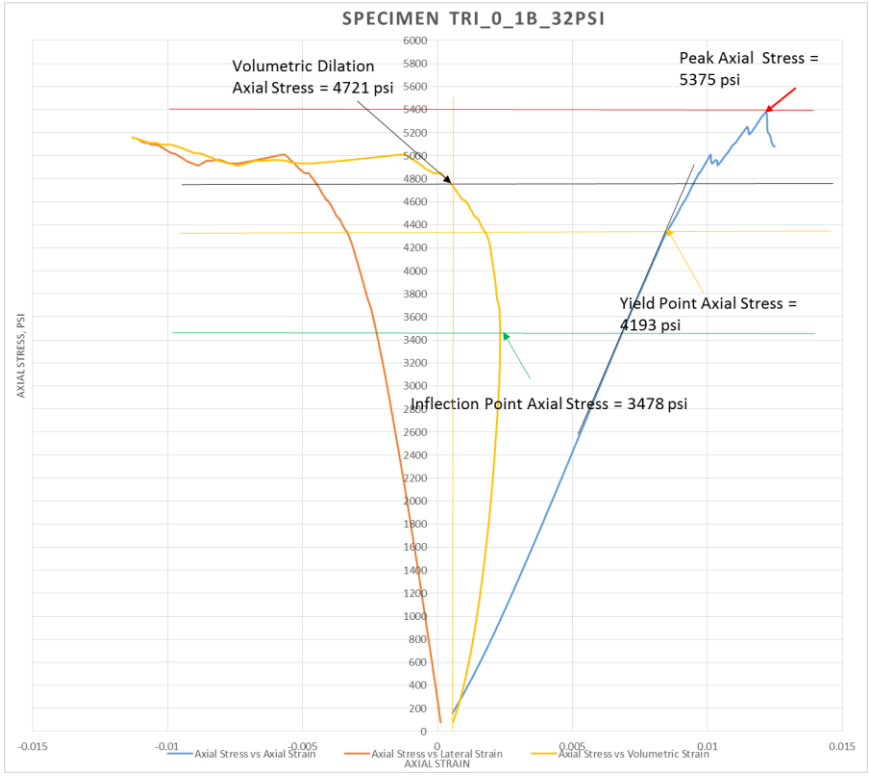
SPECIMEN TRI_0_1B_32PSI
Volumetric Dilation
Axial Stress = 4721 psi
Peak Axial Stress =
5375 psi
Yield Point Axial Stress =
4193 psi
Inflection Point Axial Stress = 3478 psi
AXIAL STRESS, PSI
AXIAL STRAIN
Axial Stress vs Axial Strain
Axial Stress vs Lateral Strain
Axial Stress vs Volumetric Strain

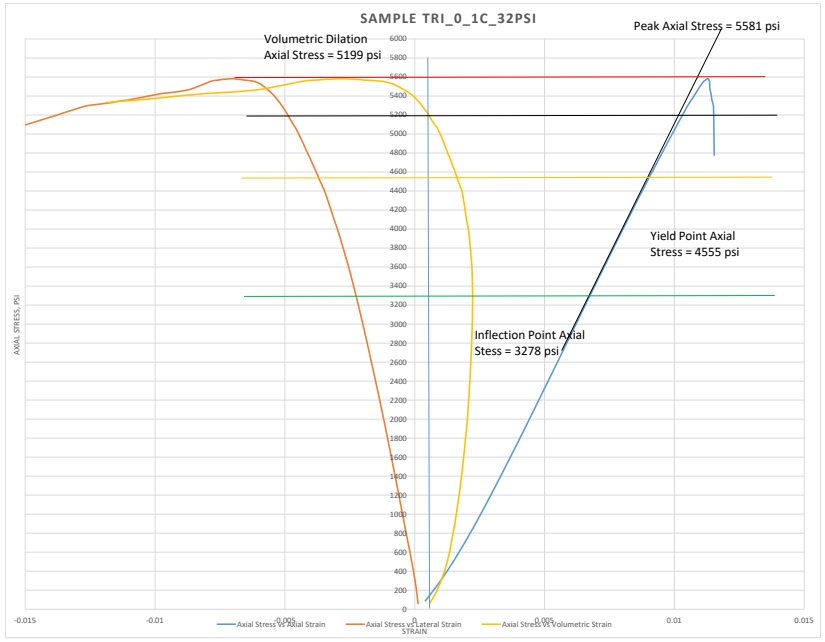
SAMPLE TRI_0_1C_32PSI
Volumetric Dilation
Axial Stress = 5199 psi
Peak Axial Stress = 5581 psi
Yield Point Axial
Stress = 4555 psi
Inflection Point Axial
Stess = 3278 psi
AXIAL STRESS, PSI
STRAIN
Axial Stress vs Axial Strain
Axial Stress vs Lateral Strain
Axial Stress vs Volumetric Strain

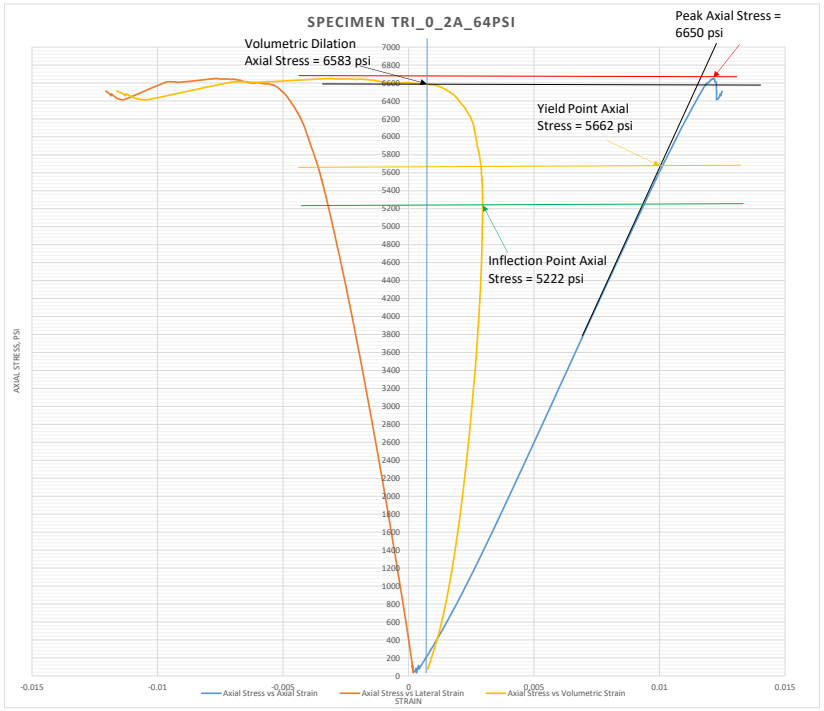
SPECIMEN TRI_0_2A_64PSI
Volumetric Dilation
Axial Stress = 6583 psi
Peak Axial Stress =
6650 psi
Yield Point Axial
Stress = 5662 psi
Inflection Point Axial
Stress = 5222 psi
AXIAL STRESS, PSI
STRAIN
Axial Stress vs Axial Strain
Axial Stress vs Lateral Strain
Axial Stress vs Volumetric Strain

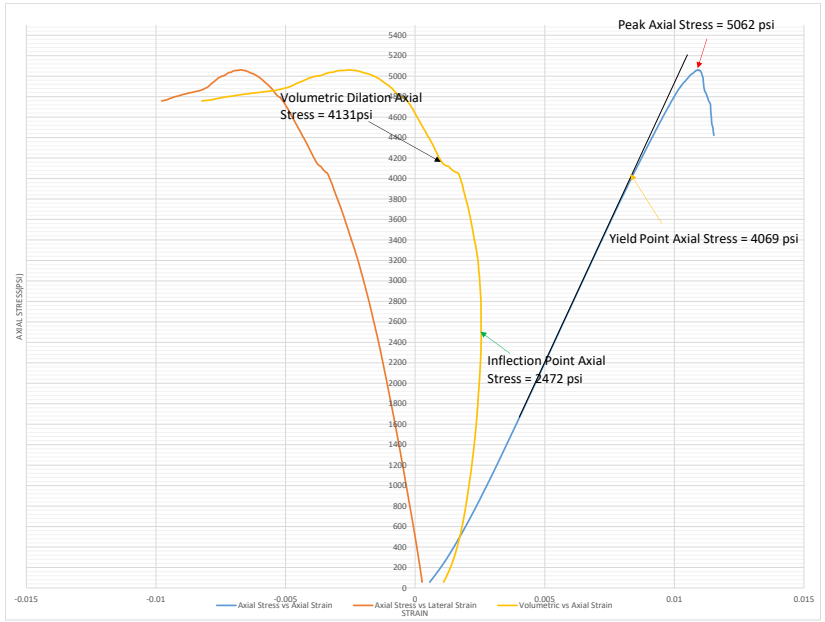
Peak Axial Stress = 5062 psi
Volumetric Dilation Axial Stress = 4131psi
Yield Point Axial Stress = 4069 psi
Inflection Point Axial Stress = 2472 psi
AXIAL STRESS(PSI)
STRAIN
Axial Stress vs Axial Strain
Axial Stress vs Lateral Strain
Volumetric vs Axial Strain

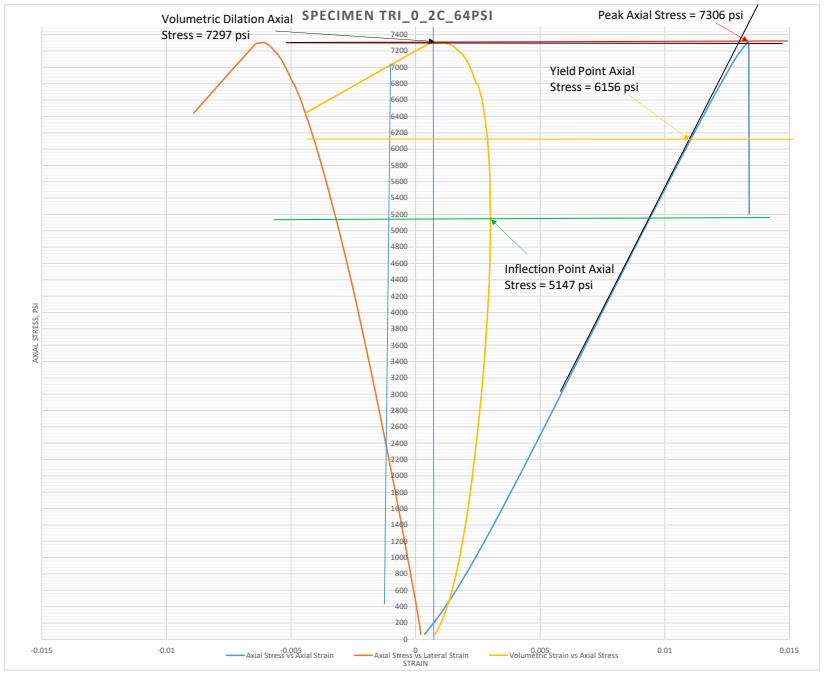
SPECIMEN TRI_0_2C_64PSI
Volumetric Dilation Axial Stress = 7297 psi
Peak Axial Stress = 7306 psi
Yield Point Axial Stress = 6156 psi
Inflection Point Axial Stress = 5147 psi
AXIAL STRESS, PSI
STRAIN
Axial Stress vs Axial Strain
Axial Stress vs Lateral Strain
Volumetric Strain vs Axial Stress

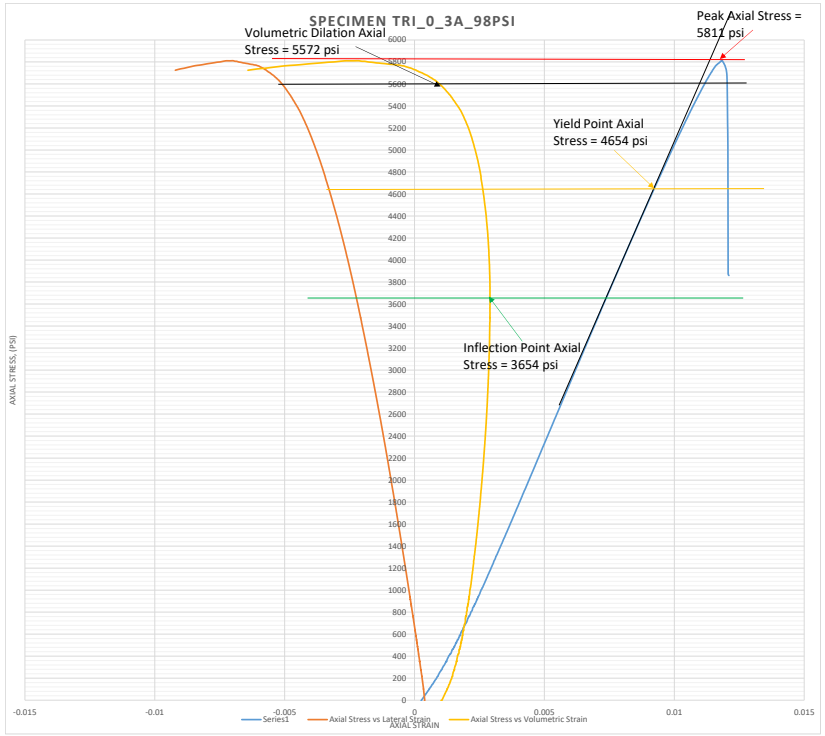
SPECIMEN TRI_0_3A_98PSI
Peak Axial Stress = 5811 psi
Volumetric Dilation Axial Stress = 5572 psi
Yield Point Axial Stress = 4654 psi
Inflection Point Axial Stress = 3654 psi
AXIAL STRESS, (PSI)
AXIAL STRAIN
Series1
Axial Stress vs Lateral Strain
Axial Stress vs Volumetric Strain

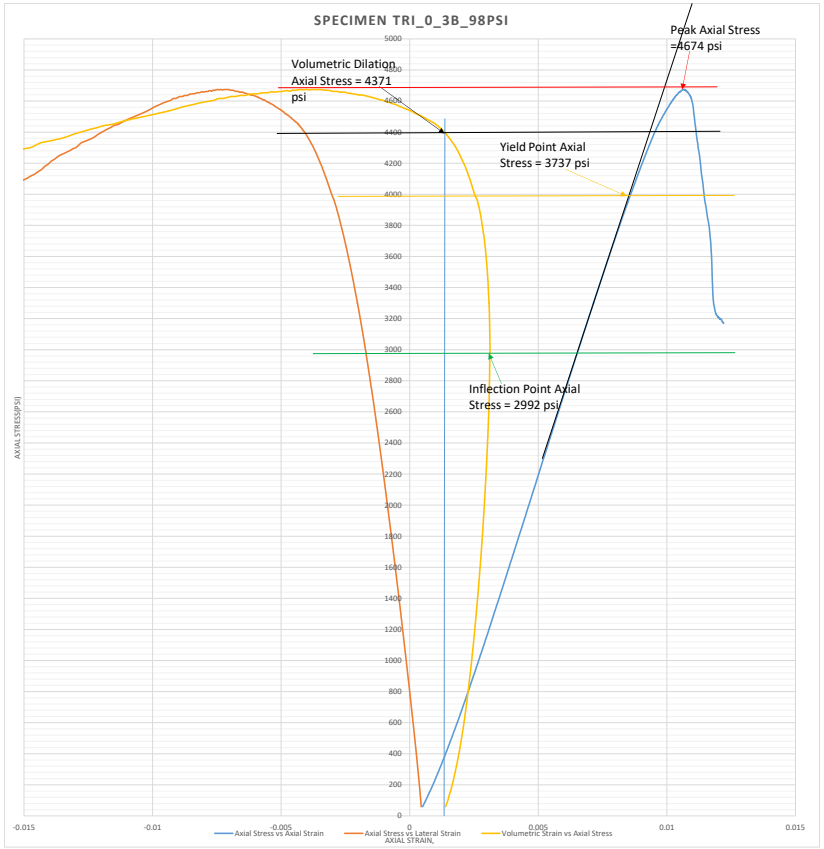
SPECIMEN TRI_0_3B_98PSI
Peak Axial Stress =4674 psi
Volumetric Dilation Axial Stress = 4371 psi
Yield Point Axial Stress = 3737 psi
Inflection Point Axial Stress = 2992 psi
AXIAL STRESS(PSI)
AXIAL STRAIN,
Axial Stress vs Axial Strain
Axial Stress vs Lateral Strain
Volumetric Strain vs Axial Stress

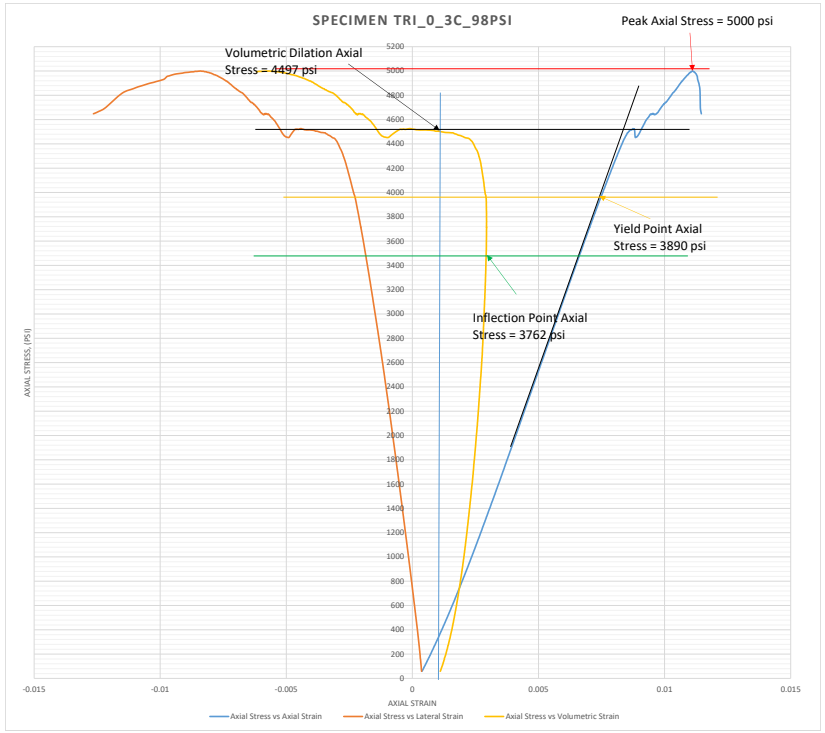
SPECIMEN TRI_0_3C_98PSI
Peak Axial Stress = 5000 psi
Volumetric Dilation Axial Stress = 4497 psi
Yield Point Axial Stress = 3890 psi
Inflection Point Axial Stress = 3762 psi
AXIAL STRESS, (PSI)
AXIAL STRAIN
Axial Stress vs Axial Strain
Axial Stress vs Lateral Strain
Axial Stress vs Volumetric Strain

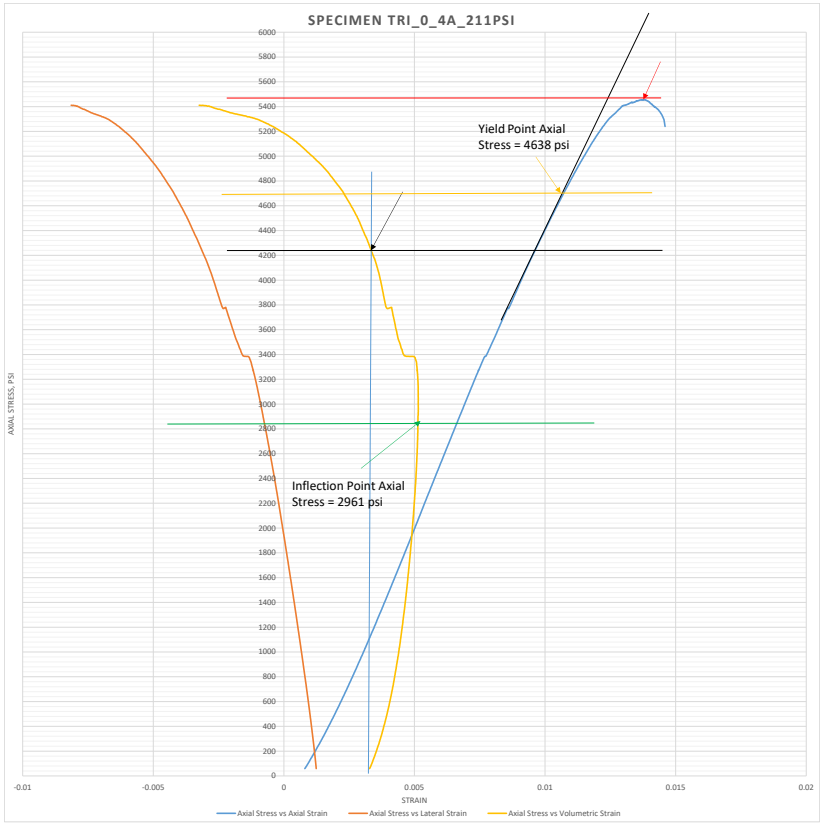
SPECIMEN TRI_0_4A_211PSI
Yield Point Axial Stress = 4638 psi
Inflection Point Axial Stress = 2961 psi
AXIAL STRESS, PSI
STRAIN
Axial Stress vs Axial Strain
Axial Stress vs Lateral Strain
Axial Stress vs Volumetric Strain

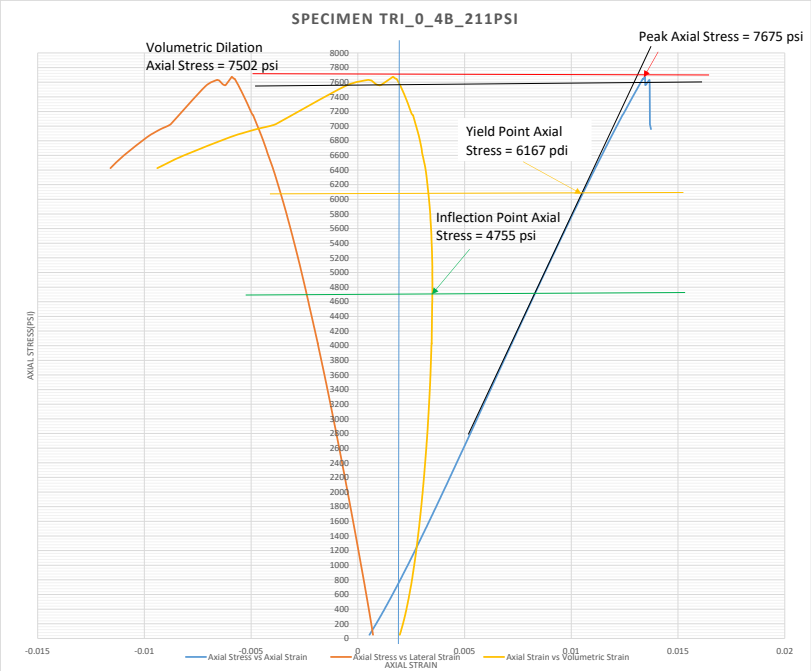
SPECIMEN TRI_0_4B_211PSI
Volumetric Dilation
Axial Stress = 7502 psi
Peak Axial Stress = 7675 psi
Yield Point Axial
Stress = 6167 pdi
Inflection Point Axial
Stress = 4755 psi
AXIAL STRESS(PSI)
AXIAL STRAIN
Axial Stress vs Axial Strain
Axial Stress vs Lateral Strain
Axial Strain vs Volumetric Strain

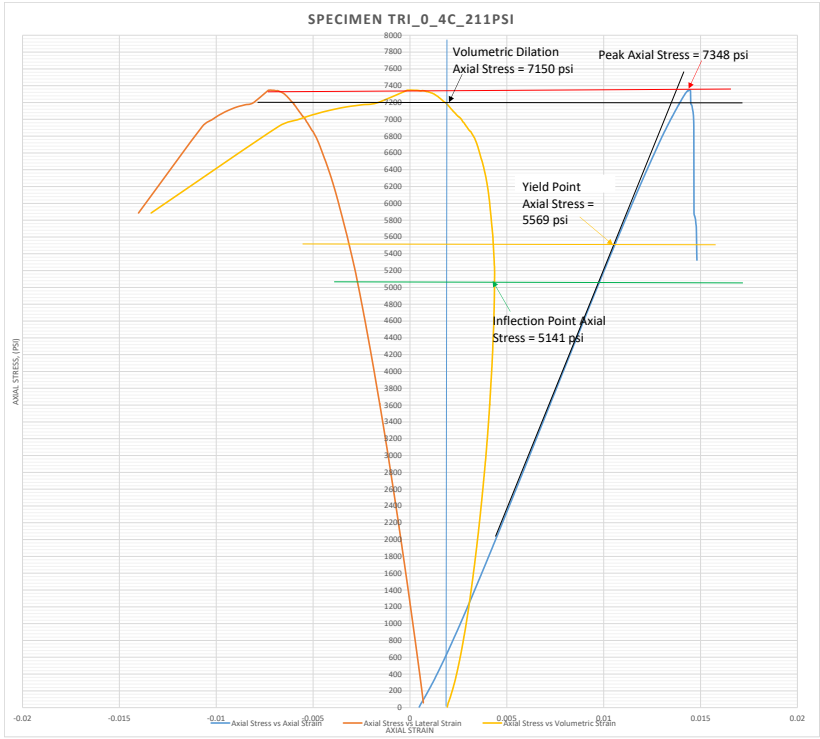
SPECIMEN TRI_0_4C_211PSI
Volumetric Dilation
Axial Stress = 7150 psi
Peak Axial Stress = 7348 psi
Yield Point
Axial Stress =
5569 psi
Inflection Point Axial
Stress = 5141 psi
AXIAL STRESS, (PSI)
AXIAL STRAIN
Axial Stress vs Axial Strain
Axial Stress vs Lateral Strain
Axial Stress vs Volumetric Strain

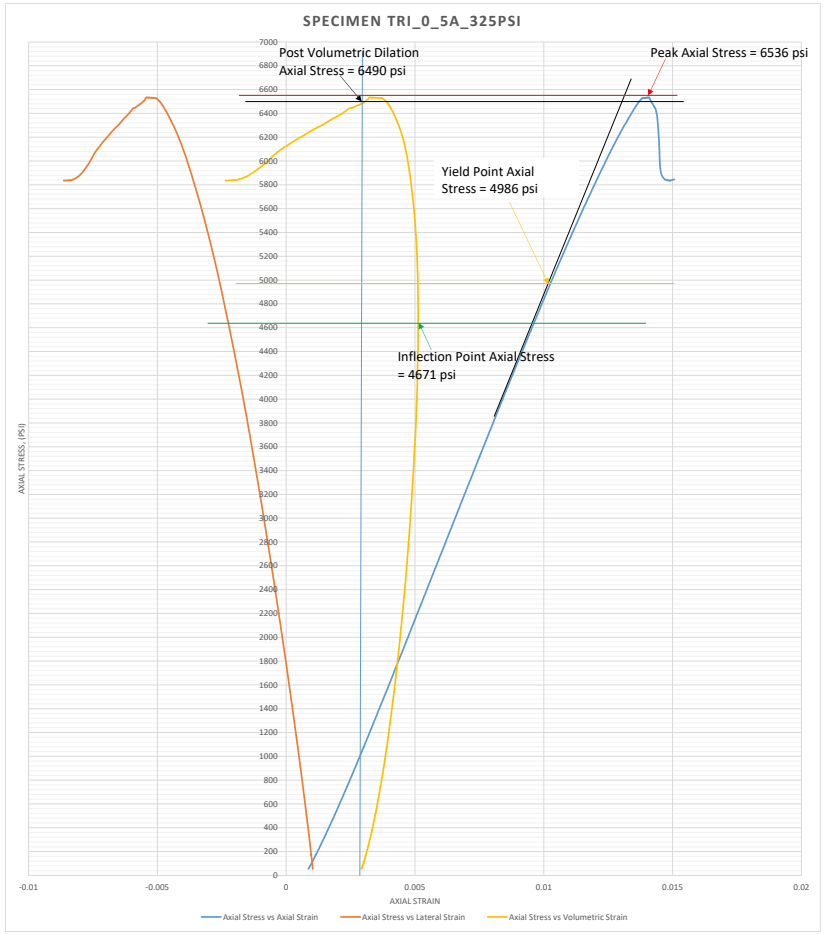
SPECIMEN TRI_0_5A_325PSI
Post Volumetric Dilation
Axial Stress = 6490 psi
Peak Axial Stress = 6536 psi
Yield Point Axial
Stress = 4986 psi
Inflection Point Axial Stress
= 4671 psi
AXIAL STRESS, (PSI)
AXIAL STRAIN
Axial Stress vs Axial Strain
Axial Stress vs Lateral Strain
Axial Stress vs Volumetric Strain

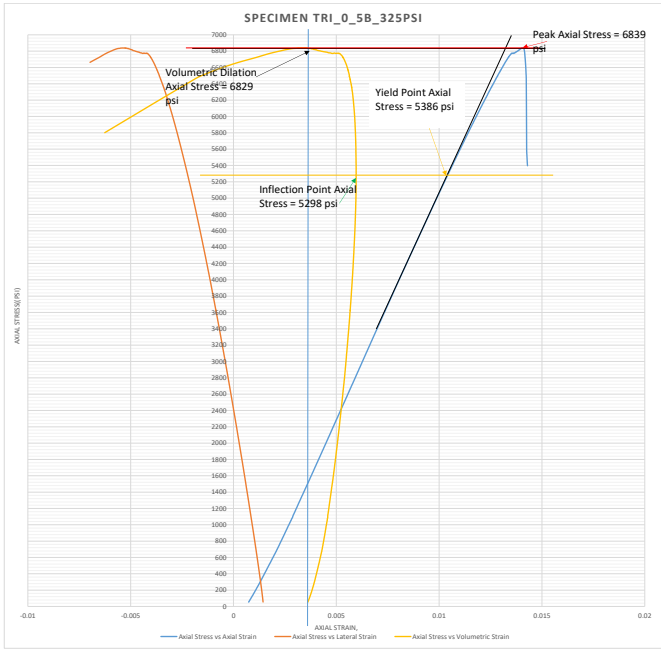
SPECIMEN TRI_0_5B_325PSI
Peak Axial Stress = 6839
psi
Volumetric Dilation
Axial Stress = 6829
psi
Yield Point Axial
Stress = 5386 psi
Inflection Point Axial
Stress = 5298 psi
AXIAL STRESS(PSI)
AXIAL STRAIN,
Axial Stress vs Axial Strain
Axial Stress vs Lateral Strain
Axial Stress vs Volumetric Strain

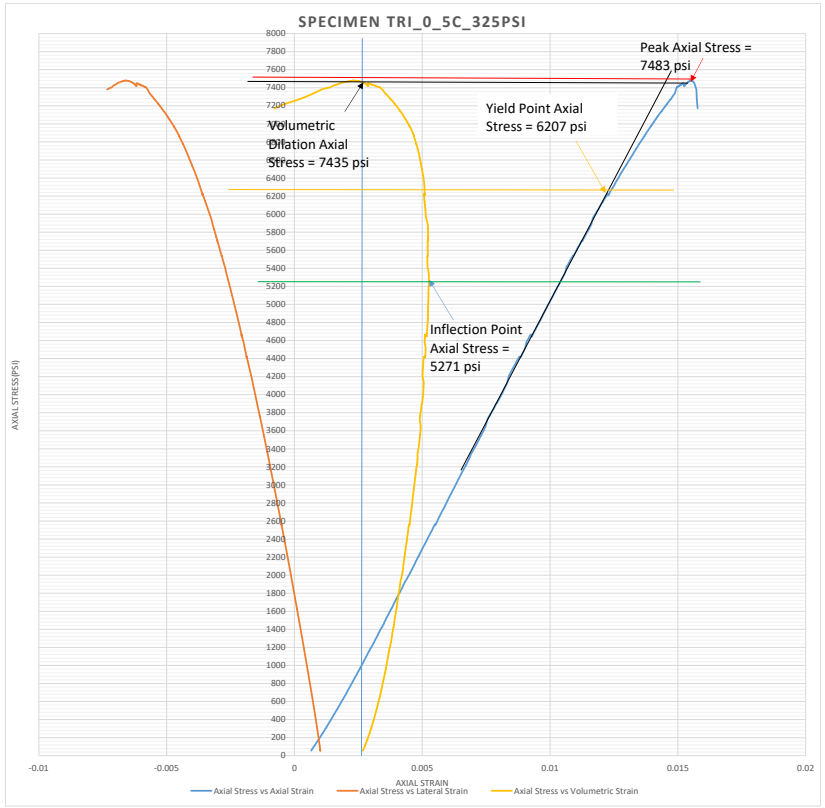
SPECIMEN TRI_0_5C_325PSI
Peak Axial Stress = 7483 psi
Yield Point Axial Stress = 6207 psi
Volumetric Dilation Axial Stress = 7435 psi
Inflection Point Axial Stress = 5271 psi
AXIAL STRESS(PSI)
AXIAL STRAIN
Axial Stress vs Axial Strain
Axial Stress vs Lateral Strain
Axial Stress vs Volumetric Strain

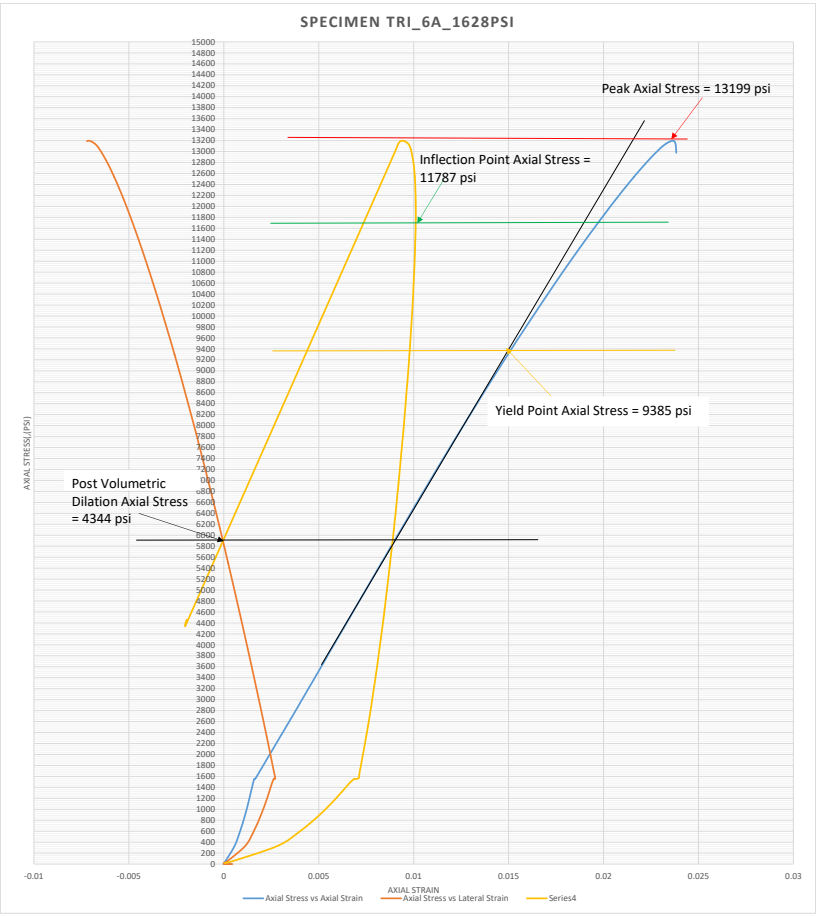
SPECIMEN TRI_6A_1628PSI
Peak Axial Stress = 13199 psi
Inflection Point Axial Stress = 11787 psi
Yield Point Axial Stress = 9385 psi
Post Volumetric Dilation Axial Stress = 4344 psi
AXIAL STRESS(PSI)
AXIAL STRAIN
Axial Stress vs Axial Strain
Axial Stress vs Lateral Strain
Series4

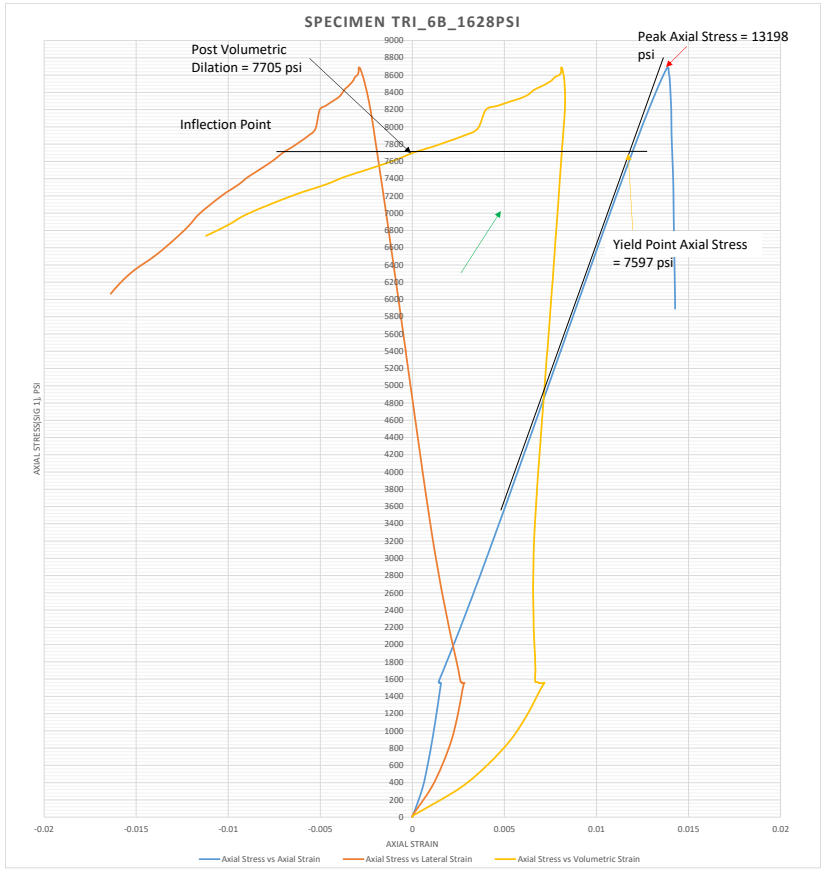
SPECIMEN TRI_6B_1628PSI
Post Volumetric Dilation = 7705 psi
Peak Axial Stress = 13198 psi
Inflection Point
Yield Point Axial Stress = 7597 psi
AXIAL STRESS(SIG 1), PSI
AXIAL STRAIN
Axial Stress vs Axial Strain
Axial Stress vs Lateral Strain
Axial Stress vs Volumetric Strain

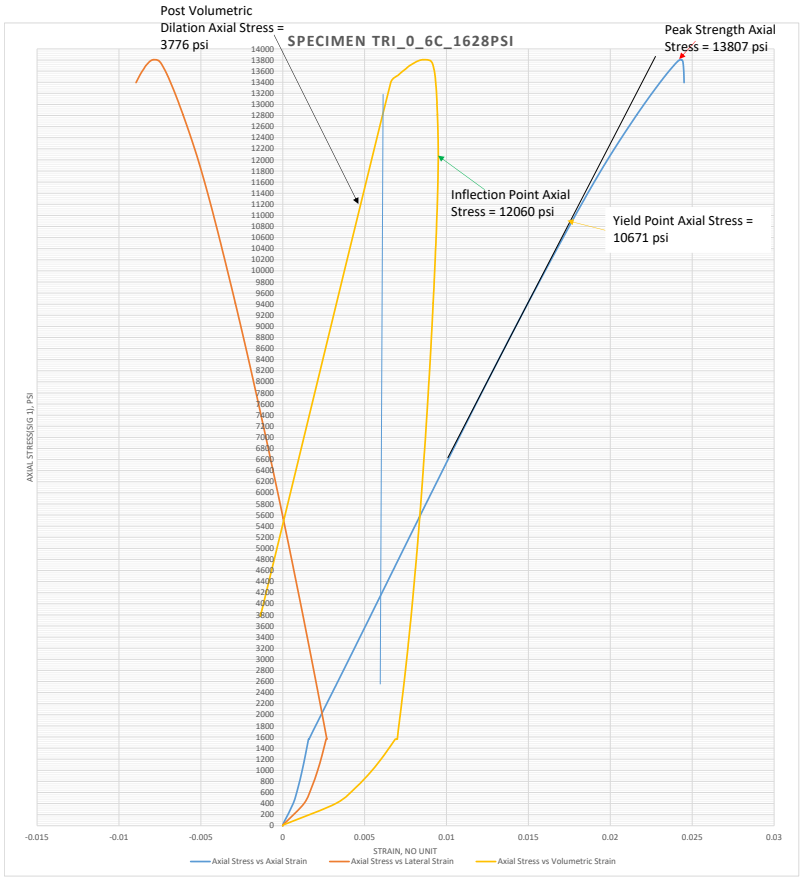
Post Volumetric Dilation Axial Stress = 3776 psi
SPECIMEN TRI_0_6C_1628PSI
Peak Strength Axial Stress = 13807 psi
Inflection Point Axial Stress = 12060 psi
Yield Point Axial Stress = 10671 psi
AXIAL STRESS(SIG 1), PSI
STRAIN, NO UNIT
Axial Stress vs Axial Strain
Axial Stress vs Lateral Strain
Axial Stress vs Volumetric Strain

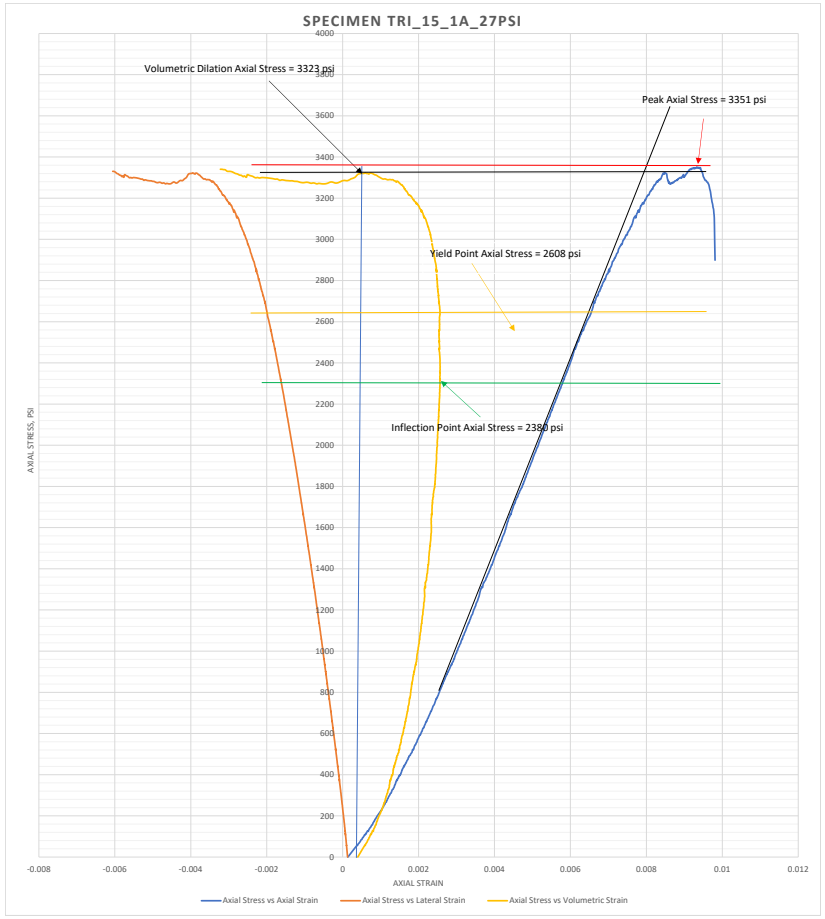
SPECIMEN TRI_15_1A_27PSI
Volumetric Dilation Axial Stress = 3323 psi
Peak Axial Stress = 3351 psi
Yield Point Axial Stress = 2608 psi
Inflection Point Axial Stress = 2380 psi
AXIAL STRESS, PSI
AXIAL STRAIN
Axial Stress vs Axial Strain
Axial Stress vs Lateral Strain
Axial Stress vs Volumetric Strain

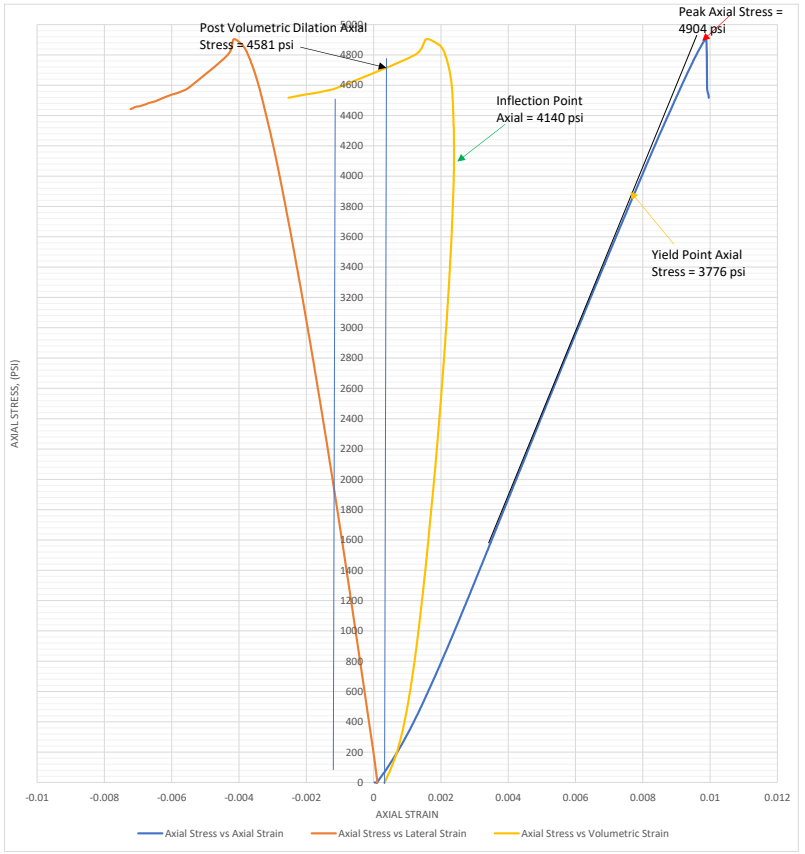
Post Volumetric Dilation Axial Stress = 4581 psi
Peak Axial Stress = 4904 psi
Inflection Point Axial = 4140 psi
Yield Point Axial Stress = 3776 psi
AXIAL STRESS, (PSI)
AXIAL STRAIN
Axial Stress vs Axial Strain
Axial Stress vs Lateral Strain
Axial Stress vs Volumetric Strain

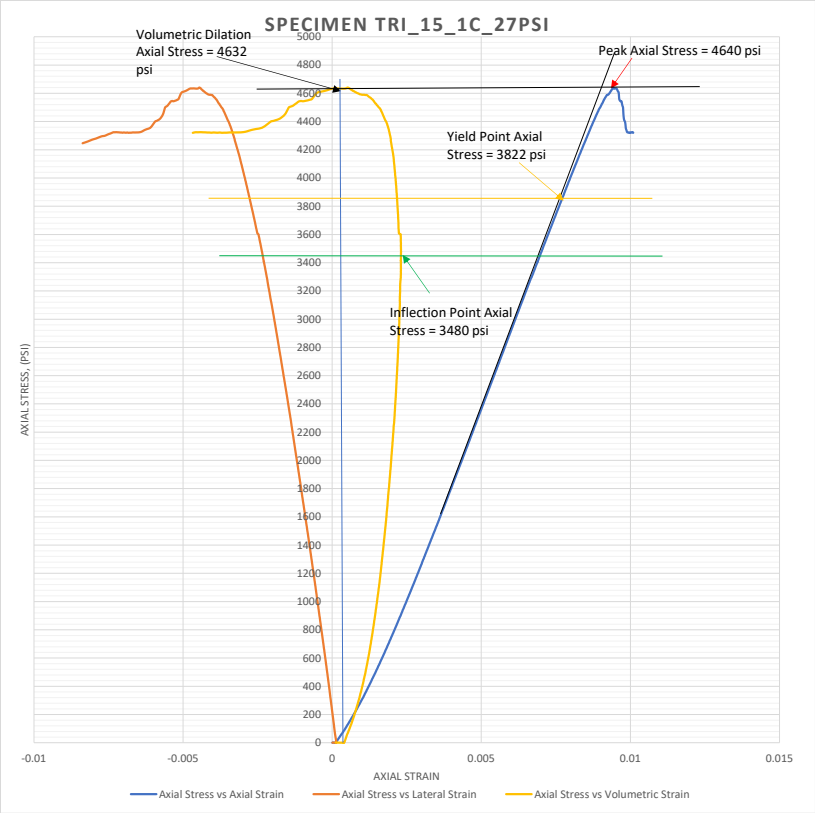
SPECIMEN TRI_15_1C_27PSI
Volumetric Dilation Axial Stress = 4632 psi
Peak Axial Stress = 4640 psi
Yield Point Axial Stress = 3822 psi
Inflection Point Axial Stress = 3480 psi
AXIAL STRESS, (PSI)
AXIAL STRAIN
Axial Stress vs Axial Strain
Axial Stress vs Lateral Strain
Axial Stress vs Volumetric Strain

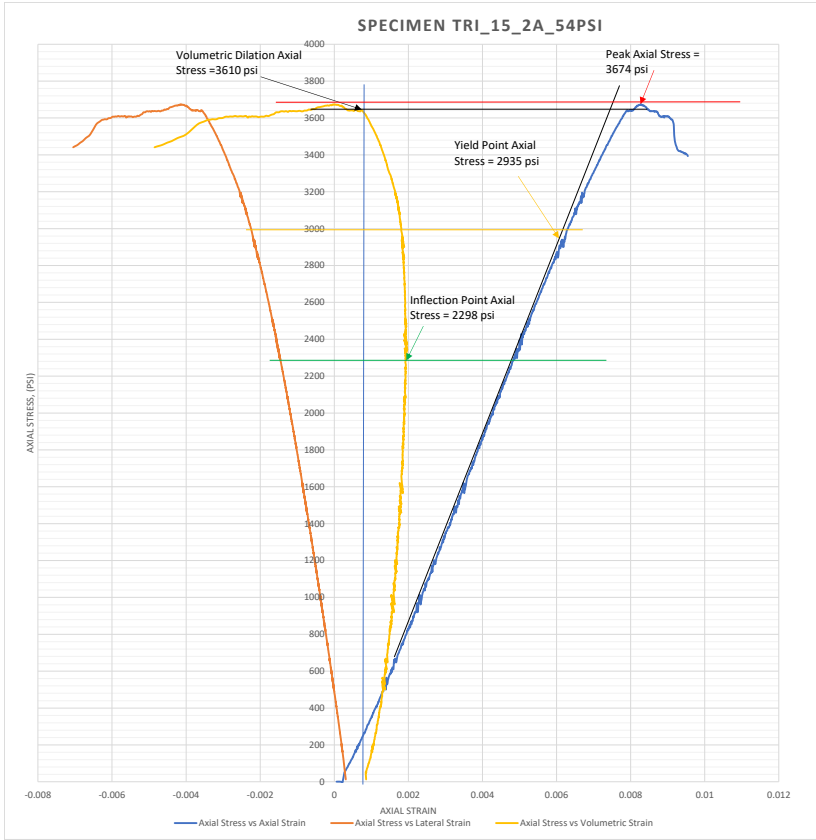
SPECIMEN TRI_15_2A_54PSI
Volumetric Dilation Axial Stress =3610 psi
Peak Axial Stress = 3674 psi
Yield Point Axial Stress = 2935 psi
Inflection Point Axial Stress = 2298 psi
AXIAL STRESS, (PSI)
AXIAL STRAIN
Axial Stress vs Axial Strain
Axial Stress vs Lateral Strain
Axial Stress vs Volumetric Strain

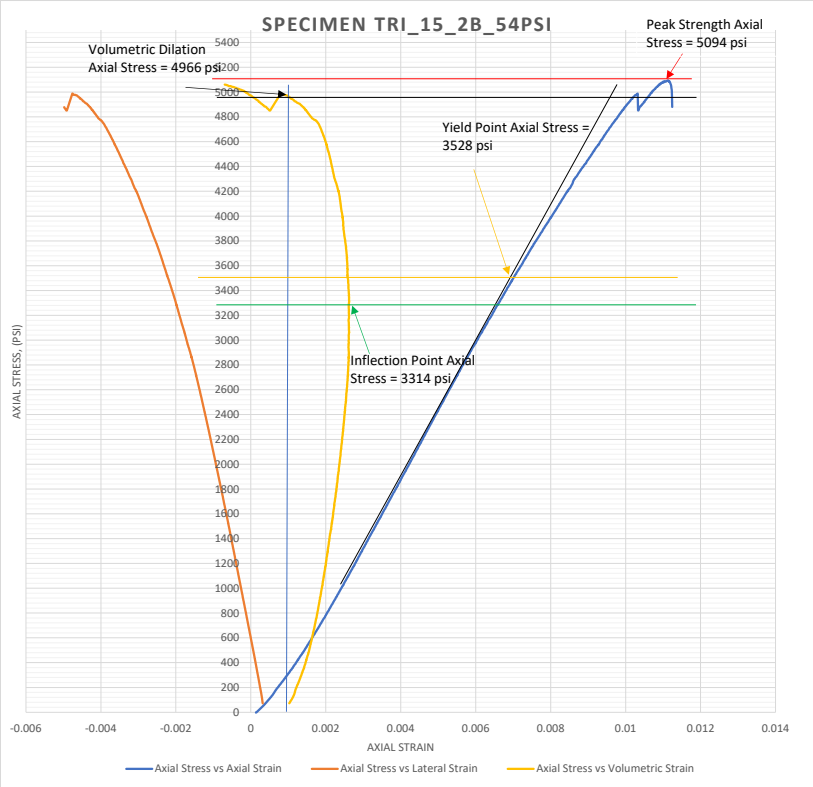
SPECIMEN TRI_15_2B_54PSI
Volumetric Dilation
Axial Stress = 4966 psi
Peak Strength Axial
Stress = 5094 psi
Yield Point Axial Stress =
3528 psi
Inflection Point Axial
Stress = 3314 psi
AXIAL STRESS, (PSI)
AXIAL STRAIN
Axial Stress vs Axial Strain
Axial Stress vs Lateral Strain
Axial Stress vs Volumetric Strain

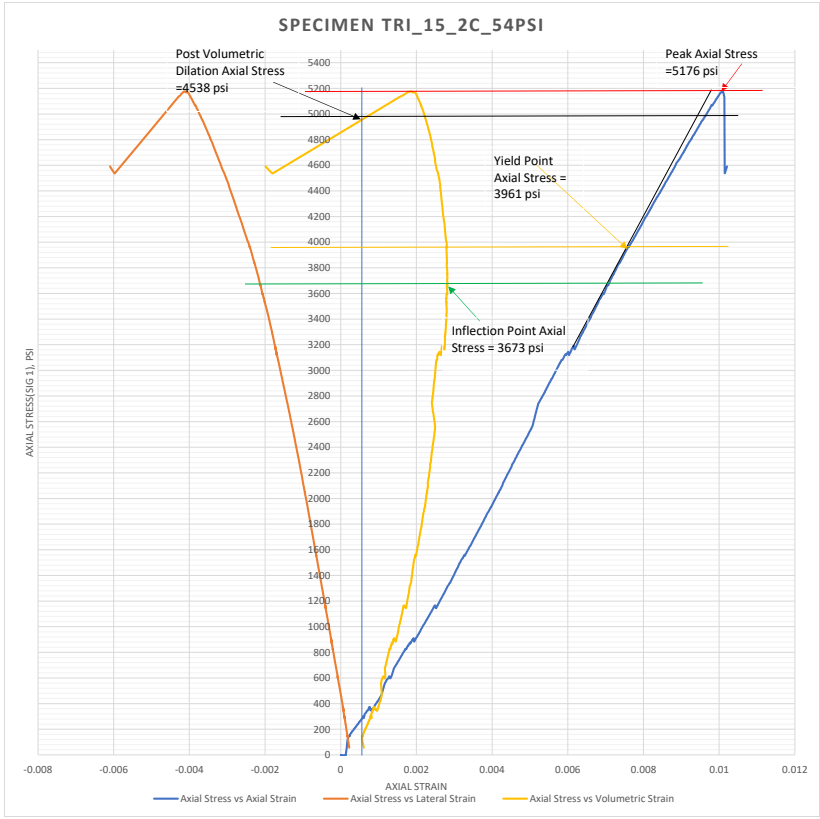
SPECIMEN TRI_15_2C_54PSI
Post Volumetric
Dilation Axial Stress
=4538 psi
Peak Axial Stress
=5176 psi
Yield Point
Axial Stress =
3961 psi
Inflection Point Axial
Stress = 3673 psi
AXIAL STRESS(SIG 1), PSI
AXIAL STRAIN
Axial Stress vs Axial Strain
Axial Stress vs Lateral Strain
Axial Stress vs Volumetric Strain

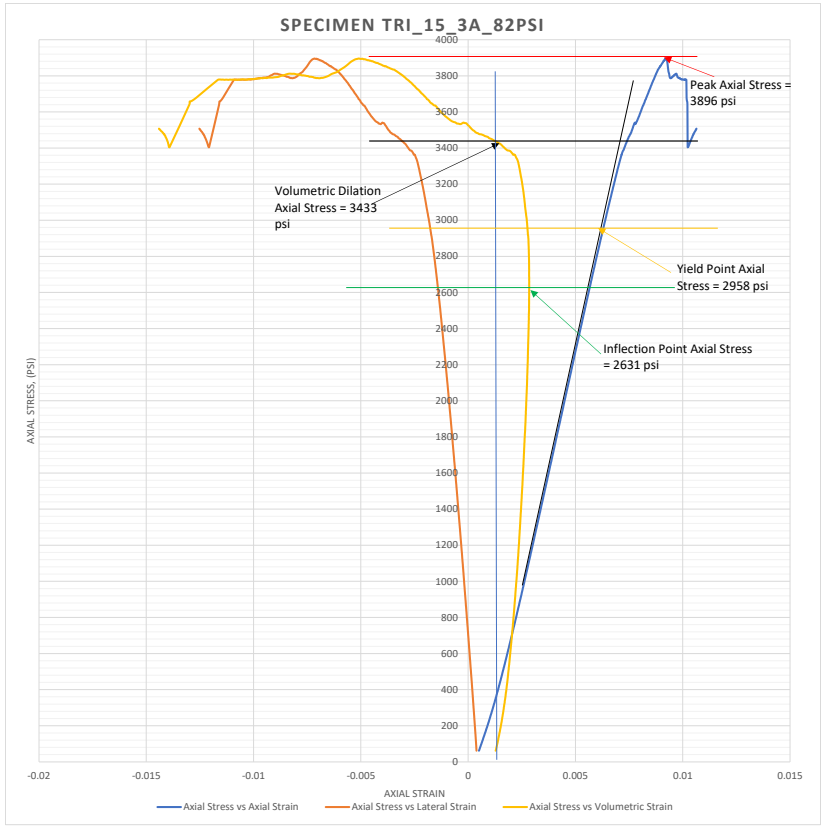
SPECIMEN TRI_15_3A_82PSI
Peak Axial Stress = 3896 psi
Volumetric Dilation Axial Stress = 3433 psi
Yield Point Axial Stress = 2958 psi
Inflection Point Axial Stress = 2631 psi
AXIAL STRESS, (PSI)
AXIAL STRAIN
Axial Stress vs Axial Strain
Axial Stress vs Lateral Strain
Axial Stress vs Volumetric Strain

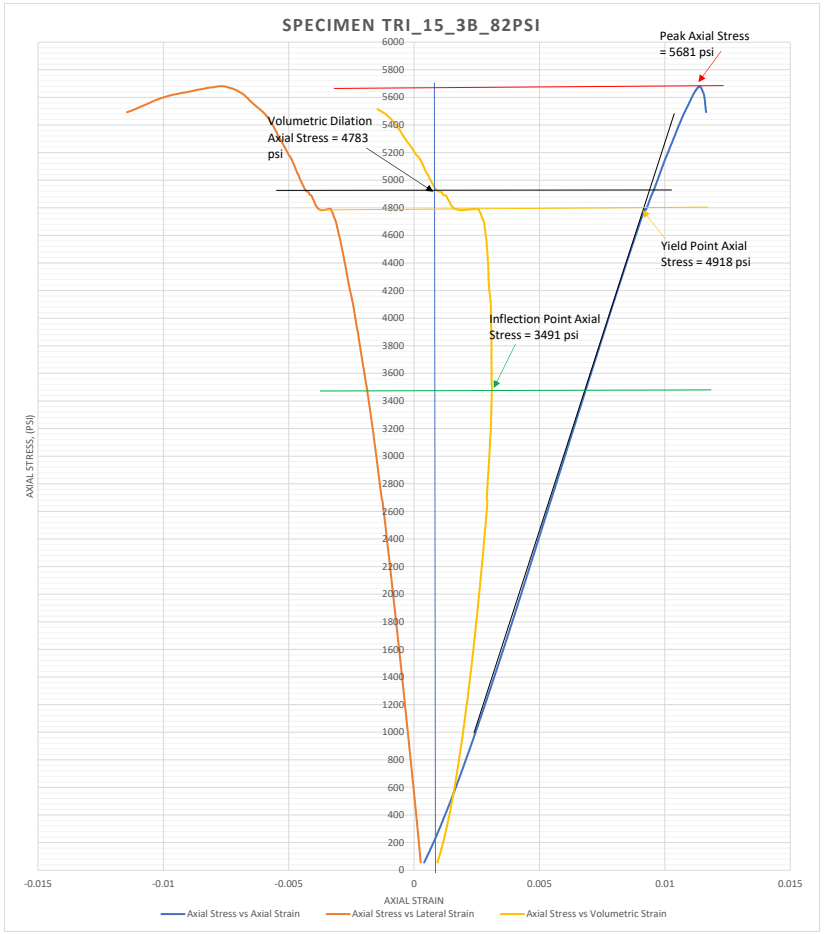
SPECIMEN TRI_15_3B_82PSI
Peak Axial Stress = 5681 psi
Volumetric Dilation Axial Stress = 4783 psi
Yield Point Axial Stress = 4918 psi
Inflection Point Axial Stress = 3491 psi
AXIAL STRESS, (PSI)
AXIAL STRAIN
Axial Stress vs Axial Strain
Axial Stress vs Lateral Strain
Axial Stress vs Volumetric Strain

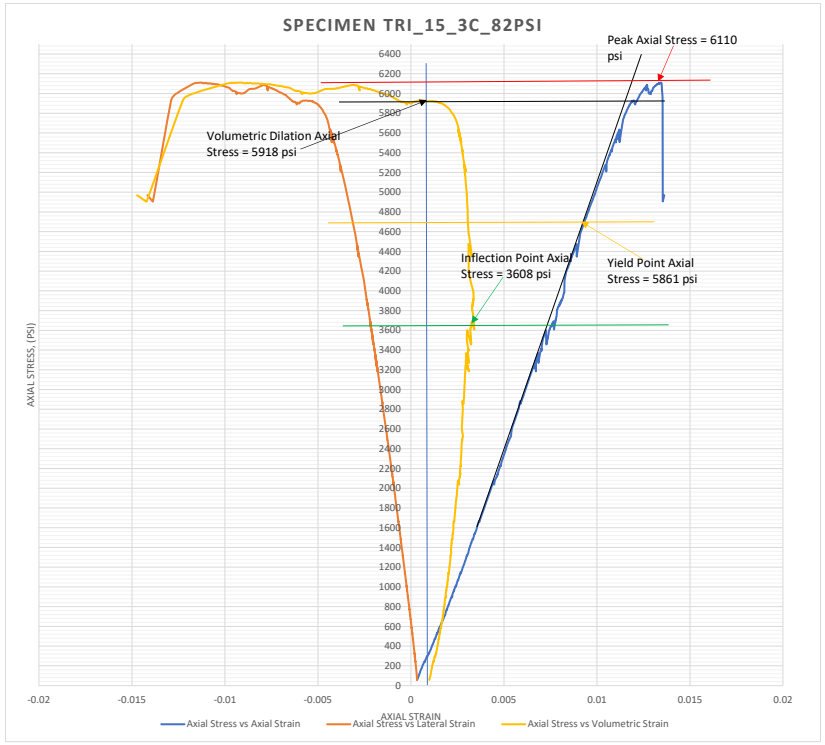
SPECIMEN TRI_15_3C_82PSI
Peak Axial Stress = 6110 psi
Volumetric Dilation Axial Stress = 5918 psi
Inflection Point Axial Stress = 3608 psi
Yield Point Axial Stress = 5861 psi
AXIAL STRESS, (PSI)
AXIAL STRAIN
Axial Stress vs Axial Strain
Axial Stress vs Lateral Strain
Axial Stress vs Volumetric Strain

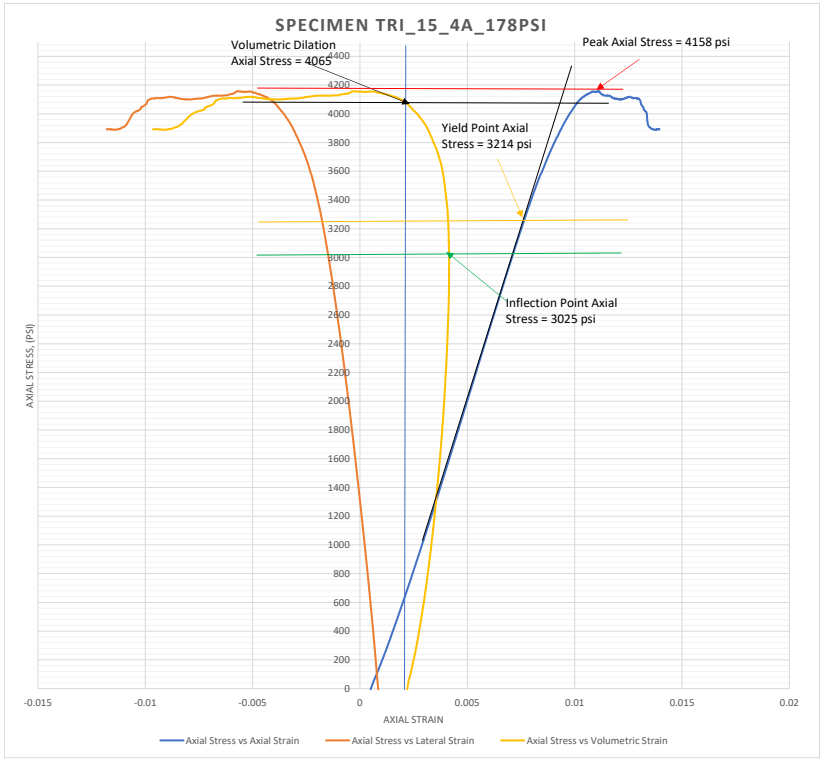
SPECIMEN TRI_15_4A_178PSI
Volumetric Dilation Axial Stress = 4065
Peak Axial Stress = 4158 psi
Yield Point Axial Stress = 3214 psi
Inflection Point Axial Stress = 3025 psi
AXIAL STRESS, (PSI)
AXIAL STRAIN
Axial Stress vs Axial Strain
Axial Stress vs Lateral Strain
Axial Stress vs Volumetric Strain

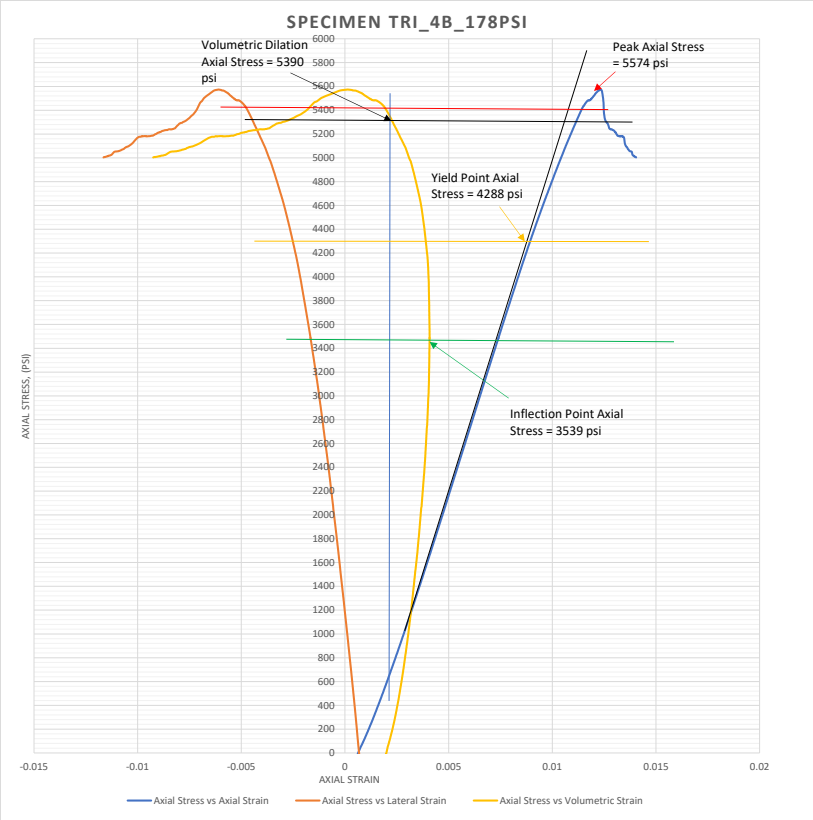
SPECIMEN TRI_4B_178PSI
Volumetric Dilation Axial Stress = 5390 psi
Peak Axial Stress = 5574 psi
Yield Point Axial Stress = 4288 psi
Inflection Point Axial Stress = 3539 psi
AXIAL STRESS, (PSI)
AXIAL STRAIN
Axial Stress vs Axial Strain
Axial Stress vs Lateral Strain
Axial Stress vs Volumetric Strain

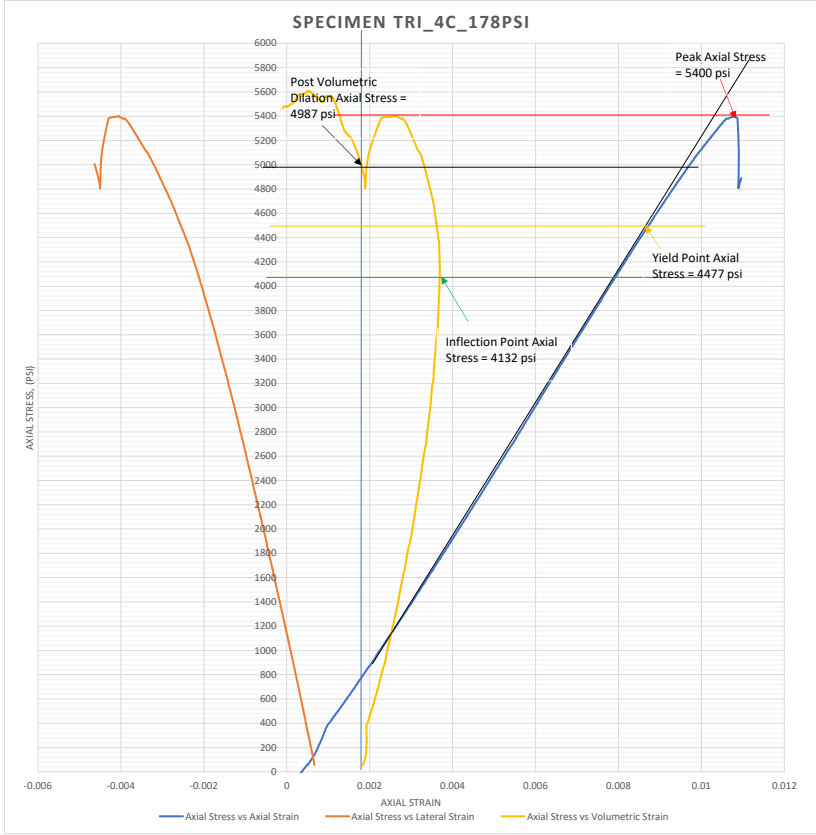
SPECIMEN TRI_4C_178PSI
Post Volumetric Dilation Axial Stress = 4987 psi
Peak Axial Stress = 5400 psi
Yield Point Axial Stress = 4477 psi
Inflection Point Axial Stress = 4132 psi
AXIAL STRESS, (PSI)
AXIAL STRAIN
Axial Stress vs Axial Strain
Axial Stress vs Lateral Strain
Axial Stress vs Volumetric Strain

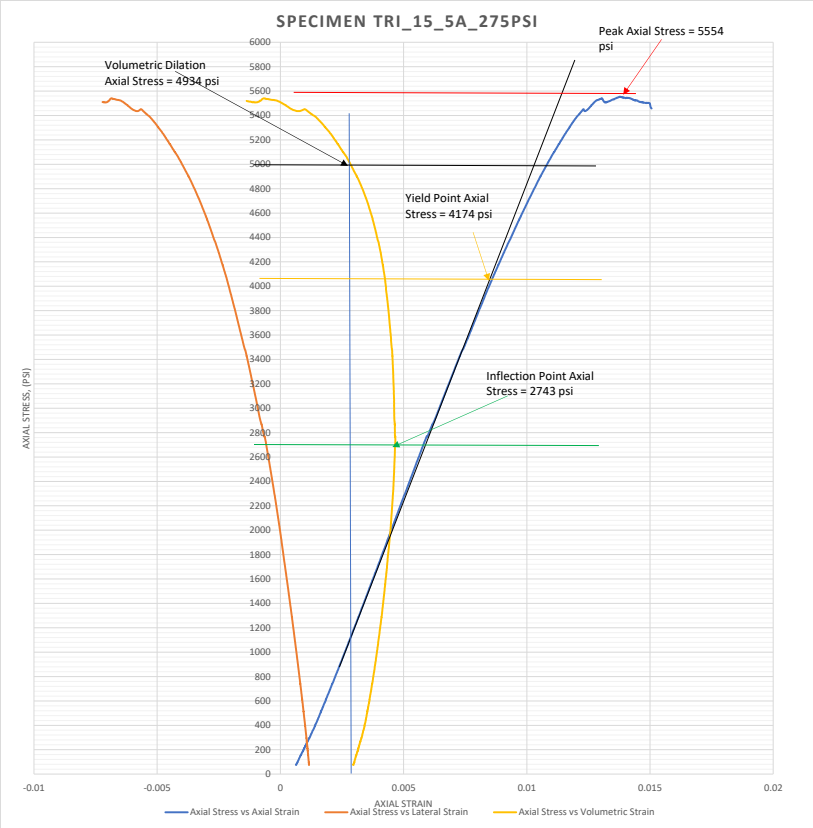
SPECIMEN TRI_15_5A_275PSI
Peak Axial Stress = 5554 psi
Volumetric Dilation Axial Stress = 4934 psi
Yield Point Axial Stress = 4174 psi
Inflection Point Axial Stress = 2743 psi
AXIAL STRESS, (PSI)
AXIAL STRAIN
Axial Stress vs Axial Strain
Axial Stress vs Lateral Strain
Axial Stress vs Volumetric Strain

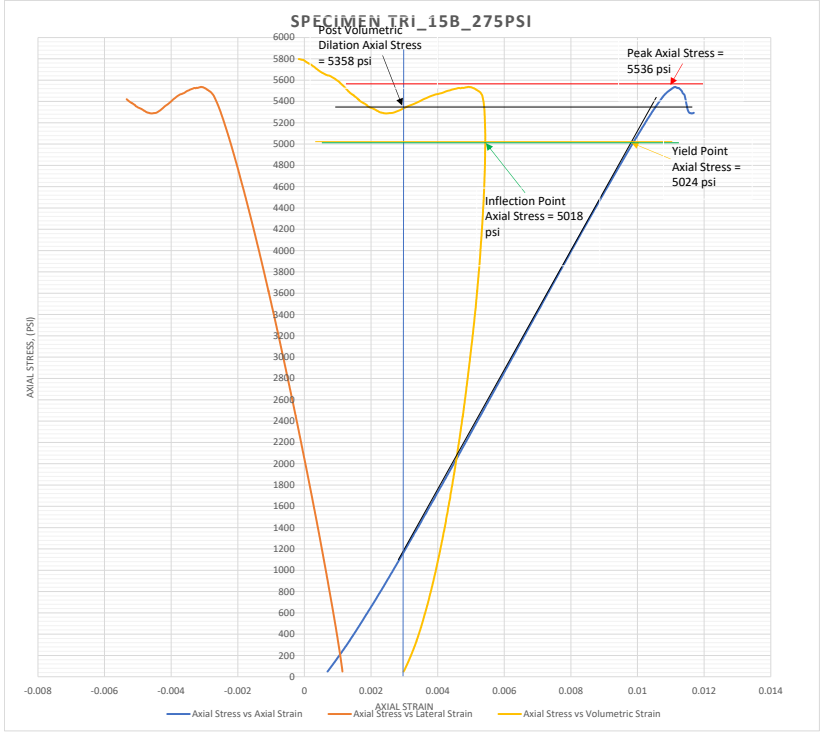
SPECIMEN TRI_15B_275PSI
Post Volumetric Dilation Axial Stress = 5358 psi
Peak Axial Stress = 5536 psi
Yield Point Axial Stress = 5024 psi
Inflection Point Axial Stress = 5018 psi
AXIAL STRESS, (PSI)
AXIAL STRAIN
Axial Stress vs Axial Strain
Axial Stress vs Lateral Strain
Axial Stress vs Volumetric Strain

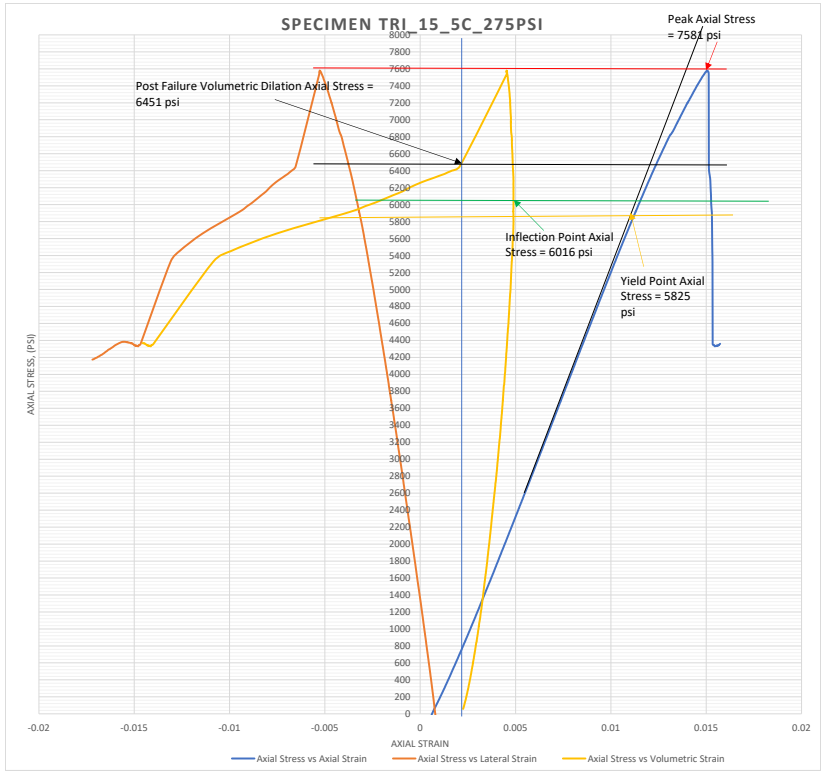
SPECIMEN TRI_15_5C_275PSI
Peak Axial Stress = 7581 psi
Post Failure Volumetric Dilation Axial Stress = 6451 psi
Inflection Point Axial Stress = 6016 psi
Yield Point Axial Stress = 5825 psi
AXIAL STRESS, (PSI)
AXIAL STRAIN
Axial Stress vs Axial Strain
Axial Stress vs Lateral Strain
Axial Stress vs Volumetric Strain

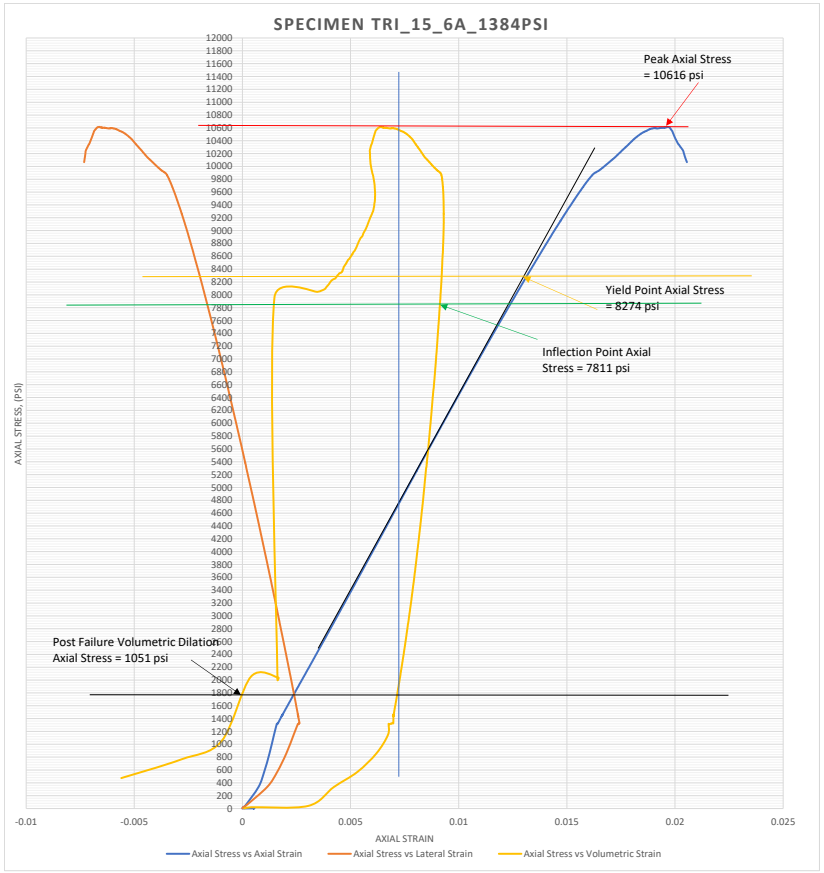
SPECIMEN TRI_15_6A_1384PSI
Peak Axial Stress = 10616 psi
Yield Point Axial Stress = 8274 psi
Inflection Point Axial Stress = 7811 psi
Post Failure Volumetric Dilation Axial Stress = 1051 psi
AXIAL STRESS, (PSI)
AXIAL STRAIN
Axial Stress vs Axial Strain
Axial Stress vs Lateral Strain
Axial Stress vs Volumetric Strain

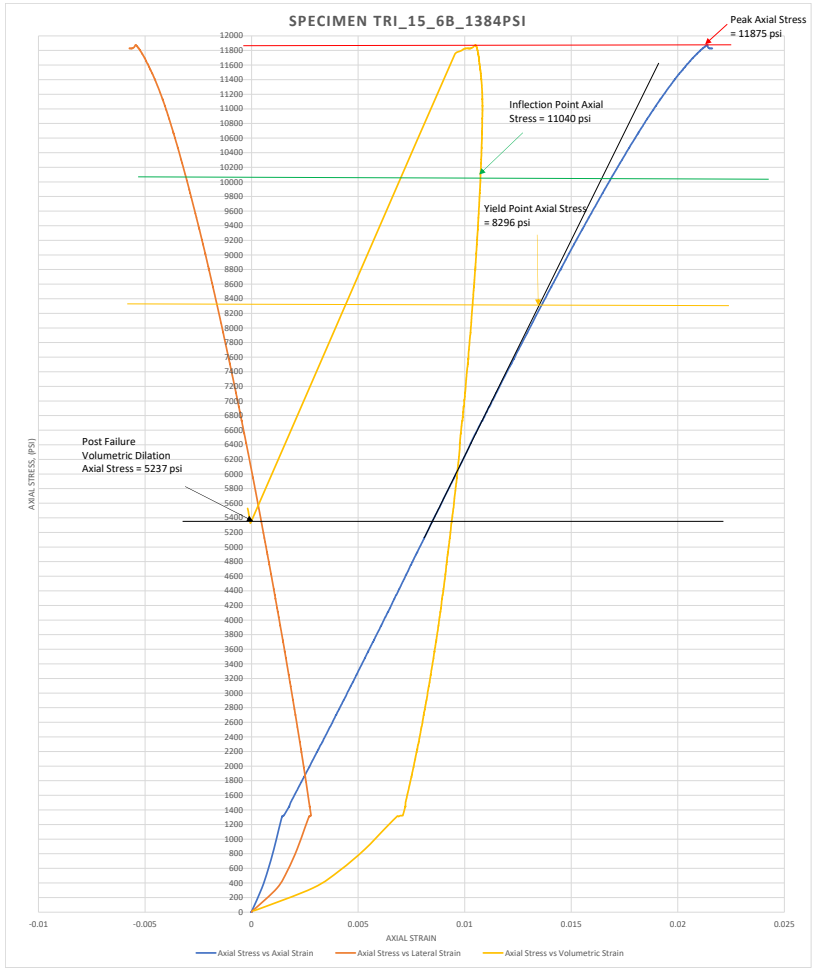
SPECIMEN TRI_15_6B_1384PSI
Peak Axial Stress = 11875 psi
Inflection Point Axial Stress = 11040 psi
Yield Point Axial Stress = 8296 psi
Post Failure Volumetric Dilation Axial Stress = 5237 psi
AXIAL STRESS, (PSI)
AXIAL STRAIN
Axial Stress vs Axial Strain
Axial Stress vs Lateral Strain
Axial Stress vs Volumetric Strain

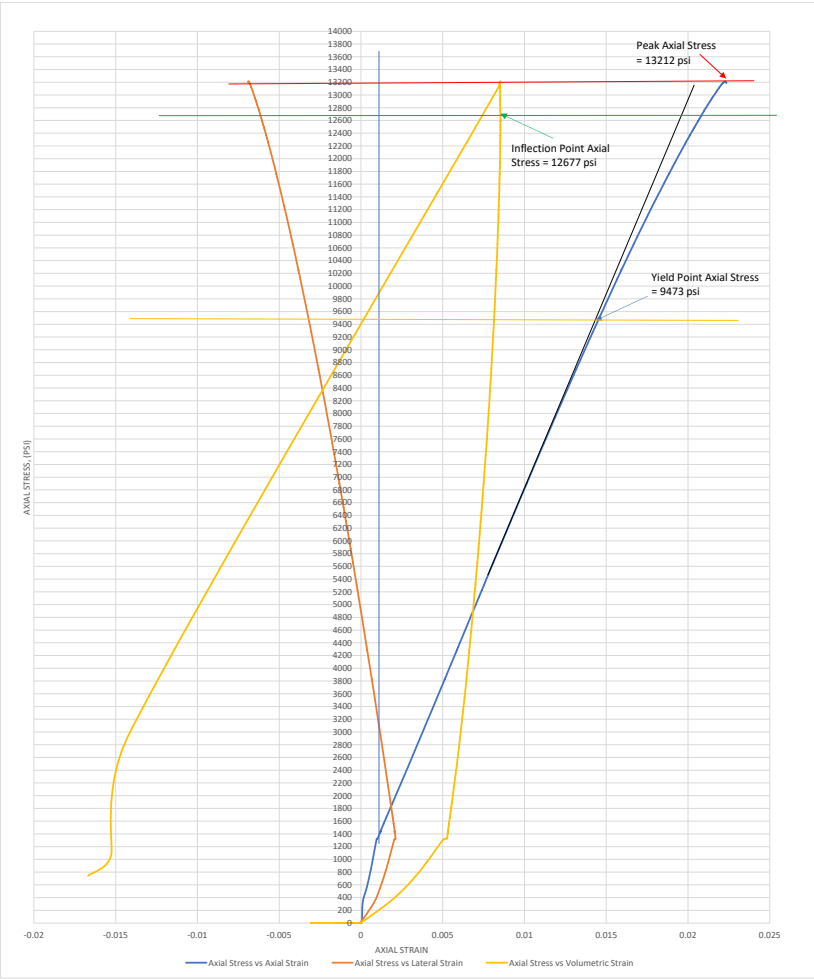
Peak Axial Stress = 13212 psi
Inflection Point Axial Stress = 12677 psi
Yield Point Axial Stress = 9473 psi
AXIAL STRESS, (PSI)
AXIAL STRAIN
Axial Stress vs Axial Strain
Axial Stress vs Lateral Strain
Axial Stress vs Volumetric Strain

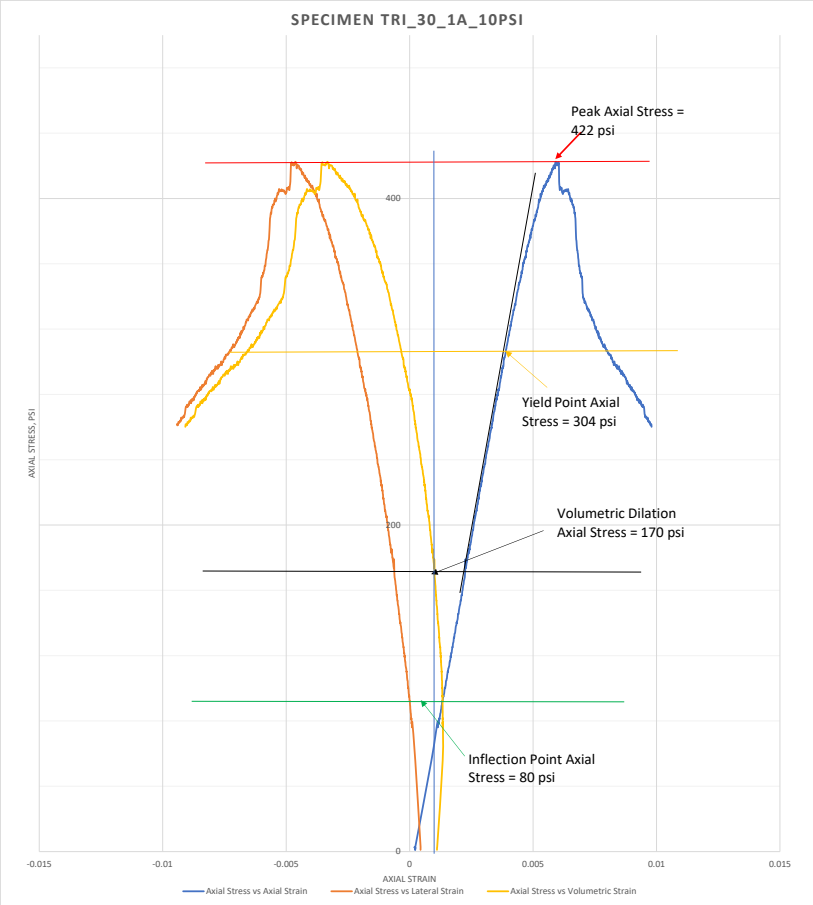
SPECIMEN TRI_30_1A_10PSI
Peak Axial Stress = 422 psi
Yield Point Axial Stress = 304 psi
Volumetric Dilation Axial Stress = 170 psi
Inflection Point Axial Stress = 80 psi
AXIAL STRESS, PSI
AXIAL STRAIN
Axial Stress vs Axial Strain
Axial Stress vs Lateral Strain
Axial Stress vs Volumetric Strain

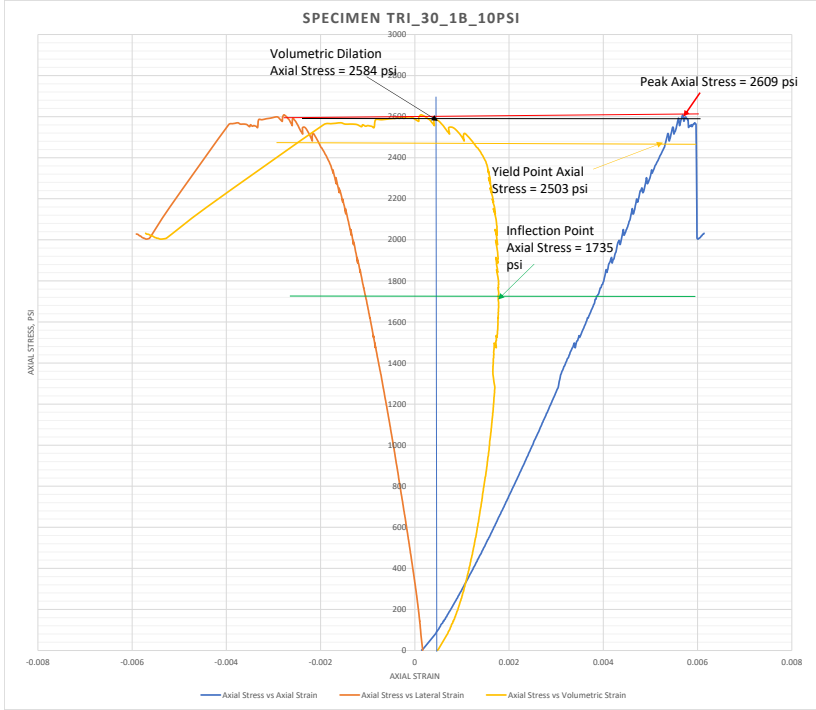
SPECIMEN TRI_30_1B_10PSI
Volumetric Dilation Axial Stress = 2584 psi
Peak Axial Stress = 2609 psi
Yield Point Axial Stress = 2503 psi
Inflection Point Axial Stress = 1735 psi
AXIAL STRESS, PSI
AXIAL STRAIN
Axial Stress vs Axial Strain
Axial Stress vs Lateral Strain
Axial Stress vs Volumetric Strain

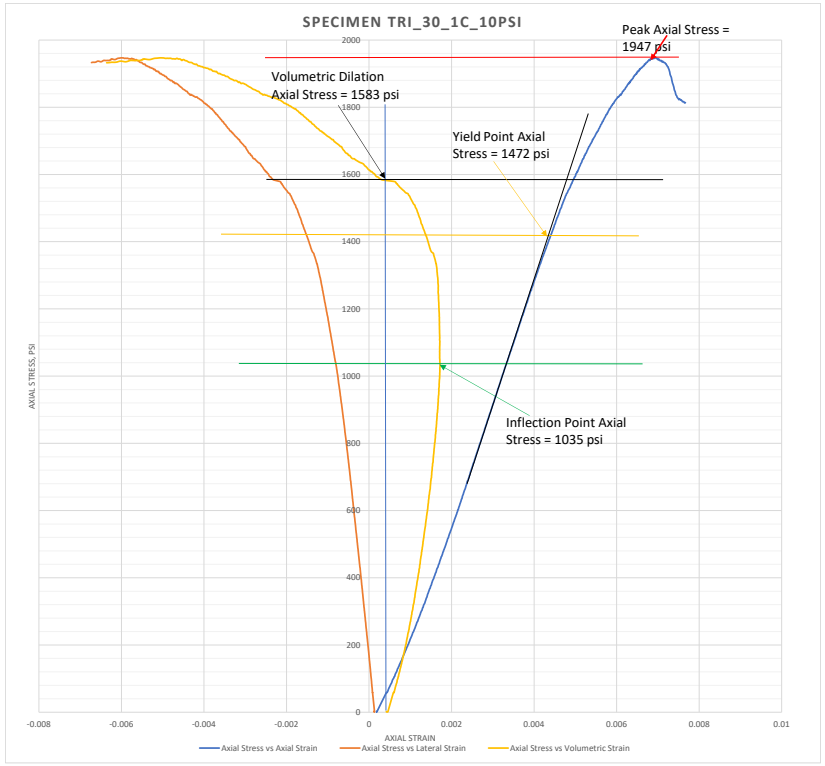
SPECIMEN TRI_30_1C_10PSI
Peak Axial Stress = 1947 psi
Volumetric Dilation Axial Stress = 1583 psi
Yield Point Axial Stress = 1472 psi
Inflection Point Axial Stress = 1035 psi
AXIAL STRESS, PSI
AXIAL STRAIN
Axial Stress vs Axial Strain
Axial Stress vs Lateral Strain
Axial Stress vs Volumetric Strain

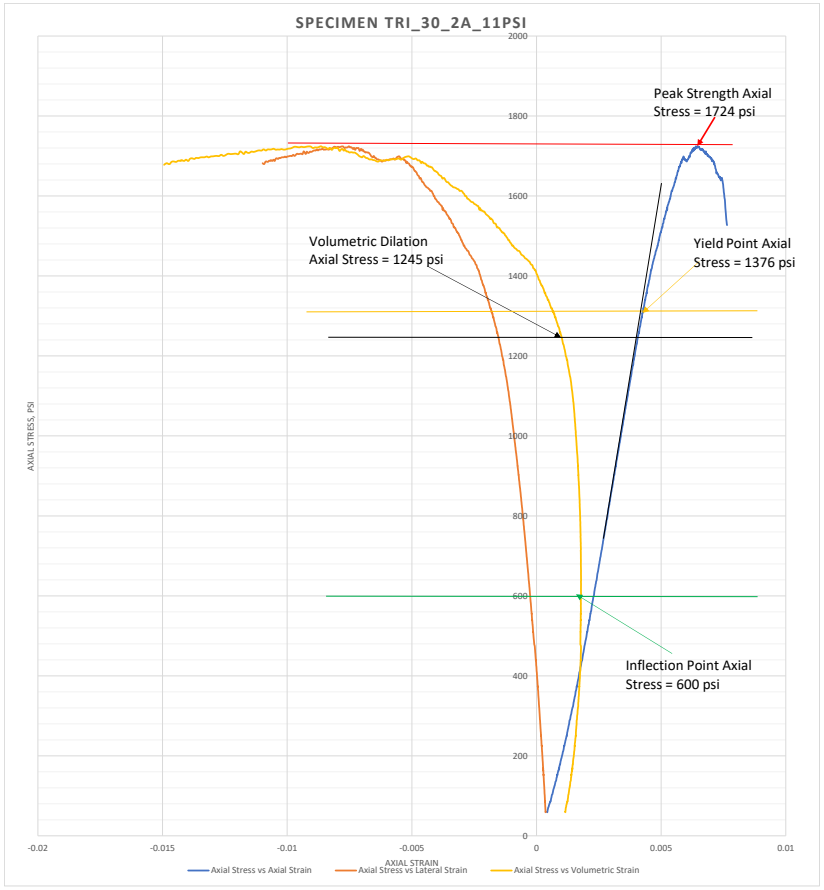
SPECIMEN TRI_30_2A_11PSI
Peak Strength Axial Stress = 1724 psi
Volumetric Dilation Axial Stress = 1245 psi
Yield Point Axial Stress = 1376 psi
Inflection Point Axial Stress = 600 psi
AXIAL STRESS, PSI
AXIAL STRAIN
Axial Stress vs Axial Strain
Axial Stress vs Lateral Strain
Axial Stress vs Volumetric Strain

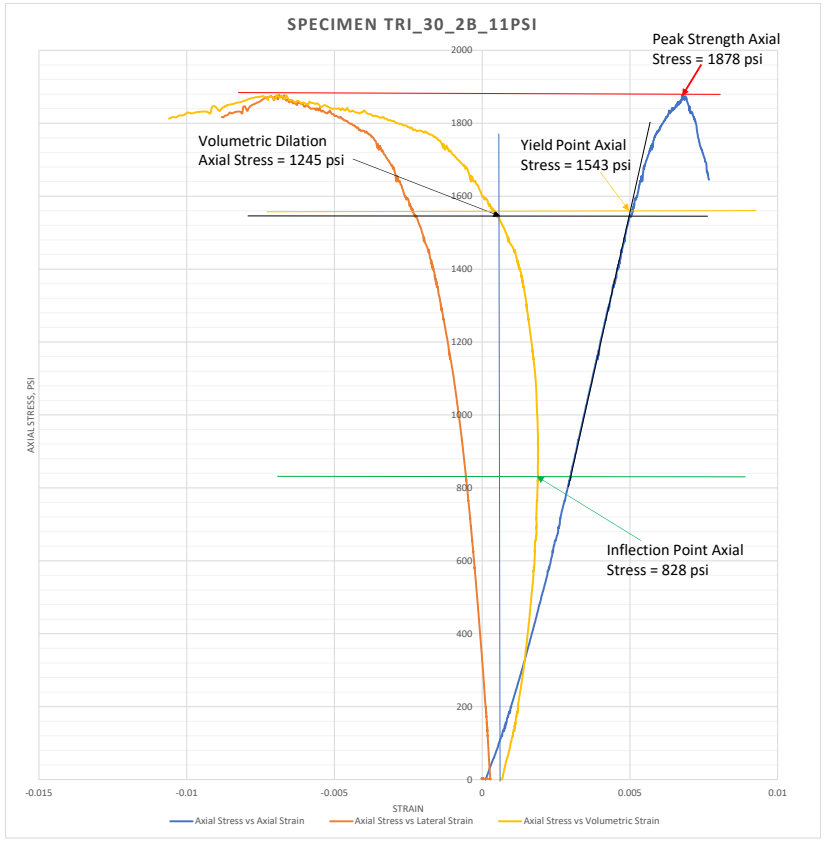
SPECIMEN TRI_30_2B_11PSI
Peak Strength Axial Stress = 1878 psi
Volumetric Dilation Axial Stress = 1245 psi
Yield Point Axial Stress = 1543 psi
Inflection Point Axial Stress = 828 psi
AXIAL STRESS, PSI
STRAIN
Axial Stress vs Axial Strain
Axial Stress vs Lateral Strain
Axial Stress vs Volumetric Strain

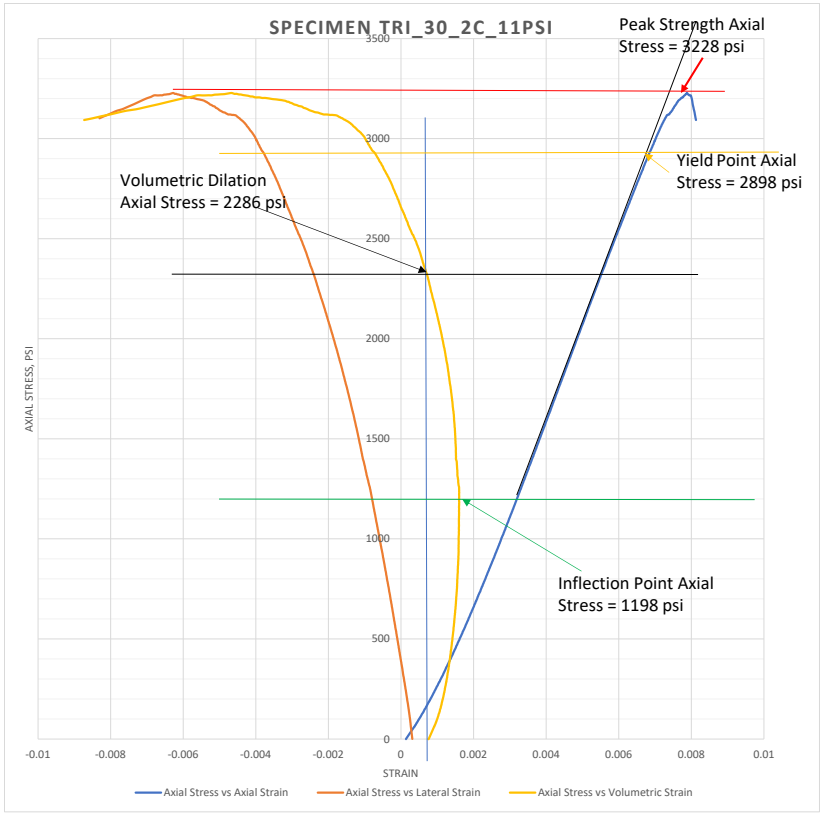
SPECIMEN TRI_30_2C_11PSI
Peak Strength Axial Stress = 3228 psi
Yield Point Axial Stress = 2898 psi
Volumetric Dilation Axial Stress = 2286 psi
Inflection Point Axial Stress = 1198 psi
AXIAL STRESS, PSI
STRAIN
Axial Stress vs Axial Strain
Axial Stress vs Lateral Strain
Axial Stress vs Volumetric Strain

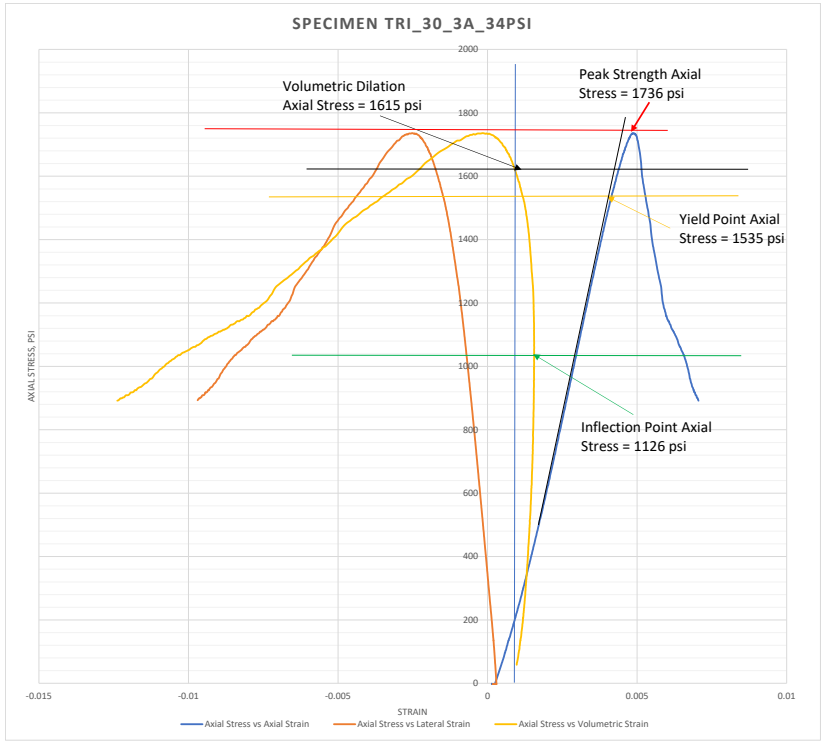
SPECIMEN TRI_30_3A_34PSI
Volumetric Dilation
Axial Stress = 1615 psi
Peak Strength Axial
Stress = 1736 psi
Yield Point Axial
Stress = 1535 psi
Inflection Point Axial
Stress = 1126 psi
AXIAL STRESS, PSI
STRAIN
Axial Stress vs Axial Strain
Axial Stress vs Lateral Strain
Axial Stress vs Volumetric Strain

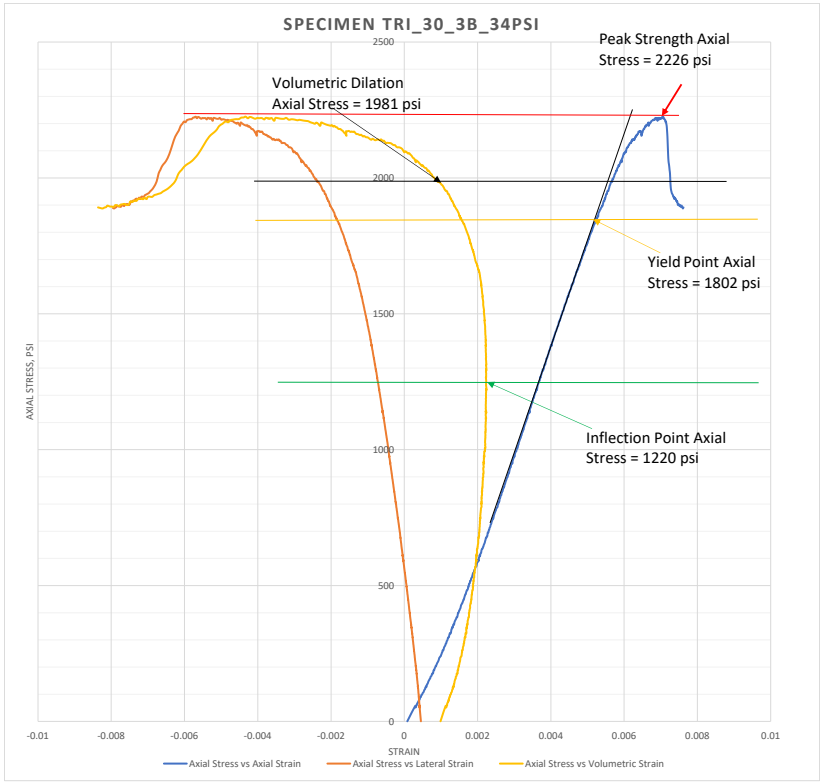
SPECIMEN TRI_30_3B_34PSI
Peak Strength Axial
Stress = 2226 psi
Volumetric Dilation
Axial Stress = 1981 psi
Yield Point Axial
Stress = 1802 psi
Inflection Point Axial
Stress = 1220 psi
AXIAL STRESS, PSI
STRAIN
Axial Stress vs Axial Strain
Axial Stress vs Lateral Strain
Axial Stress vs Volumetric Strain

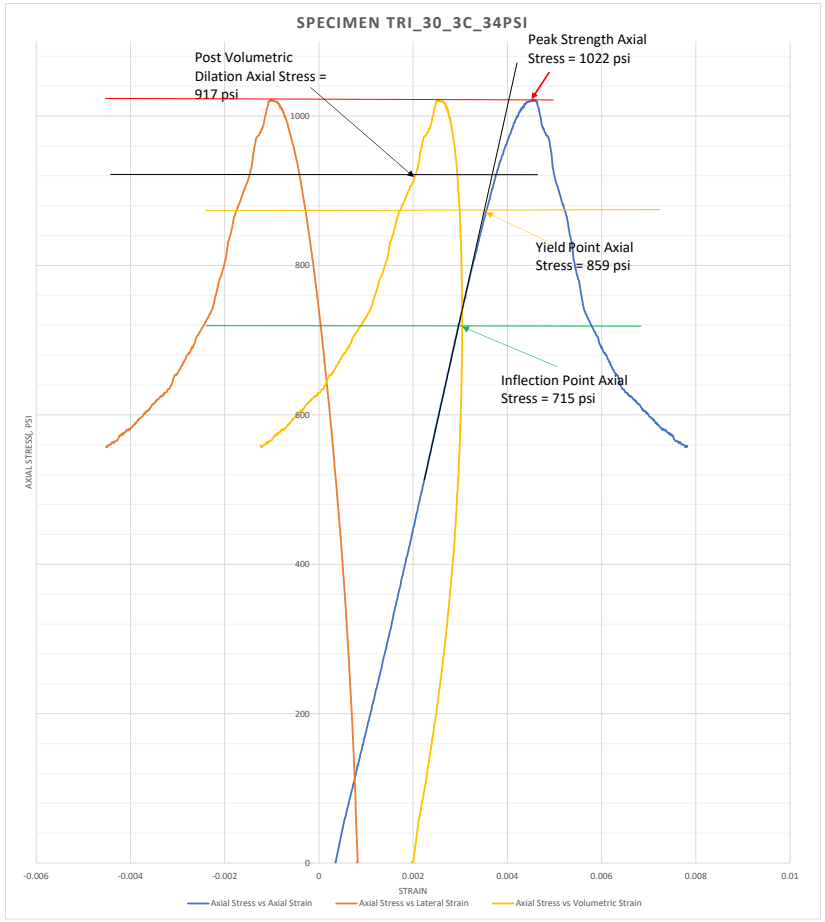
SPECIMEN TRI_30_3C_34PSI
Post Volumetric Dilation Axial Stress = 917 psi
Peak Strength Axial Stress = 1022 psi
Yield Point Axial Stress = 859 psi
Inflection Point Axial Stress = 715 psi
AXIAL STRESS, PSI
STRAIN
Axial Stress vs Axial Strain
Axial Stress vs Lateral Strain
Axial Stress vs Volumetric Strain

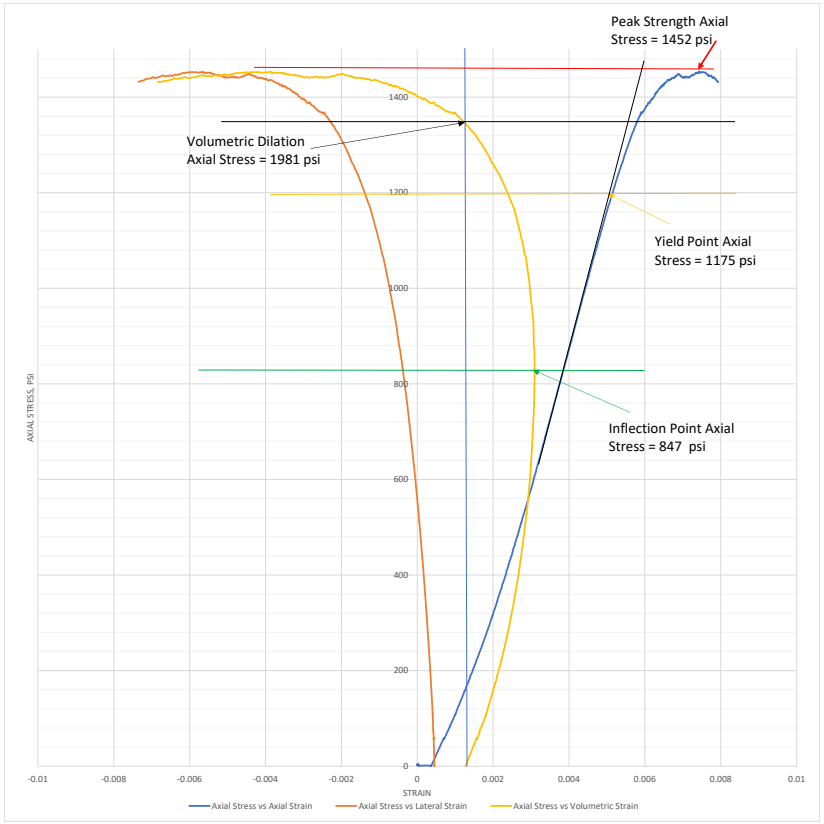
Peak Strength Axial Stress = 1452 psi
Volumetric Dilation Axial Stress = 1981 psi
Yield Point Axial Stress = 1175 psi
Inflection Point Axial Stress = 847 psi
AXIAL STRESS, PSI
STRAIN
Axial Stress vs Axial Strain
Axial Stress vs Lateral Strain
Axial Stress vs Volumetric Strain

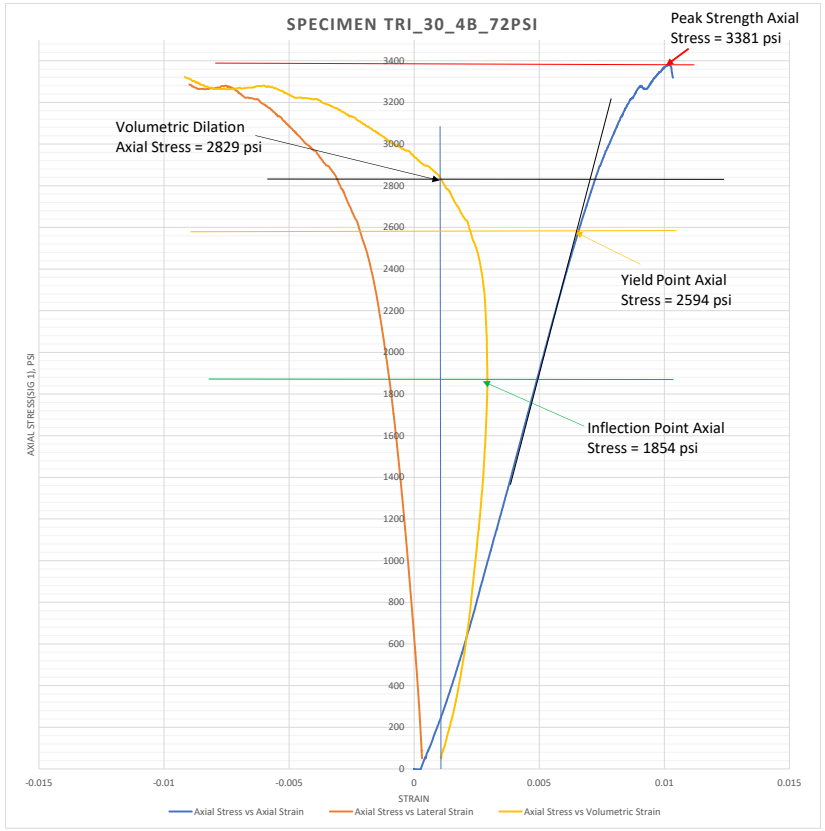
SPECIMEN TRI_30_4B_72PSI
Peak Strength Axial Stress = 3381 psi
Volumetric Dilation Axial Stress = 2829 psi
Yield Point Axial Stress = 2594 psi
Inflection Point Axial Stress = 1854 psi
AXIAL STRESS(SIG 1), PSI
STRAIN
Axial Stress vs Axial Strain
Axial Stress vs Lateral Strain
Axial Stress vs Volumetric Strain

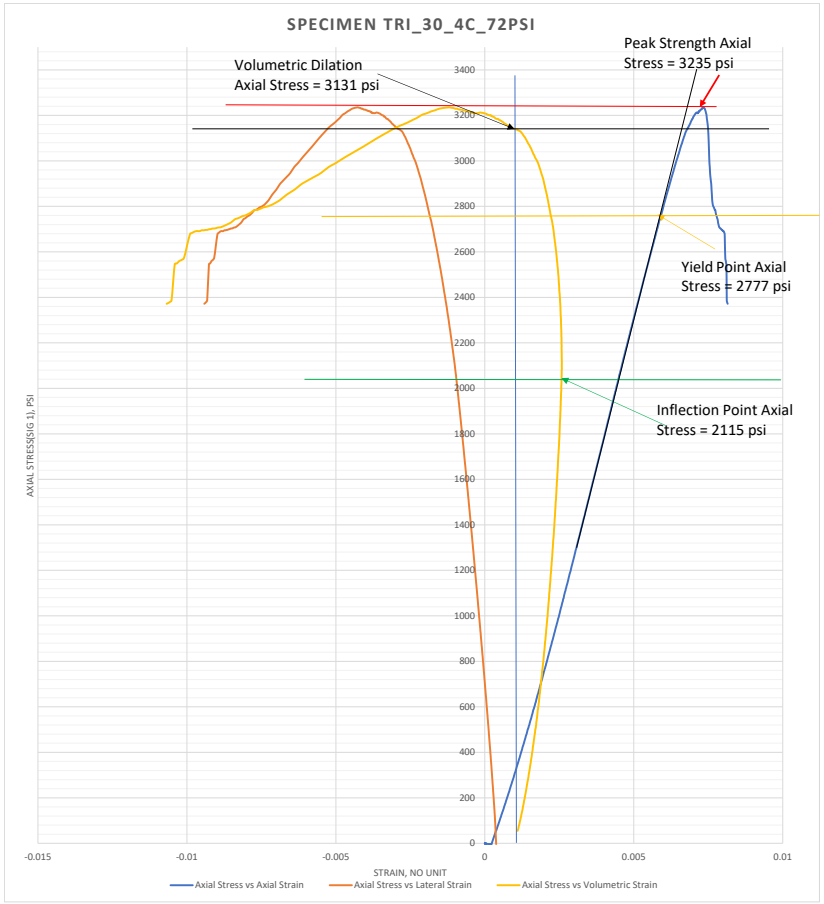
SPECIMEN TRI_30_4C_72PSI
Peak Strength Axial Stress = 3235 psi
Volumetric Dilation Axial Stress = 3131 psi
Yield Point Axial Stress = 2777 psi
Inflection Point Axial Stress = 2115 psi
AXIAL STRESS(SIG 1), PSI
STRAIN, NO UNIT
Axial Stress vs Axial Strain
Axial Stress vs Lateral Strain
Axial Stress vs Volumetric Strain

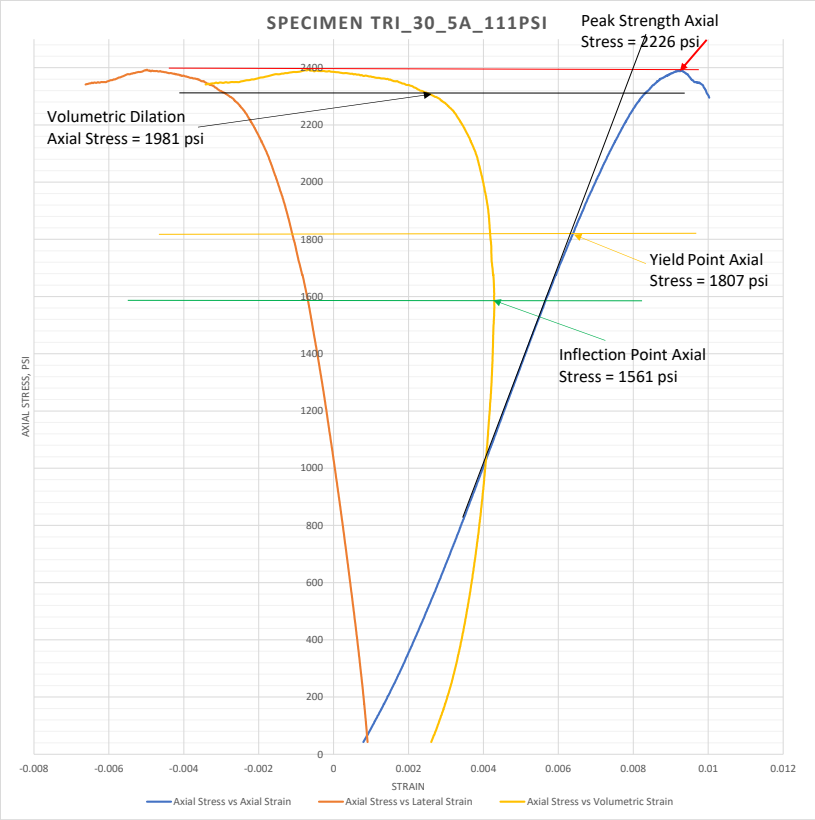
SPECIMEN TRI_30_5A_111PSI
Peak Strength Axial Stress = 2226 psi
Volumetric Dilation Axial Stress = 1981 psi
Yield Point Axial Stress = 1807 psi
Inflection Point Axial Stress = 1561 psi
AXIAL STRESS, PSI
STRAIN
Axial Stress vs Axial Strain
Axial Stress vs Lateral Strain
Axial Stress vs Volumetric Strain

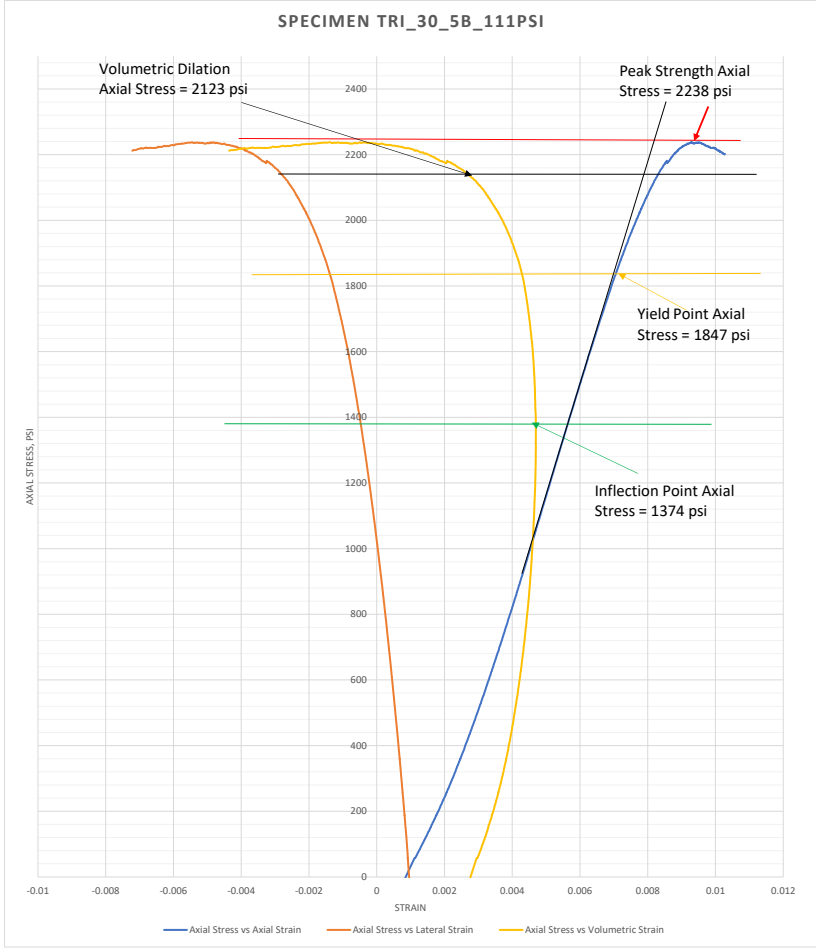
SPECIMEN TRI_30_5B_111PSI
Volumetric Dilation Axial Stress = 2123 psi
Peak Strength Axial Stress = 2238 psi
Yield Point Axial Stress = 1847 psi
Inflection Point Axial Stress = 1374 psi
AXIAL STRESS, PSI
STRAIN
Axial Stress vs Axial Strain
Axial Stress vs Lateral Strain
Axial Stress vs Volumetric Strain

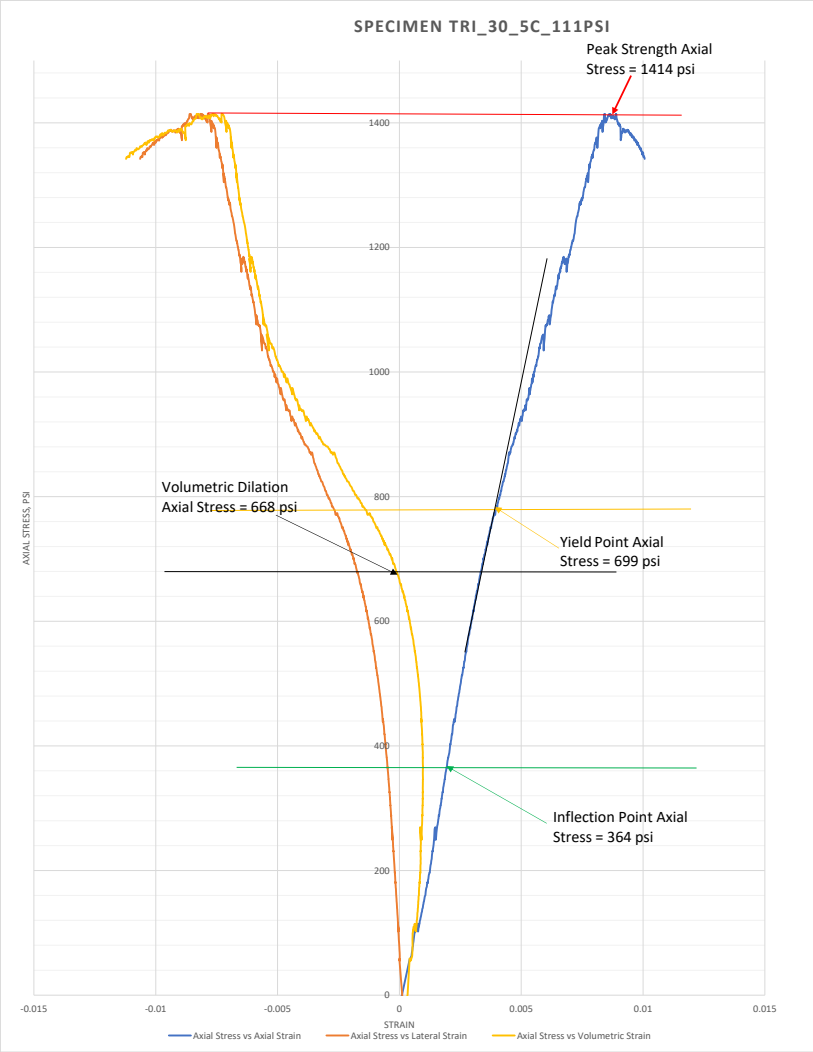
SPECIMEN TRI_30_5C_111PSI
Peak Strength Axial Stress = 1414 psi
Volumetric Dilation Axial Stress = 668 psi
Yield Point Axial Stress = 699 psi
Inflection Point Axial Stress = 364 psi
AXIAL STRESS, PSI
STRAIN
Axial Stress vs Axial Strain
Axial Stress vs Lateral Strain
Axial Stress vs Volumetric Strain

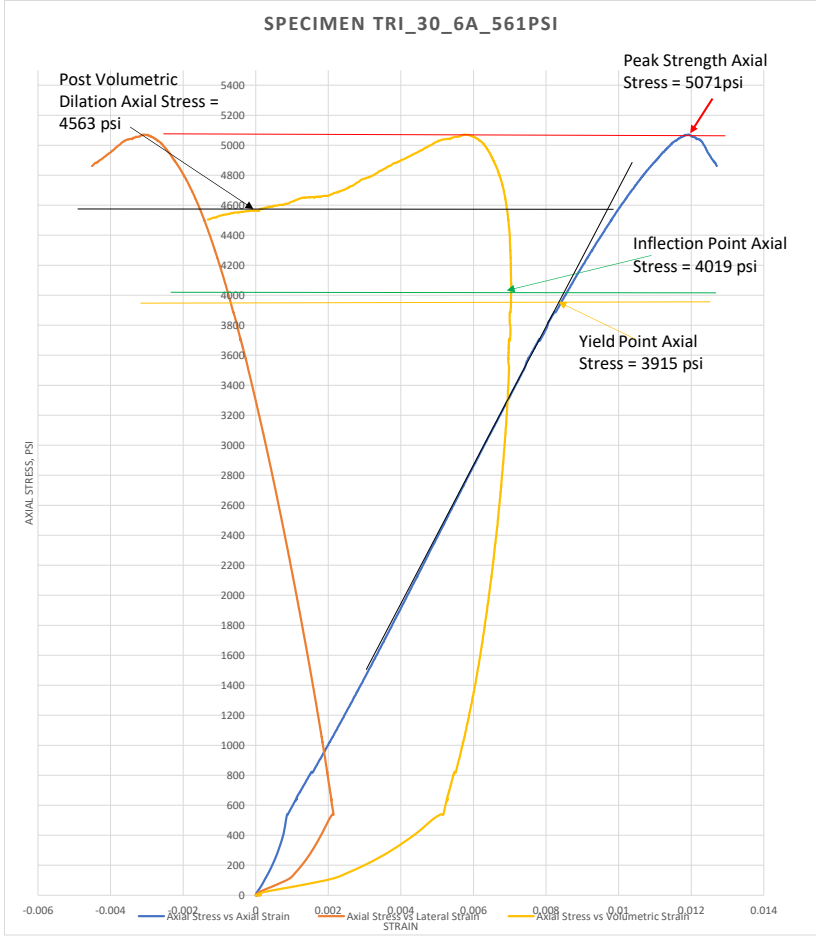
SPECIMEN TRI_30_6A_561PSI
Post Volumetric Dilation Axial Stress = 4563 psi
Peak Strength Axial Stress = 5071psi
Inflection Point Axial Stress = 4019 psi
Yield Point Axial Stress = 3915 psi
AXIAL STRESS, PSI
STRAIN
Axial Stress vs Axial Strain
Axial Stress vs Lateral Strain
Axial Stress vs Volumetric Strain

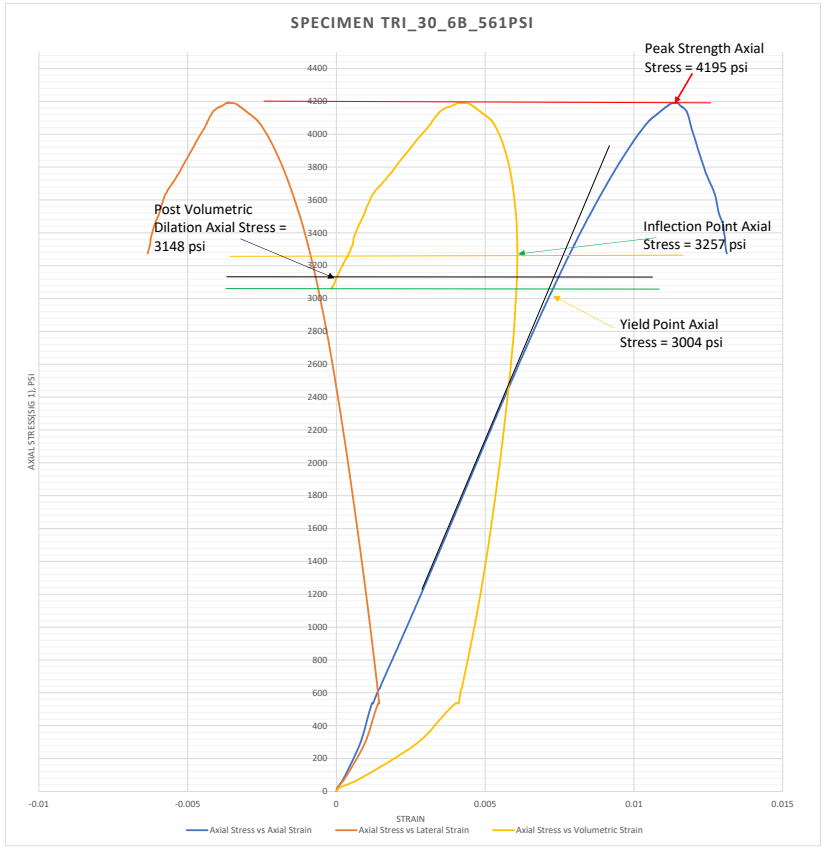
SPECIMEN TRI_30_6B_561PSI
Peak Strength Axial Stress = 4195 psi
Post Volumetric Dilation Axial Stress = 3148 psi
Inflection Point Axial Stress = 3257 psi
Yield Point Axial Stress = 3004 psi
AXIAL STRESS(SIG 1), PSI
STRAIN
Axial Stress vs Axial Strain
Axial Stress vs Lateral Strain
Axial Stress vs Volumetric Strain

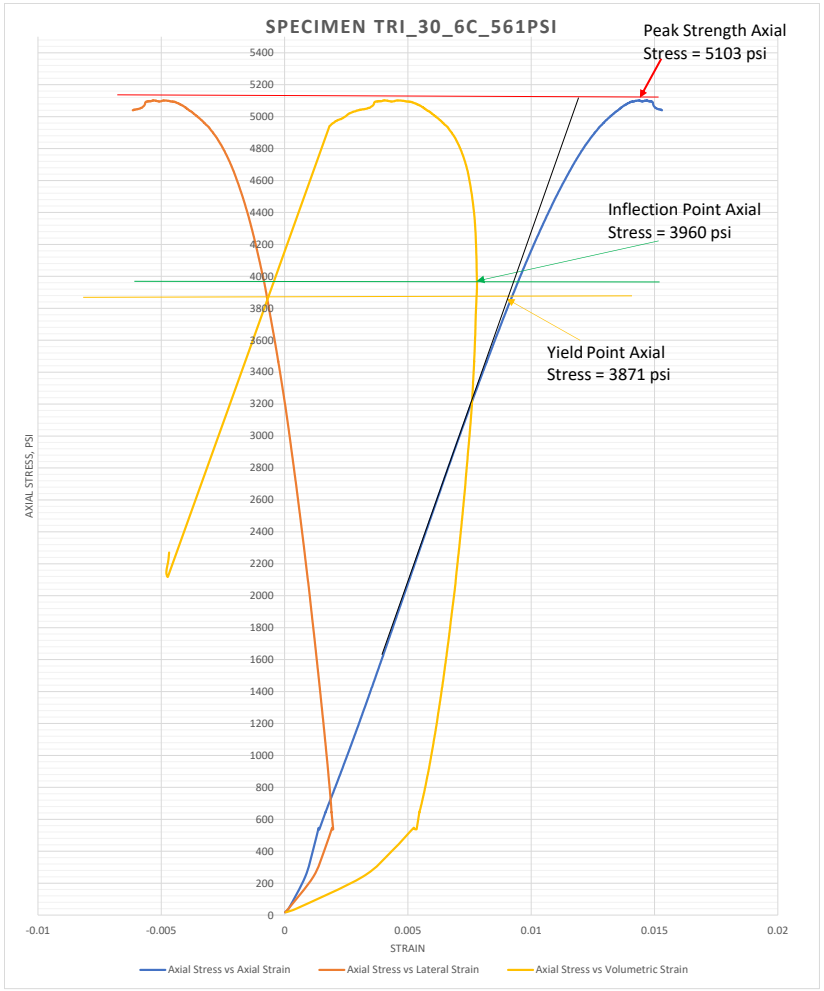
SPECIMEN TRI_30_6C_561PSI
Peak Strength Axial Stress = 5103 psi
Inflection Point Axial Stress = 3960 psi
Yield Point Axial Stress = 3871 psi
AXIAL STRESS, PSI
STRAIN
Axial Stress vs Axial Strain
Axial Stress vs Lateral Strain
Axial Stress vs Volumetric Strain

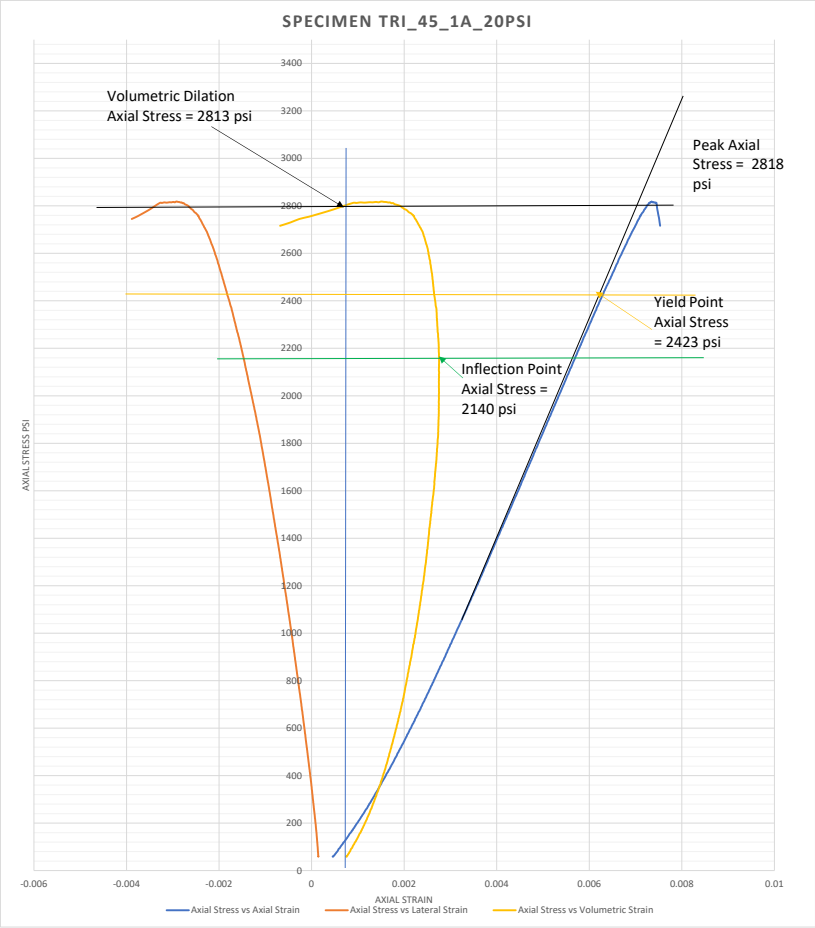
SPECIMEN TRI_45_1A_20PSI
Volumetric Dilation
Axial Stress = 2813 psi
Peak Axial
Stress = 2818
psi
Yield Point
Axial Stress
= 2423 psi
Inflection Point
Axial Stress =
2140 psi
AXIAL STRESS PSI
AXIAL STRAIN
Axial Stress vs Axial Strain
Axial Stress vs Lateral Strain
Axial Stress vs Volumetric Strain

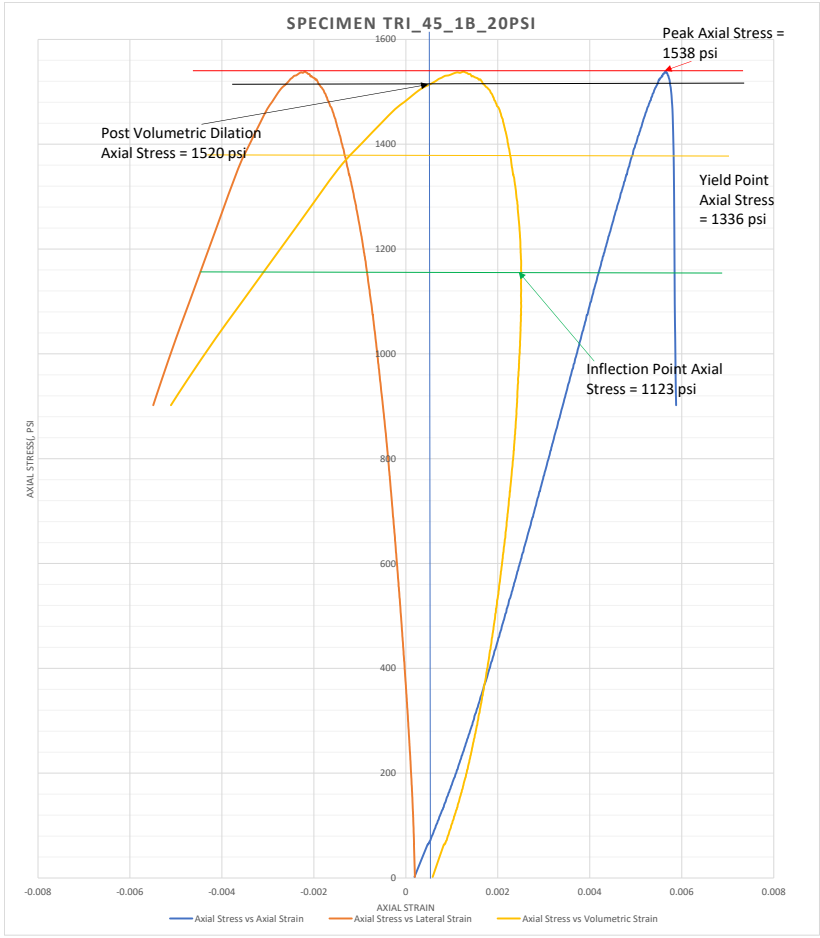
SPECIMEN TRI_45_1B_20PSI
Peak Axial Stress =
1538 psi
Post Volumetric Dilation
Axial Stress = 1520 psi
Yield Point
Axial Stress
= 1336 psi
Inflection Point Axial
Stress = 1123 psi
AXIAL STRESS, PSI
AXIAL STRAIN
Axial Stress vs Axial Strain
Axial Stress vs Lateral Strain
Axial Stress vs Volumetric Strain

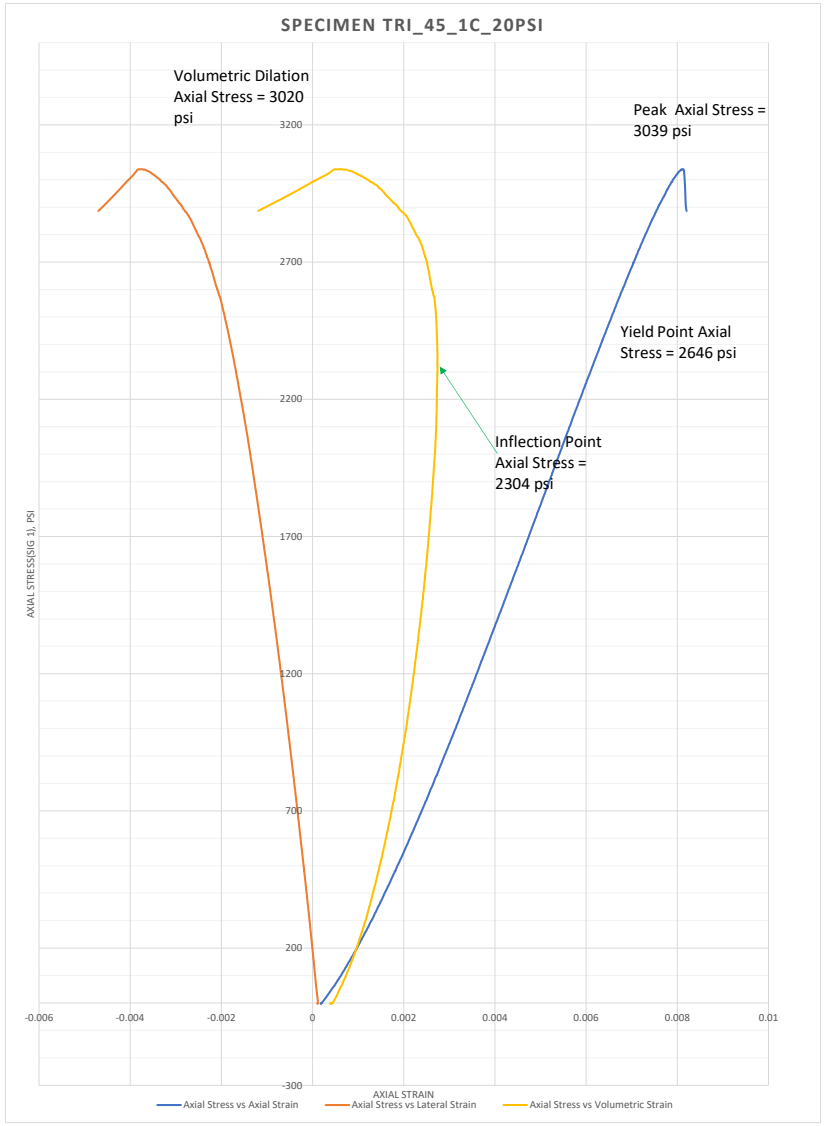
SPECIMEN TRI_45_1C_20PSI
Volumetric Dilation
Axial Stress = 3020
psi
Peak Axial Stress =
3039 psi
Yield Point Axial
Stress = 2646 psi
Inflection Point
Axial Stress =
2304 psi
AXIAL STRESS(SIG 1), PSI
AXIAL STRAIN
Axial Stress vs Axial Strain
Axial Stress vs Lateral Strain
Axial Stress vs Volumetric Strain

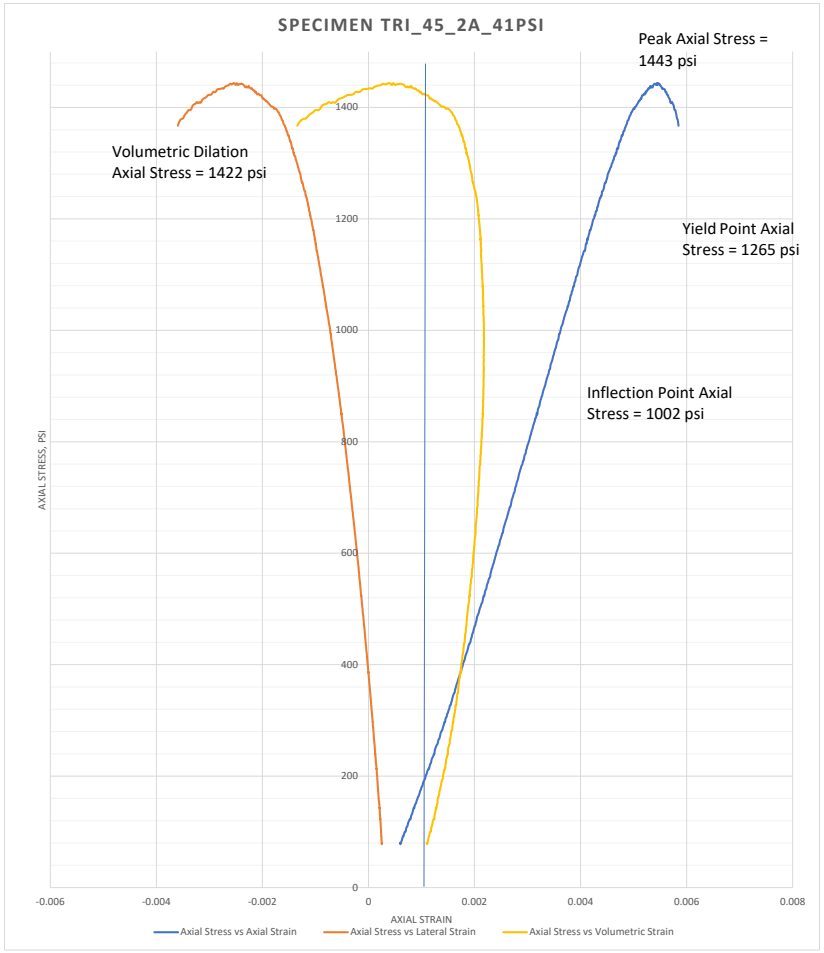
SPECIMEN TRI_45_2A_41PSI
Peak Axial Stress =
1443 psi
Volumetric Dilation
Axial Stress = 1422 psi
Yield Point Axial
Stress = 1265 psi
Inflection Point Axial
Stress = 1002 psi
AXIAL STRESS, PSI
AXIAL STRAIN
Axial Stress vs Axial Strain
Axial Stress vs Lateral Strain
Axial Stress vs Volumetric Strain

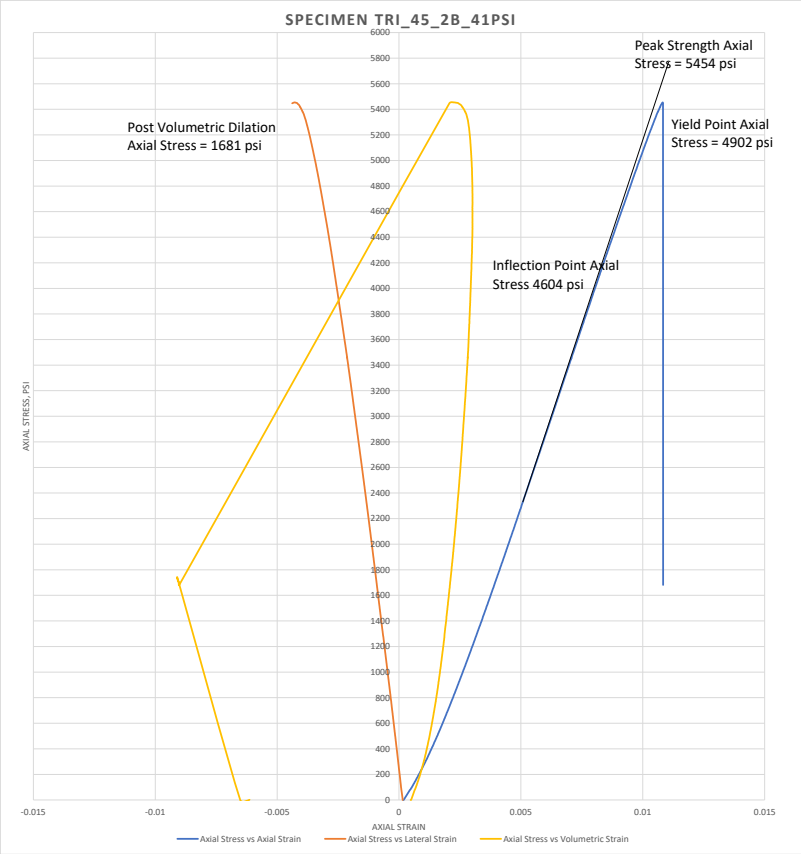
SPECIMEN TRI_45_2B_41PSI
Peak Strength Axial Stress = 5454 psi
Post Volumetric Dilation Axial Stress = 1681 psi
Yield Point Axial Stress = 4902 psi
Inflection Point Axial Stress 4604 psi
AXIAL STRESS, PSI
AXIAL STRAIN
Axial Stress vs Axial Strain
Axial Stress vs Lateral Strain
Axial Stress vs Volumetric Strain

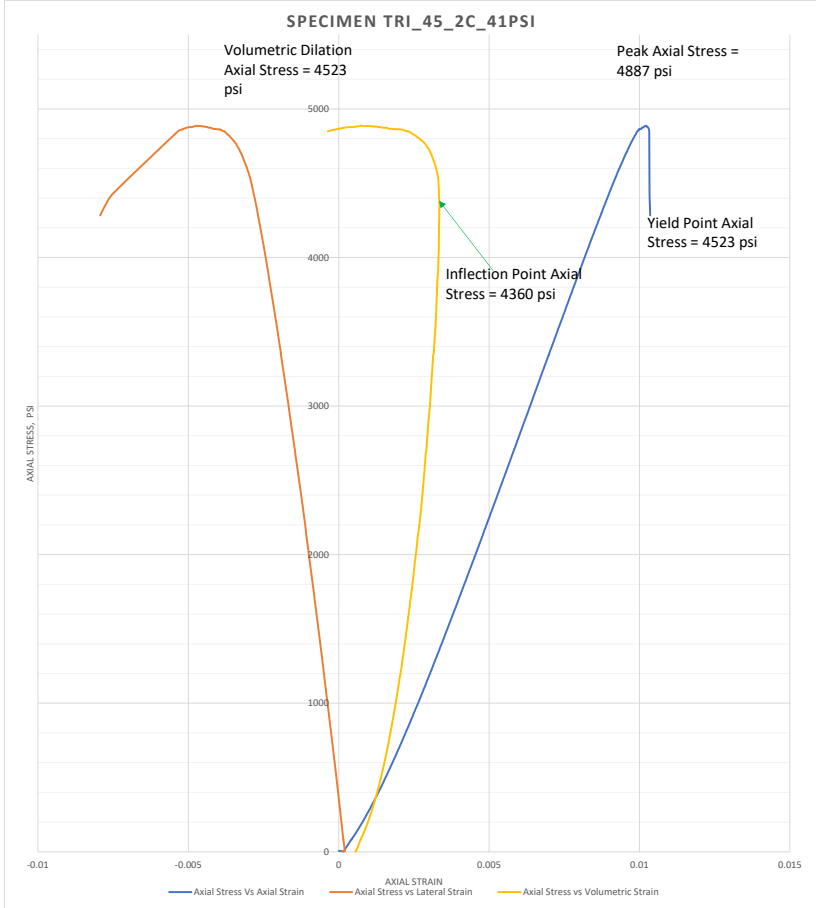
SPECIMEN TRI_45_2C_41PSI
Volumetric Dilation Axial Stress = 4523 psi
Peak Axial Stress = 4887 psi
Yield Point Axial Stress = 4523 psi
Inflection Point Axial Stress = 4360 psi
AXIAL STRESS, PSI
AXIAL STRAIN
Axial Stress Vs Axial Strain
Axial Stress vs Lateral Strain
Axial Stress vs Volumetric Strain

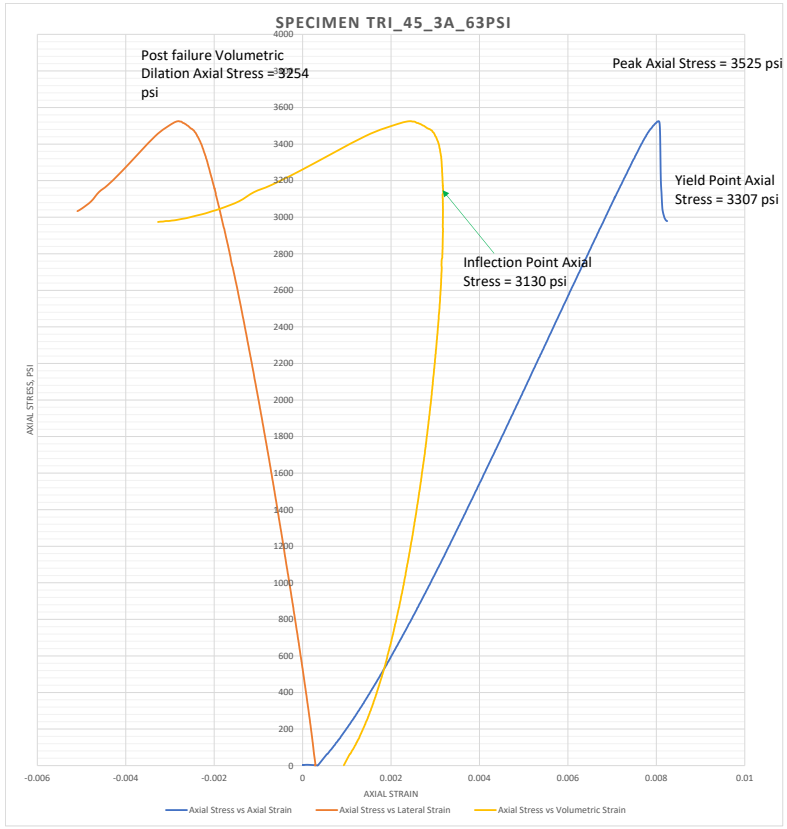
SPECIMEN TRI_45_3A_63PSI
Post failure Volumetric Dilation Axial Stress = 3254 psi
Peak Axial Stress = 3525 psi
Yield Point Axial Stress = 3307 psi
Inflection Point Axial Stress = 3130 psi
AXIAL STRESS, PSI
AXIAL STRAIN
Axial Stress vs Axial Strain
Axial Stress vs Lateral Strain
Axial Stress vs Volumetric Strain

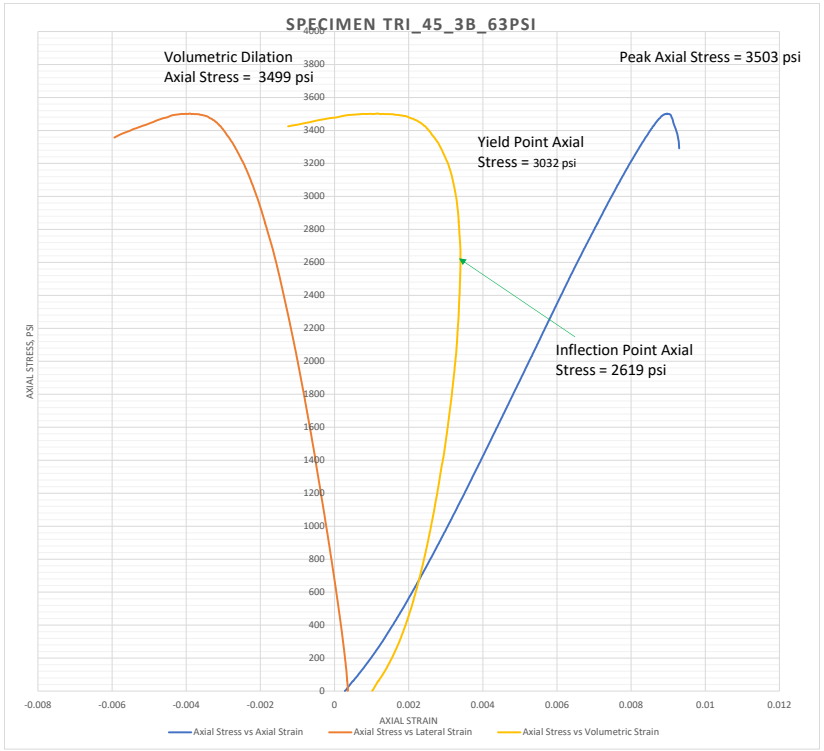
SPECIMEN TRI_45_3B_63PSI
Volumetric Dilation Axial Stress = 3499 psi
Peak Axial Stress = 3503 psi
Yield Point Axial Stress = 3032 psi
Inflection Point Axial Stress = 2619 psi
AXIAL STRESS, PSI
AXIAL STRAIN
Axial Stress vs Axial Strain
Axial Stress vs Lateral Strain
Axial Stress vs Volumetric Strain

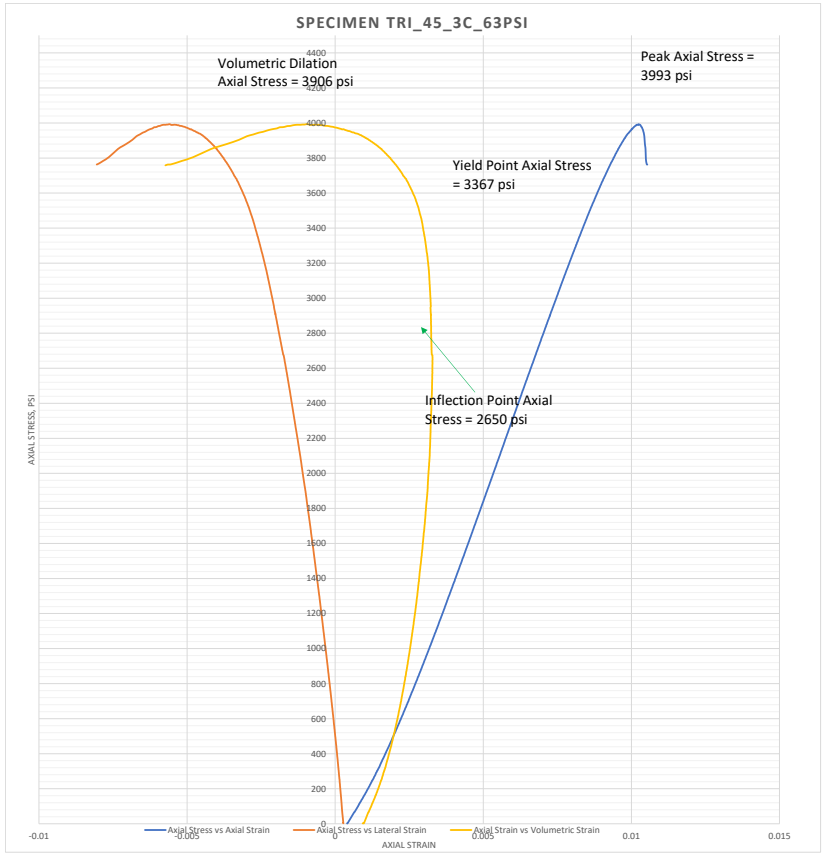
SPECIMEN TRI_45_3C_63PSI
Volumetric Dilation
Axial Stress = 3906 psi
Peak Axial Stress =
3993 psi
Yield Point Axial Stress
= 3367 psi
Inflection Point Axial
Stress = 2650 psi
AXIAL STRESS, PSI
AXIAL STRAIN
Axial Stress vs Axial Strain
Axial Stress vs Lateral Strain
Axial Strain vs Volumetric Strain

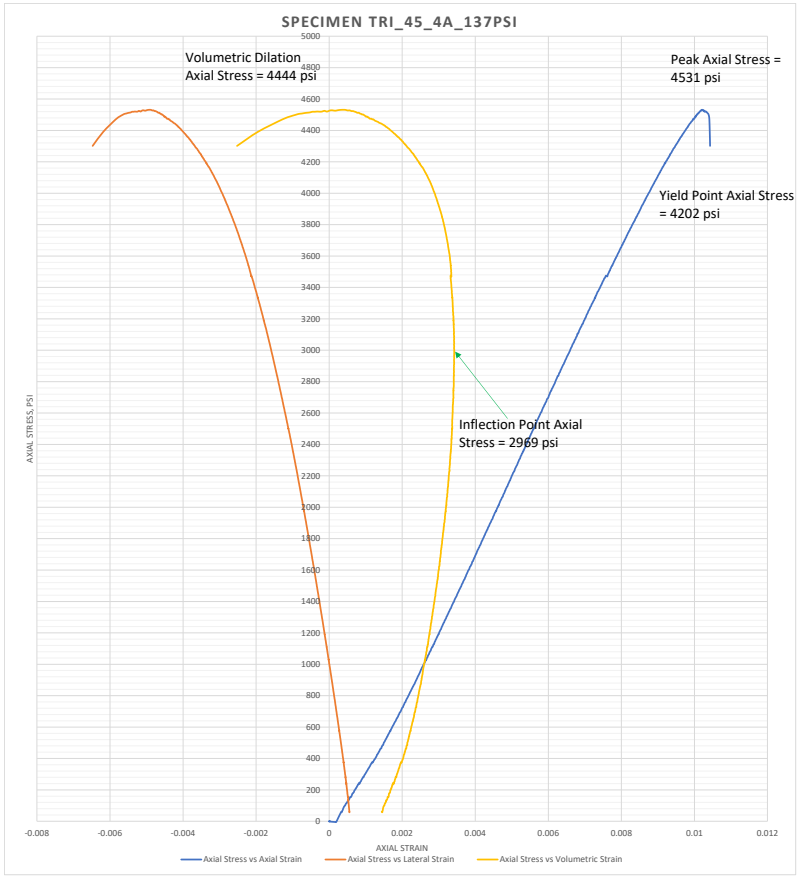
SPECIMEN TRI_45_4A_137PSI
Volumetric Dilation
Axial Stress = 4444 psi
Peak Axial Stress =
4531 psi
Yield Point Axial Stress
= 4202 psi
Inflection Point Axial
Stress = 2969 psi
AXIAL STRESS, PSI
AXIAL STRAIN
Axial Stress vs Axial Strain
Axial Stress vs Lateral Strain
Axial Stress vs Volumetric Strain

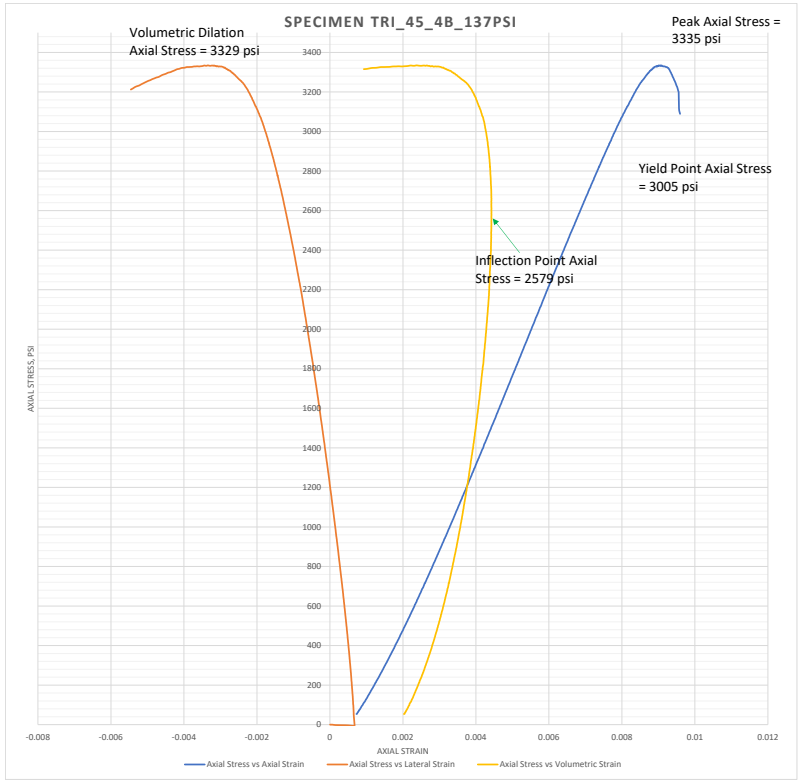
SPECIMEN TRI_45_4B_137PSI
Volumetric Dilation
Axial Stress = 3329 psi
Peak Axial Stress = 3335 psi
Yield Point Axial Stress = 3005 psi
Inflection Point Axial Stress = 2579 psi
AXIAL STRESS, PSI
AXIAL STRAIN
Axial Stress vs Axial Strain
Axial Stress vs Lateral Strain
Axial Stress vs Volumetric Strain

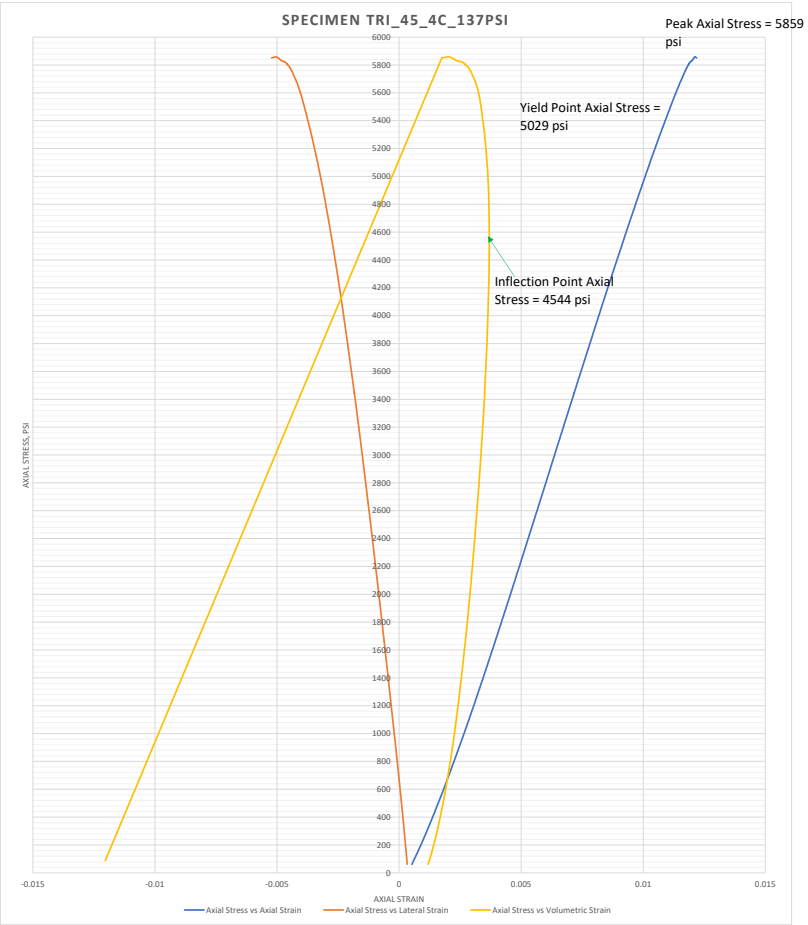
SPECIMEN TRI_45_4C_137PSI
Peak Axial Stress = 5859 psi
Yield Point Axial Stress = 5029 psi
Inflection Point Axial Stress = 4544 psi
AXIAL STRESS, PSI
AXIAL STRAIN
Axial Stress vs Axial Strain
Axial Stress vs Lateral Strain
Axial Stress vs Volumetric Strain

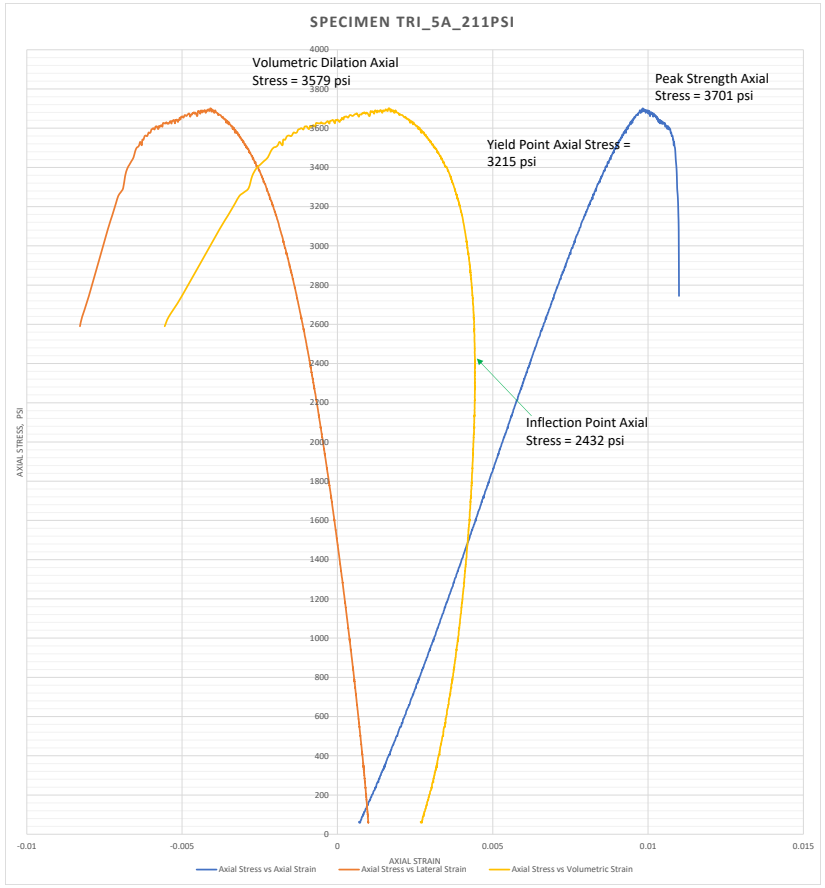
SPECIMEN TRI_5A_211PSI
Volumetric Dilation Axial Stress = 3579 psi
Peak Strength Axial Stress = 3701 psi
Yield Point Axial Stress = 3215 psi
Inflection Point Axial Stress = 2432 psi
AXIAL STRESS, PSI
AXIAL STRAIN
Axial Stress vs Axial Strain
Axial Stress vs Lateral Strain
Axial Stress vs Volumetric Strain

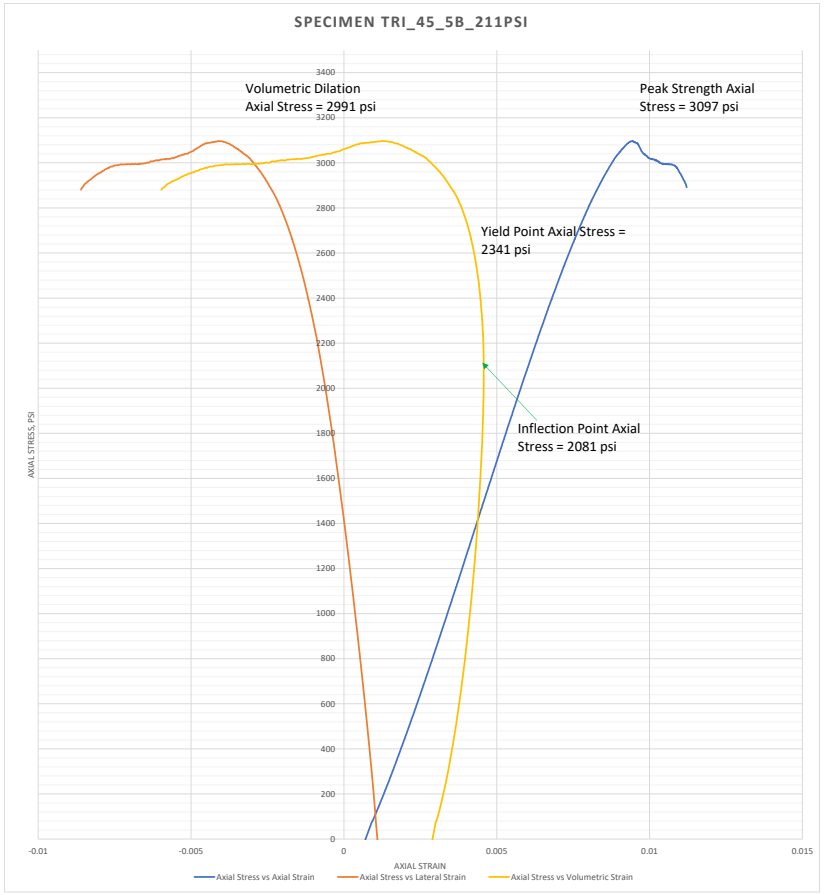
SPECIMEN TRI_45_5B_211PSI
Volumetric Dilation Axial Stress = 2991 psi
Peak Strength Axial Stress = 3097 psi
Yield Point Axial Stress = 2341 psi
Inflection Point Axial Stress = 2081 psi
AXIAL STRESS, PSI
AXIAL STRAIN
Axial Stress vs Axial Strain
Axial Stress vs Lateral Strain
Axial Stress vs Volumetric Strain

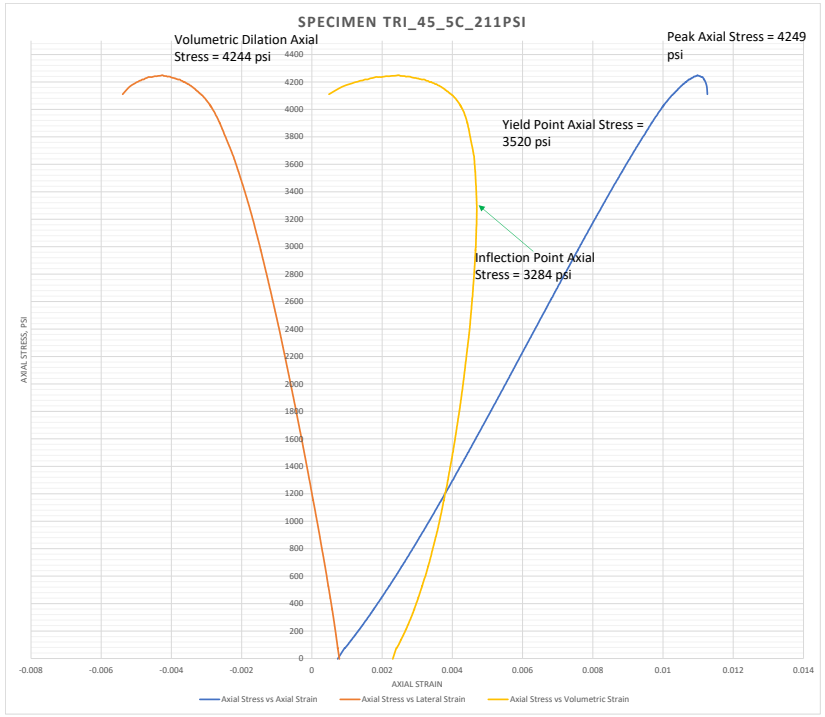
SPECIMEN TRI_45_5C_211PSI
Volumetric Dilation Axial Stress = 4244 psi
Peak Axial Stress = 4249 psi
Yield Point Axial Stress = 3520 psi
Inflection Point Axial Stress = 3284 psi
AXIAL STRESS, PSI
AXIAL STRAIN
Axial Stress vs Axial Strain
Axial Stress vs Lateral Strain
Axial Stress vs Volumetric Strain

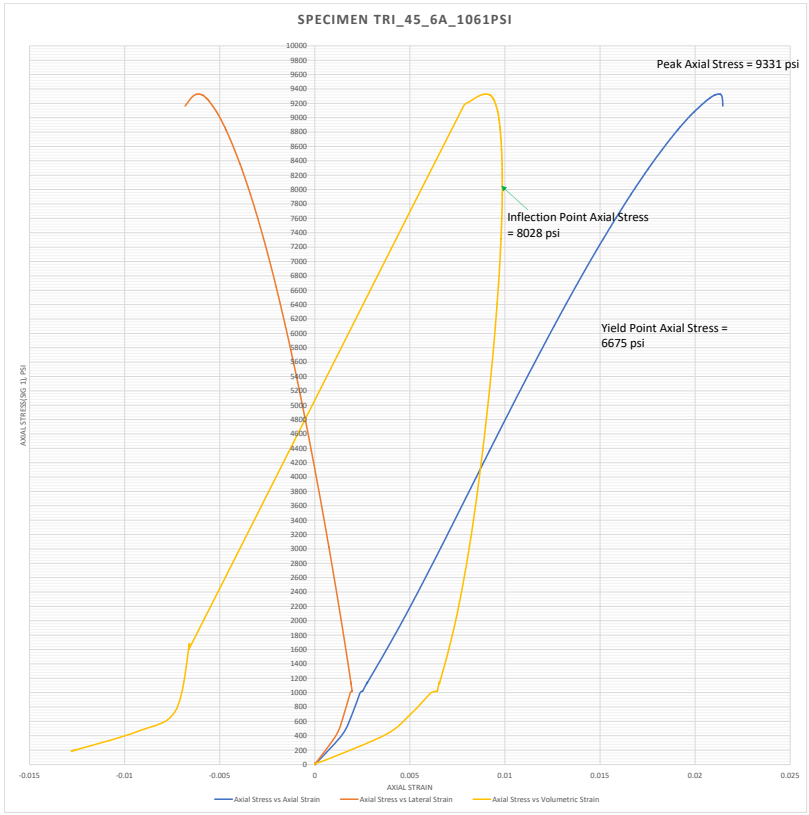
SPECIMEN TRI_45_6A_1061PSI
Peak Axial Stress = 9331 psi
Inflection Point Axial Stress = 8028 psi
Yield Point Axial Stress = 6675 psi
AXIAL STRESS(SIG 11, PSI
AXIAL STRAIN
Axial Stress vs Axial Strain
Axial Stress vs Lateral Strain
Axial Stress vs Volumetric Strain

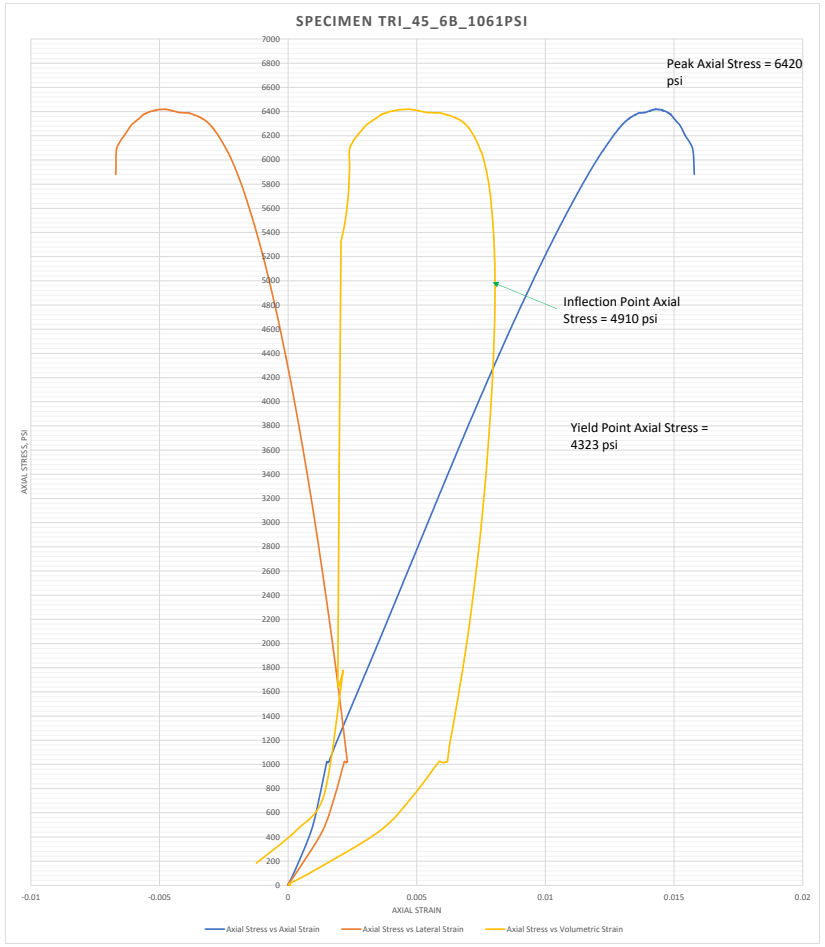
SPECIMEN TRI_45_6B_1061PSI
Peak Axial Stress = 6420 psi
Inflection Point Axial Stress = 4910 psi
Yield Point Axial Stress = 4323 psi
AXIAL STRESS, PSI
AXIAL STRAIN
Axial Stress vs Axial Strain
Axial Stress vs Lateral Strain
Axial Stress vs Volumetric Strain

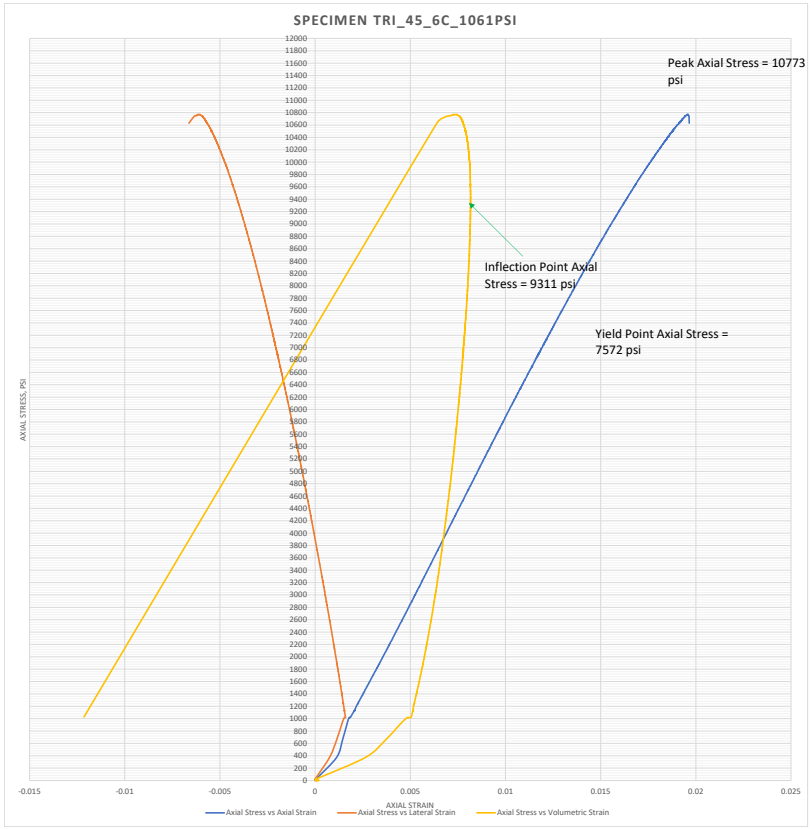
SPECIMEN TRI_45_6C_1061PSI
Peak Axial Stress = 10773 psi
Inflection Point Axial Stress = 9311 psi
Yield Point Axial Stress = 7572 psi
AXIAL STRESS, PSI
AXIAL STRAIN
Axial Stress vs Axial Strain
Axial Stress vs Lateral Strain
Axial Stress vs Volumetric Strain

Appendix C: Crucial Points on Stress-Strain Curves for All 72 Specimens

Table C-1: Crucial points (peak, yield, inflection, dilation) on the stress-strain curves for all 72 conventional triaxial tests

Specimen	Peak Stress	Yield Stress	Infection Point Stress	Volumetric Dilation Stress
Tri_0_1a_32psi	5121	4190	3265	4941
Tri_0_1b_32psi	5375	4391	3478	4703
Tri_0_1c_32psi	5581	4520	3290	5216
Tri_0_2a_64psi	6606	5689	5222	6582
Tri_0_2b_64psi	5060	4219	2472	4124
Tri_0_2c_64psi	7305	6384	5147	7291
Tri_0_3a_98psi	5811	4654	3627	5536
Tri_0_3b_98psi	4674	3718	2992	4344
Tri_0_3c_98psi	5000	3938	3762	4450
Tri_0_4a_211psi	5456	4638	2961	4159
Tri_0_4b_211psi	7675	6361	4755	7567
Tri_0_4c_211psi	7348	5838	5166	7096
Tri_0_5a_325psi	6536	5406	4671	6482
Tri_0_5b_325psi	6839	5507	5298	6827
Tri_0_5c_325psi	7483	6179	5271	7418
Tri_0_6a_1628psi	13199	8575	11787	13183
Tri_0_6b_1628psi	8689	8037	8354	8625
Tri_0_6c_1628psi	13807	11633	12060	13800
Tri_15_1a_27psi	3351	2778	2380	3316
Tri_15_1b_27psi	4904	4192	4166	n/a
Tri_15_1c_27psi	4640	4159	3481	4632
Tri_15_2a_54psi	3674	2935	2298	3543
Tri_15_2b_54psi	5094	3211	3183	4927
Tri_15_2c_54psi	5176	3961	3750	n/a
Tri_15_3a_82psi	3896	2958	2645	3433
Tri_15_3b_82psi	5681	4728	3491	4893
Tri_15_3c_82psi	6110	5902	3608	5918
Tri_15_4a_178psi	4158	3476	3025	4065
Tri_15_4b_178psi	5574	4288	3519	5390
Tri_15_4c_178psi	5607	4394	4132	n/a
Tri_15_5a_275psi	5554	4174	2756	4934
Tri_15_5b_275psi	5832	5024	5050	5532
Tri_15_5c_275psi	7581	5825	6016	n/a
Tri_15_6a_275psi	10616	8274	9126	n/a
Tri_15_6b_275psi	11875	8296	11040	n/a
Tri_15_6c_275psi	13212	9473	12598	n/a
Tri_30_1a_10psi	422	304	80	147
Tri_30_1b_10psi	2609	2503	1760	2584
Tri_30_1c_10psi	1947	1472	1034	1583
Tri_30_2a_11psi	1724	1376	620	1211
Tri_30_2b_11psi	1878	1543	828	1520
Tri_30_3a_11psi	3228	2898	1198	2324
Tri_30_3a_34psi	1736	1535	1059	1730
Tri_30_3b_34psi	2226	1802	1220	1981
Tri_30_3c_34psi	1022	859	719	n/a
Tri_30_4a_72psi	1453	1175	847	1345
Tri_30_4b_72psi	3381	2804	1854	2829
Tri_30_4c_72psi	3235	2597	2113	3131
Tri_30_5a_111psi	2393	2038	1561	2300
Tri_30_5b_111psi	2238	1847	1374	2123
Tri_30_5c_111psi	1414	652	364	616
Tri_30_6a_561psi	5071	3909	4048	n/a
Tri_30_6b_561psi	4195	3004	3269	n/a
Tri_30_6c_561psi	5103	3871	3962	n/a
Tri_45_1a_20psi	2808	2423	2145	2813
Tri_45_1b_20psi	1538	1336	1140	n/a
Tri_45_1c_20psi	3039	2646	2304	3020
Tri_45_2a_41psi	1443	1265	1002	1422
Tri_45_2b_41psi	5454	4902	4668	n/a
Tri_45_2c_41psi	4887	4523	4360	4878
Tri_45_3a_63psi	3525	3307	3130	n/a
Tri_45_3b_63psi	3502	3032	2613	3499
Tri_45_3c_63psi	3993	3367	2650	3906
Tri_45_4a_137psi	4532	4202	2976	4444
Tri_45_4b_137psi	3335	3005	2579	3329
Tri_45_4c_137psi	5859	5029	4544	n/a
Tri_45_5a_211psi	3701	3215	2284	3579
Tri_45_5b_211psi	3097	2341	2081	2991
Tri_45_5c_211psi	4249	3520	3284	4244
Tri_45_6a_1061psi	9331	6675	8028	9328
Tri_45_6b_1061psi	6420	4323	4911	n/a
Tri_45_6c_1061psi	10773	7572	9369	n/a

Appendix D: Dilation & Inflection as a Percentage of Yield & Peak

Table D-1: Dilation and inflection point stresses as a percentage of yield and peak stresses, for all 72 conventional triaxial tests

Specimen	Dilation Yield	Dilation Peak	Infection Yield	Inflection Peak
Tri_0_1a_32psi	118	96	78	64
Tri_0_1b_32psi	107	87	79	65
Tri_0_1c_32psi	115	93	73	59
Tri_0_2a_64psi	116	100	92	79
Tri_0_2b_64psi	98	82	59	49
Tri_0_2c_64psi	114	100	81	70
Tri_0_3a_98psi	119	95	78	62
Tri_0_3b_98psi	117	93	80	64
Tri_0_3c_98psi	113	89	96	75
Tri_0_4a_211psi	90	76	64	54
Tri_0_4b_211psi	119	99	75	62
Tri_0_4c_211psi	122	97	88	70
Tri_0_5a_325psi			86	71
Tri_0_5b_325psi	124	100	96	77
Tri_0_5c_325psi	120	99	85	70
Tri_0_6a_1628psi	154	100	137	89
Tri_0_6b_1628psi	107	99	104	96
Tri_0_6c_1628psi	119	100	104	87
Tri_15_1a_27psi	119	99	86	71
Tri_15_1b_27psi			99	85
Tri_15_1c_27psi	111	100	84	75
Tri_15_2a_54psi	121	96	78	63
Tri_15_2b_54psi	153	97	99	62
Tri_15_2c_54psi			95	72
Tri_15_3a_82psi	116	88	89	68
Tri_15_3b_82psi	103	86	74	61
Tri_15_3c_82psi	100	97	61	59
Tri_15_4a_178psi	117	98	87	73
Tri_15_4b_178psi	126	97	82	63
Tri_15_4c_178psi			94	74
Tri_15_5a_275psi	118	89	66	50
Tri_15_5b_275psi	110	95	101	87
Tri_15_5c_275psi			103	79
Tri_15_6a_275psi			110	86
Tri_15_6b_275psi			133	93
Tri_15_6c_275psi			133	95

Specimen	Dilation Yield	Dilation Peak	Infection Yield	Inflection Peak
Tri_30_1a_10psi	48	35	26	19
Tri_30_1b_10psi	103	99	70	67
Tri_30_1c_10psi	108	81	70	53
Tri_30_2a_11psi	88	70	45	36
Tri_30_2b_11psi	99	81	54	44
Tri_30_3a_11psi	80	72	41	37
Tri_30_3a_34psi	105	93	69	61
Tri_30_3b_34psi	110	89	68	55
Tri_30_3c_34psi			84	70
Tri_30_4a_72psi	114	93	72	58
Tri_30_4b_72psi	101	84	66	55
Tri_30_4c_72psi	121	97	81	65
Tri_30_5a_111psi	113	96	77	65
Tri_30_5b_111psi	115	95	74	61
Tri_30_5c_111psi	95	44	56	26
Tri_30_6a_561psi			104	80
Tri_30_6b_561psi			109	78
Tri_30_6c_561psi			102	78
Tri_45_1a_20psi			88	76
Tri_45_1b_20psi			85	74
Tri_45_1c_20psi			87	76
Tri_45_2a_41psi	112	99	79	69
Tri_45_2b_41psi			95	86
Tri_45_2c_41psi	108	100	96	89
Tri_45_3a_63psi			95	89
Tri_45_3b_63psi	115	100	86	75
Tri_45_3c_63psi	116	98	79	66
Tri_45_4a_137psi	106	98	71	66
Tri_45_4b_137psi	111	100	86	77
Tri_45_4c_137psi			90	78
Tri_45_5a_211psi	111	97	71	62
Tri_45_5b_211psi	128	97	89	67
Tri_45_5c_211psi	121	100	93	77
Tri_45_6a_1061psi	140	100	120	86
Tri_45_6b_1061psi			114	76
Tri_45_6c_1061psi			124	87

Appendix E: All Possible MC Parameters from Conventional Triaxial Tests for Group 1 Specimens

Table E-1: Mohr-Coulomb parameters from all possible combinations of conventional triaxial tests (Group 1 specimens only, cleats at 0°). Sets containing the outlier are highlighted in yellow and yield friction angles that are much lower (and cohesion values that are higher) than the other sets.

Peak Stress Values			Mohr Coulomb Parameters	
212 psi Confining Pressure	326 psi Confining Pressure	1628 psi Confining Pressure	Cohesion, psi	Friction Angle, degree
5456	6536	13197	987	43
5456	6536	8689	1911	19
5456	6536	13807	924	44
5456	6839	13197	1034	42
5456	6839	8689	2021	18
5456	6839	13807	967	44
5456	7481	13197	1136	41
5456	7481	8689	2276	15
5456	7481	13807	1063	44
7675	6536	13197	1418	39
7675	6536	8689	3248	3
7675	6536	13807	1325	41
7675	6839	13197	1475	39
7675	6839	8689	3485	0.3
7675	6839	13807	1377	41
7675	7481	13197	1601	37
7675	7481	8689	4108	6
7675	7481	13807	1493	40
7348	6536	13197	1349	40
7348	6536	8689	2974	6
7348	6536	13807	1260	42
7348	6839	13197	1404	39
7348	6839	8689	3178	4
7348	6839	13807	1311	41
7348	7481	13197	1526	38
7348	7481	13807	1424	40